THE JOURNAL
OF
CHEMICAL PHYSICS

VOLUME 6 OCTOBER, 1938 NUMBER 10

Exchange of Deuterium Between Methanol and Water: Vibrations of the Hydroxyl Group in Methanol and Methanol-*d*: The Entropy of Methanol

J. O. HALFORD AND B. PECHERER
Department of Chemistry, University of Michigan, Ann Arbor, Michigan
(Received April 19, 1938)

New measurements of the equilibrium in the exchange reaction between methanol and heavy water, in conjunction with data in the literature, are considered in relation to the vibrations of the hydroxyl group, including the torsional degree of freedom. An interpretation is presented which allows for a torsional frequency of 250 cm^{-1}, a value which is shown to be in reasonable agreement with the entropy from thermal data.

THROUGH the courtesy of Professor E. F. Barker of the Physics Department, new data on the infra-red absorption of methanol and methanol-*d* have been made available in advance of publication. In addition to frequencies which can be ascribed to motions of the methyl and methoxy groups, they include the OH and OD valence vibrations at 3683 and 2720 cm^{-1} and the distortion of the C−O−D angle at 863, but the corresponding distortion of the C−O−H angle unaccountably fails to appear. The torsional motion produces a broad complicated band system which is spread over a large part of the low frequency region.

The data are not adequate to permit a calculation of the equilibrium constant of the reaction,

$$CH_3OH+DOH=CH_3OD+HOH,$$

by the statistical method. However, the constant can be obtained experimentally to a good degree of accuracy, and it is the purpose of this paper to determine its value and apply it toward the search for the missing deformation and torsional frequencies. The exchange constant turns out to be insensitive to variations of the torsional frequency. For this reason, little specific information about the torsional motion is obtained, but the deformation frequency is consequently quite closely determined.

EXPERIMENTAL

A recent measurement by Okamoto[1] gives the distribution ratio of deuterium between methanol and water as 1.00±0.01 at 0°C, corresponding to an equilibrium constant for the exchange reaction of 0.50±0.005. This result was obtained from two sets of experiments, in which H_2 or D_2 was brought to equilibrium with water or methanol with the aid of platinum black, so that no use was made of water-alcohol solutions, and consequently any peculiar activity effects which such solutions might introduce were eliminated.

In our measurements, equilibrium solutions were made by mixing equimolar quantities of methanol and dilute deuterium oxide, and the alcohol and water were separated by fractional

[1] G. Okamoto, Sci. Papers Inst. Phys. Chem. Research (Tokyo), **31**, 211 (1936).

TABLE I. *Methanol exchange equilibrium at 80°C.*

DOH Initial	DOH Final	Difference	Moles water / Moles alc.	$\frac{CH_3OD}{CH_3OH}\times 100$	$\frac{DOH}{HOH}\times 100$	$K(l)_{353}$
2.644	1.798	0.846	0.982	0.848	1.811	0.468
7.610	5.086	2.524	0.990	2.575	5.194	.496
7.610	5.116	2.494	0.985	2.529	5.225	.484
9.844	6.762	3.122	1.027	3.322	6.955	.478
17.44	11.90	5.54	1.005	5.91	12.52	.472
17.44	11.86	5.58	0.990	5.85	12.47	.469
24.90	16.92	7.98	1.012	8.79	18.20	.483
24.90	16.74	8.16	1.005	8.94	17.99	.496

Mean value, $K(l)_{353}=0.481\pm0.015$.

distillation, using a 90 cm vacuum-jacketed fractionating column. The equilibrium constant was calculated from the decrease in density of the water, as shown by the balance temperature of a glass diver. Initial D_2O concentrations from 1.3 percent to 12.5 percent were employed. The conversion of balance temperatures to D_2O percentages assumes that there is no significant volume change upon mixing D_2O and H_2O, and that the density difference between the two kinds of water is constant in the working temperature range. The second assumption might introduce an error which would appear as a trend in the resulting constant, such that the equilibrium quotient would be a function of the total deuterium content. No trend was observed, and the error introduced is therefore within the limits imposed by the total experimental error. The temperature measurements upon individual samples of water were reproducible to within $\pm0.02°$, corresponding to an uncertainty of ±0.006 percent D_2O at the highest concentrations. The spread of the results is somewhat larger than this figure would allow, probably because of differences in the completeness of separation of the water from the alcohol, and because of fractionation of the water during the distillation so that the sample analyzed was not quite representative.

The fact that the separation was not isothermal was not serious because the heat of reaction is very small. The result is assumed to be correct at 80°C. In the calculation of the equilibrium quotient, the ratio of H_2O to DOH was obtained for each concentration from the constant $K=3.37$ for the reaction,

$$D_2O+H_2O=2DOH.$$

The ratio is not sensitive to the selected value of this constant, but since the constant is a property of the vapor equilibrium, it should be remembered that its application to the liquid phase reaction assumes that the partial pressure of DOH is the geometrical mean of the partial pressures which D_2O and H_2O would have at the same concentration.

The results are summarized in Table I, which shows, in successive columns, the initial and final total deuterium content (expressed as DOH percent of the water content), the decrease produced by reaction, the ratio of total moles of water to total moles of methanol, the ratio of DOH to H_2O, and the equilibrium quotient $K(l)_{353}$ for the liquid phase reaction at 80°C.

The relation between the measured quantity $K(l)$ and the vapor phase constant $K(g)$ must now be considered, since only the latter can be calculated from available data. The transformation would require that $K(l)$ be multiplied by a factor

$$\frac{p^0(HOH)\times p^0(CH_3OD)}{p^0(DOH)\times p^0(CH_3OH)},$$

in which the symbol p° refers to the vapor pressure of the pure substance, in order to give the first approximation to $K(g)$. From the vapor pressure of the three kinds of water published by Wahl and Urey,[2] the correction factor to be applied for the HOH/DOH ratio would increase the constant by about 3 percent. It is probable that this correction would be at least partially compensated by the corresponding effect with the methanols. Thus the vapor phase quotient should be slightly greater than the measured quotient $K(l)$. However, the principal error, incomplete separation of the methanol and water, would operate to give a high result. It is known from the spread of the results that the error of measurement is of roughly the same magnitude as the estimated difference between the liquid and vapor quotients. It appears, therefore, that the mean value of $K(l)$ from Table I is probably very close to the correct vapor phase constant.

At 0°C, the temperature of Okamoto's measurements, the HOH/DOH ratio is about 1.1.

[2] M. H. Wahl and H. C. Urey, J. Chem. Phys. **3**, 411 (1935).

If it is assumed that the corresponding ratio for the methanols is nearer to 1.0, say 1.05, the quotient for the vapor equilibrium at the ice point should be 0.525, which differs from the result for the liquid state by about five times the estimated experimental error.

The statistical constant

The calculation of the equilibrium constant of the exchange reaction from the masses, moments of inertia, and fundamental vibration frequencies by the well-established statistical method has been considered in detail by a number of authors.[3] The paper by Urey and Greiff gives the fundamental equation except for the question of the character of the rotational function for molecules with more than three rotational degrees of freedom. This has been treated rigorously by Eidinoff and Aston,[4] who have worked with certain special cases, and has been generalized by Kassel.[5] In addition, the function has been derived for ethane by Mayer, Brunauer and Mayer,[6] and approximate methods of calculation have been employed by Halford[7] and by Wirtz.[8]

The equilibrium quotient is given by the expression,

$$K(g)=\frac{L(\text{alc.})}{L(\text{aq.})}=\frac{f(CH_3OD)\times f(HOH)}{f(CH_3OH)\times f(DOH)},$$

in which f is the quantity frequently called the partition function and L may conveniently be designated as a partition ratio, such that

$$L(\text{alc.})=\left[\frac{M_D}{M_H}\right]^{\frac{1}{2}}\times\left[\frac{R_D}{R_H}\right]^{\frac{1}{2}}\times\prod_i\frac{(e^{-hc\nu_i/2kT})_D(1-e^{-hc\nu_i/kT})_H}{(e^{-hc\nu_i/2kT})_H(1-e^{-hc\nu_i/kT})_D},$$

[3] H. C. Urey and D. Rittenberg, J. Chem. Phys. **1**, 137 (1933). R. H. Crist and G. A. Dalin, J. Chem. Phys. **1**, 677 (1933). D. Rittenberg, W. Bleakey and H. C. Urey, J. Chem. Phys. **2**, 48 (1934). H. C. Urey and L. J. Greiff, J. Am. Chem. Soc. **57**, 321 (1935). K. Wirtz, Z. physik Chem. **B31**, 309 (1936); **B34**, 121 (1936). P. A. Small, Trans. Faraday Soc. **33**, 820 (1937). T. Jones and A. Sherman, J. Chem. Phys. **5**, 375 (1937).

[4] M. L. Eidinoff and J. G. Aston, J. Chem. Phys. **3**, 379 (1935).

[5] L. S. Kassel, J. Chem. Phys. **4**, 276 (1936).

[6] J. E. Mayer, S. Brunauer and M. G. Mayer, J. Am. Chem. Soc. **55**, 37 (1933).

[7] J. O. Halford, J. Chem. Phys. **2**, 694 (1934).

[8] K. Wirtz, Zeits. f. physik. Chemie **B34**, 121 (1936).

TABLE II. *Methanol moments of inertia (approximate, $\times 10^{40}$).*

Axis	CH_3OH	CH_3OD
Transverse, in COH plane	33.16	34.59
Transverse, perpendicular to COH plane	34.55	37.27
Methyl group	5.268	5.268
Hydroxyl group, axis through its C.G., parallel to CO bond	1.344	2.537
Product $=R'\times 10^{156}$	0.811	1.723

M is the molecular weight, R is Kassel's determinant which reduces to the product of the principal moments of inertia if there is no internal rotation, and h, c, k and T have their usual significance. The subscripts H and D refer to the protium and deuterium compounds, respectively. The corresponding ratio for water contains a symmetry factor of two and in this case R is perhaps more conveniently expressed in terms of the principal moments of inertia.

The water partition ratio

The fundamental frequencies of the H_2O and DOH molecules have been taken from a paper by Barker and Sleator.[9] For the ratio of the moment products R it has seemed safer to use the result of a calculation which assumes that the valence angle and the interatomic distances are the same in the two kinds of water. The values of L(aq.) at 0°C and 80°C are, respectively, 70.176 and 35.807. These numbers are somewhat sensitive to the values of the constants h and k, but the effect of the sensitivity upon the equilibrium quotient is negligible. The constants used here have been taken from a table in Pauling and Wilson.[10]

Rotational functions of the methanols

In the evaluation of Kassel's determinant for the methanols, the C−O−H angle has been taken as 105° and the interatomic distances as C−H=1.09, C−O=1.42 and O−H=0.96 angstrom units. The values of R for methanol and methanol-d, respectively, are 0.7989 and $1.6671(\times 10^{-156})$, and the square root of their ratio, which enters directly into the exchange quotient, is 1.444_6.

[9] E. F. Barker and W. W. Sleator, J. Chem. Phys. **3**, 660 (1935).

[10] Pauling and Wilson, *Introduction to Quantum Mechanics*, McGraw-Hill Book Company (1935), p. 439.

It becomes desirable to compare this result with one which may be reached by an approximate method, as a partial justification of the ratio used further on in the calculations concerned with the possibility of torsional vibration. In addition to the three principal moments of inertia which the methanol molecule would possess as a rigid body, a reduced internal moment is assigned, such as could be ascribed to a molecule like CH_3CD_3, equal to the ratio of the product to the sum of the moments of two coaxial rotators. Since the sum is equal to one of the principal moments, the quantity calculated as substitute for R in the exact equation becomes the quadruple product of the remaining principal moments and the two internal moments. Table II shows the results of the calculations.

The square root of the ratio of the products becomes 1.457, about one percent higher than the correct value. Consequently, no significant error would be introduced into the exchange quotient by the use of these approximate moments. If the entropy of methanol-*d* were calculated with the moments of Table II, it would be high by 0.07 unit at 25°C.

The hydroxyl deformation frequency

If free rotation is assumed, the expression for the equilibrium quotient may be put into the form

$$K(g)\cdot L(\text{aq.}) = (M_D/M_H)^{\frac{3}{2}}\cdot(R_D/R_H)^{\frac{1}{2}}\cdot V,$$

where $$2.303 \log V = (hc/2kT)\sum_i \nu_i.$$

The factors $(1-e^{-hc\nu/kT})$ are omitted because for all the frequencies with which this calculation is concerned they are negligibly different from unity. The one unknown frequency is evaluated by these equations directly from the equilibrium quotient. Numerical solution yields $V_{353}=11.382$ from the new data presented here and $V_{273}=23.188$ from Okamoto's data. The same result, 1199 within a wave number, is obtained for $\sum_i \nu_i$ from both values of V, but the close agreement is obviously fortuitous, in view of the probable magnitude of the vapor pressure corrections associated with the low temperature measurement. The algebraic sum of the known methanol frequencies, including a correction for the shift of ν_6 from 1034 to 1040, is then introduced to give for the missing deformation frequency 1105 cm^{-1}.

This is in very close agreement with the value selected from the Raman spectrum by Bates, Anderson and Halford,[11] and independently by Mizushima, Morino and Okamoto,[12] at 1110.

The spread of the experimental results of Table I corresponds to an uncertainty of ± 15 cm^{-1}. Comparison with the observed OD deformation at 863 in conjunction with known isotope shifts for other hydrogen frequencies suggests that the upper limit of 1120 is the most reasonable result. Ratios of protium to deuterium frequencies are: limiting value 1.414, oxygen-hydrogen valence vibration 1.354, carbon-hydrogen valence vibration 1.34, carbon-hydrogen deformation from methane 1.308, oxygen-hydrogen deformation as above 1.280 ± 0.018. The higher value is further indicated by the frequent observation that Raman lines for liquids are a few wave numbers below the correct frequencies.

The above calculation suggests practically unrestricted internal rotation in the methanol molecule. In order to allow for deviation from free rotation, it would be necessary to adopt one of the lower values of the deformation frequency or to increase the equilibrium quotient. However, as will be shown below, a precise independent deformation frequency and a more accurate study of the equilibrium than is feasible at present would be required before this conclusion could be confidently drawn. In order to illustrate this point, an approximation to the equilibrium constant will be derived from the entropy, which is itself different from the free rotation value by about one entropy unit in the ordinary temperature range.

The entropy of methanol

The entropy of methanol, as a hypothetical perfect gas at atmospheric pressure and 25°C, based upon free rotation and the new set of fundamental frequencies, is 57.72, as against the value 58.38 recently published by Kassel.[13]

[11] J. R. Bates, L. C. Anderson and J. O. Halford, J. Chem. Phys. **4**, 535 (1936). J. O. Halford, L. C. Anderson and G. H. Kissin, J. Chem. Phys. **5**, 927 (1937).

[12] Mizushima, Morino and Okamoto, Bull. Chem. Soc. Japan **11**, 699 (1936).

[13] L. S. Kassel, J. Chem. Phys. **4**, 493 (1936).

The difference arises primarily from the new frequencies. The third law value obtained by combining the result of Kelley,[14] $S(l)_{298}=30.26 \pm 0.2$, with the heat of vaporization measured by Fiock, Ginnings and Holton,[15] and the vapor pressure from *International Critical Tables*[16] is $56.6_3 \pm 0.2$. The excess above 55.72 is the contribution of the torsional motion. The harmonic frequency required to bring the entropy to the upper experimental limit of 56.83 is 370 cm^{-1}. If any reasonable smooth curve of entropy against frequency is drawn in such a way as to approach the harmonic oscillator curve at high frequencies and the free rotation contribution of 2.00 entropy units at zero frequency, it will indicate that a frequency not far from 250 cm^{-1} in the lowest vibrational state corresponds to the harmonic value of 370.

The case of torsional vibration

The statistical expression for the equilibrium constant is rewritten with the contribution of the torsional motion expressed separately as W, so that

$$K(g)\cdot L(\text{aq.})=(M_D/M_H)^{\frac{3}{2}}\cdot(R_D/R_H)^{\frac{1}{2}}\cdot V\cdot W.$$

Only three rotational degrees of freedom are now included in each moment product R. The factor W is obtained from the torsional frequencies, y for CH_3OH and y' for CH_3OD, by means of two equations,

$$W=e^{hc(y-y')/2kT}\frac{(1-e^{-hcy/kT})}{(1-e^{-hcy'/kT})}$$

and

$$y=1.265y',$$

in the second of which the quantity y/y' is set equal to the ratio of the square roots of the reduced internal moments of inertia from Table II. Although W is here expressed by means of a function derived from the harmonic oscillator, it appears to depend primarily on the frequency of the ground state. This follows from the fact that it approaches y/y', the ratio for free rotation, as the frequency approaches zero, and becomes equal to $e^{hc(y-y')/2kT}$ for high frequencies, in much the same way as a theoretically correct expression in terms of the actual frequency would be expected to behave.

For this reason the computation of W is based on the value $y=250$ estimated from the entropy. The introduction of the Raman frequency 1110 for the OH deformation gives $V_{353}=11.493$ and $V_{273}=23.480$. For the exchange constant, then, based on the above interpretation of the entropy and the function W, $K(g)_{353}=0.495$ and $K(g)_{273}=0.522$. The first of these lies within the spread of the experimental values and the second comes within the range of the vapor pressure correction.

It is evident that the exchange constant would be a good measure of the torsional frequency and the deviation from free rotation only if it were known to three significant figures. Although the accuracy could be improved, it is difficult to see how the required degree of precision could be attained. Agreement between the entropy and the exchange reaction occurs only in the region near the upper limit of the experimental values of both quantities, and then only when the deformation frequency is not too close to the most probable value. This study suggests, but does not prove, that either the exchange constant or the entropy is low.

A minimum potential barrier of 2500 cal. may be estimated for methyl alcohol from the entropy by means of the tables recently published by Pitzer.[17] This is nearly as high as the estimate of 3000 for ethane, and appears to be too high, relatively, for the number of hydrogen atoms involved in the effect. It would be unwise, however, to conclude from this comparison that the entropy is low, because the underlying factors are not well enough understood. In this connection, the surprisingly high potential barriers for ethyl alcohol and isopropyl alcohol, 9000 and 6000 cal., which Schumann[18] and Aston have shown to be consistent with equilibrium data and experimental entropies, are particularly interesting.

[14] Kelley, J. Am. Chem. Soc. **51**, 181 (1929).
[15] Fiock, Ginnings and Holton, Bur. Standards J. Research **6**, 881 (1931).
[16] *International Critical Tables*, vol. 3, p. 216.
[17] K. S. Pitzer, J. Chem. Phys. **5**, 469 (1937).
[18] S. C. Schumann and J. G. Aston, J. Am. Chem. Soc. **60**, 985 (1938).

The Absorption Spectra of Cyclopropane, Ethylene Oxide, Ethylene Sulfide, and Ethylene Imine in the Photographic Infra-Red*

EUGENE H. EYSTER
University of Michigan, Ann Arbor, Michigan

(Received July 18, 1938)

The absorption spectra of cyclopropane, ethylene oxide, ethylene sulfide, and ethylene imine have been investigated in the region between 7000 and 12,000A and the stronger bands have been assigned as third harmonics of the fundamental C−H stretching frequencies of these molecules. Rotational fine structure was not observed under high dispersion, but the well-defined band envelopes of the three asymmetric rotators provide interesting examples of these little investigated band types.

INTRODUCTION

ALTHOUGH the majority of compounds of chemical interest are asymmetric rotators, comparatively little is known about the types of band envelopes which may be expected in the absorption spectra of any molecules of large asymmetry. The only molecule of considerable asymmetry whose spectrum has been investigated in great detail is water. This is a spindle-shaped rotator, and unfortunately the simplicity of the molecule prevents the occurrence of one of the three elementary band types. Still less is known about the spectrum of the asymmetric disk-shaped molecule, and hence it has been thought of interest to investigate a number of disk-shaped molecules of considerable asymmetry, and of sufficient complexity to insure the appearance of all of the elementary band types. The ethylene oxide and ethylene sulfide molecules were chosen because their moments of inertia are not too large, and their C−H frequencies are high enough to bring their third harmonics well within the range of the present Eastman I-Z plates. Ethylene imine was included in order to observe the envelope of the hybrid third N−H harmonic. Cyclopropane, the related symmetric rotator, whose fundamentals have been carefully investigated, was also studied to assist in making the vibrational assignments.

EXPERIMENTAL

The cyclopropane employed in these experiments was a pure commercial product prepared by the Ohio Chemical Company for use as an anaesthetic, and was used directly from the ampoule. Photographs were taken at pressures ranging from 120 mm to 1 atmosphere, the gas being confined in a 6-meter absorption tube.

Commercial ethylene oxide, obtained from the Ohio Chemical Company, was also used directly from the tank, photographs being taken at pressures ranging from 120 mm to 1.5 atmospheres in the 6-meter tube, and at a pressure of 1 atmosphere in the 72-foot absorption tube of this laboratory.

The ethylene sulfide was prepared from ethylene dithiocyanate kindly furnished by Dr. E. R. Buchman, according to the method of Delépine and Eschenbrenner.[1] The product was simply distilled, as it is decomposed by the ordinary drying agents, and photographed at a pressure of 200 mm in the 6-meter tube.

The ethylene imine sample was prepared from redistilled monoethanolamine by the method of Wenker,[2] and the product, twice distilled and dried over metallic sodium, was photographed at pressures ranging from 240 to 40 mm in the 6-meter tube. A second sample, kindly prepared by Mr. Herbert Sargent, Jr. according to the same method, was photographed at a pressure of 1 atmosphere in a 3-meter absorption tube.

Low dispersion spectrograms were first taken on a Bausch and Lomb glass Littrow spectrograph, and the strong bands were then photographed under the high dispersion of the 21-foot grating spectrograph.

* Contribution from the Gates and Crellin Laboratories of Chemistry, California Institute of Technology, No. 659.

[1] Delépine and Eschenbrenner, Bull. Soc. Chim. France, **33**, 703 (1923).
[2] Wenker, J. Am. Chem. Soc. **57**, 2328 (1935).

Vibrational Structure

From the standpoint of their fundamental frequencies, the molecules cyclopropane, ethylene oxide and sulfide, and ethylene imine form an interesting sequence. The four C−H stretching frequencies π_s, $\pi_a(2)$, σ_s, $\sigma_a(2)$ of cyclopropane,[3] go over to the four nondegenerate frequencies π_s, π_a, σ_s, σ_a of ethylene oxide as the symmetry is reduced from that of D_{3h} to C_{2v}, and the number of H atoms from six to four. In ethylene imine, which undoubtedly has the symmetry C_s, with the symmetry plane normal to the ring, the four C−H frequencies will remain rather similar to those of ethylene oxide, and may be characterized as π_s', π_a', σ_s', σ_a', where the π' and σ' indicate, respectively, symmetry and antisymmetry with respect to the symmetry plane of the C_2H_4 group, normal to the actual plane of symmetry of the molecule. The N−H stretching frequency, which may be called simply s, will be symmetric with respect to the symmetry plane. Table I shows the distribution of these frequencies among the irreducible representations of the appropriate point groups, and the infra-red activities of their fundamentals. It should be noted that Table I defines the location of the z axis normal to the plane of the three-membered ring, and of the x and y axes in the plane of the ring, with the former passing through the hetero-atom. The selection rules for the third harmonics and combinations of these frequencies, which are of greatest importance in this region of the spectrum, may be obtained by the usual group-theoretical methods.[4] This process yields the information that when only the above frequencies are considered, seven parallel and seven perpendicular bands are permitted for cyclopropane in the third harmonic region, while for ethylene oxide and sulfide fifteen bands are permitted, five of each of the three types A, B, and C. In ethylene imine, no less than twenty bands are permitted. While many of these bands will, of course, not be strong enough to be observed, the spectra do prove to be so complex that assignments can be made in only a few cases. In Table II are listed the observed frequencies, as well as a correlation of bands which appear to be analogous, and assignments of the active third harmonics in the four compounds. Wherever possible, the probable rotational structure types, A, B, or C, whose identification will be discussed in more detail in the next section, have also been indicated.

Table I. *Infra-red activity and irreducible representations of the high frequency fundamental modes of* C_3H_6, C_2H_4O, C_2H_4S, *and* C_2H_5N.

$D_{3h}(C_3H_6)$	$C_{2v}(C_2H_4O, C_2H_4S)$	$C_s(C_2H_5N)$
π_s, A_1',	π_s, A_1, M_x	π_s', A', M_x, M_z
π_a, E', $M_\perp$	π_a, B_1, M_y	π_a', A'', M_y
σ_s, A_2'', $M_\parallel$	σ_s, B_2, M_z	σ_s', A', M_x, M_z
σ_a, E''	σ_a, A_2	σ_a', A'', M_y
		s, A', M_x, M_z

Table II. *Observed bands, rotational structure types, and assignments.*

C_3H_6	C_2H_4O	C_2H_4S	C_2H_5N
	8333		
	8466		
	8602.1 *A* or *C*		
	8667.0 *B*, $3\pi_s$	8637 *A*, $3\pi_s$	8642.3 *B*, $3\pi_s'$
8691.4∥			
	8767.3 *C*		
8770.5⊥, $3\pi_a$	8773.8 *A*, $3\pi_a$	8771.9 *B*, $3\pi_a$	8775.0 *A*, $3\pi_a'$
8806.0∥	8815.8 *B*		
	8835.8 *C*	8833.8 *C*	
	8881.3 *A*	8909	8921
9006.8∥		8982	
9114.4∥, $3\sigma_s$	9021.7 *C*, $3\sigma_s$	9080.2 *C*, $3\sigma_s$	9065.3 *C*, $3\sigma_s'$
	9483		
			9552.5 $3s$
	9704		
	9807		
11448 complex	11333 complex	11413 complex	11390 complex
			12420 $4s$

Band Envelopes

As might well be expected, none of the observed bands showed a resolvable rotational structure, but the unresolved band envelopes do possess considerable significance in themselves. The envelopes of symmetric rotator bands have been calculated theoretically by Gerhard and Dennison,[5] and the observed cyclopropane bands seem in satisfactory agreement with the theory, though overlapping of the 8770 and 8806 cm^{-1} bands makes the interpretation of the microphotometer traces of the perpendicular band rather difficult. The envelopes of the asymmetric rotator bands, however, are of the greatest interest. When the normal modes of vibration of an asymmetric rotator are such that the changes of electric moment are along single principal

[3] See King, Armstrong, and Harris, J. Am. Chem. Soc. **58**, 1580 (1936) for diagrams of symmetry coordinates corresponding to these cyclopropane frequencies.

[4] L. Tisza, Zeits. f. Physik **82**, 48 (1933).

[5] Gerhard and Dennison, Phys. Rev. **43**, 147 (1933).

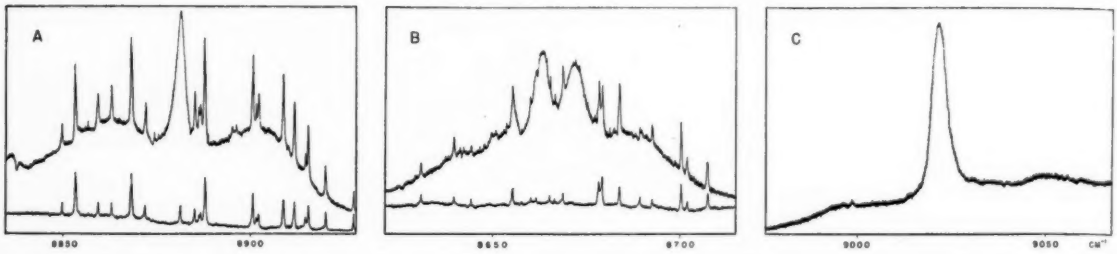

FIG. 1. Microphotometer traces of the three types of band envelopes of ethylene oxide. A trace of the water spectrum is included with the *A* and *B* type bands, which are contaminated with strong water lines.

axes of inertia of the molecule, the resulting rotational structures may be said to be of pure types, and are conveniently characterized as of types *A*, *B*, or *C*, as the change of electric moment is along the minor, intermediate, or major axis of the inertial ellipsoid. In molecules of symmetry C_1, C_i, C_2, or C_s, where the change of electric moment may have components along more than one axis, bands of a twofold (C_2, C_s) or threefold (C_1, C_i) hybrid type may appear, whose envelopes are linear combinations of the intensity distribution functions for the three related pure band types, with coefficients proportional to the squares of the components of the change of electric moment along the corresponding principal axes. In order to know which type of band should be associated with each of the C−H frequencies, it is necessary to know the location of the three different inertial axes in the molecule. For this purpose, approximate moments of inertia of ethylene oxide and ethylene sulfide were calculated on the basis of reasonable molecular models,[6] giving the following values, in g cm$^2\times10^{-40}$:

Ethylene Oxide	Ethylene Sulfide
$I_y=A=31.8$	$I_x=A=38.8$
$I_x=B=39.2$	$I_y=B=74.8$
$I_z=C=59.0$	$I_z=C=102.0$

The moments of inertia of ethylene imine are very nearly equal to those of ethylene oxide. These results, in conjunction with Table I, make possible the following correlation between the band types and the irreducible representations of the normal modes:

Ethylene Oxide	$A\sim B_1$, $B\sim A_1$, $C\sim B_2$
Ethylene Sulfide	$A\sim A_1$, $B\sim B_1$, $C\sim B_2$
Ethylene Imine	$A\sim A''$, *B*, *C* hybrid$\sim A'$

[6] Dr. H. A. Lévy has kindly informed me of preliminary results of his electron diffraction studies of the compounds.

The A' harmonics in ethylene imine may possess hybrid rotational structure, but this could hardly be observable for the C−H harmonics unless they also involve a considerable stretching of the N−H bond. The N−H bands, on the other hand, would be expected to present a twofold hybrid structure involving the band types *B* and *C*.

These predictions are confirmed in every respect by the observed band envelopes. The ethylene oxide bands at 8667, 8881, and 9022 cm^{-1}, shown in Fig. 1, are definitely of three different types, of which two are indeed somewhat similar in appearance but differ greatly in the relative intensities of the side and central branches. Since the 9022 cm^{-1} band appears to be the analogue of the 9114 cm^{-1} band of cyclopropane, one may with confidence identify the former as of type *C*. The 8667 cm^{-1} band, appears to be of type *B*, which will differ from the perpendicular band of the symmetric disk-shaped rotator principally in the appearance of a minimum of intensity at the origin. The remaining band at 8881 cm^{-1} may consequently be designated as type *A*. This identification may seem a little less arbitrary after the publication of theoretical calculations of the three types of band envelopes, which are now in progress in this laboratory. The C−H bands of ethylene imine showed no evidence of hybrid structure, and were very similar in appearance to the corresponding ethylene oxide bands. The type *C* band of ethylene sulfide showed scarcely a trace of side branches, and even when microphotometered seemed to be little more than a single intense central branch. The type *A* bands were weak, yet seemed rather similar in appearance to the type *A* bands of ethylene oxide. However, the type *B* band, shown in Fig. 2,

demonstrates in a very striking manner the effects of the change in the moments of inertia from those of ethylene oxide. The band is obviously considerably distorted as a result of the difference in the moments of inertia in the two vibrational states, but the important feature is that the double maxima about the band center have here become more widely separated, and much less intense relative to the rest of the band.

The ethylene imine band at 9553 cm^{-1} does indeed show the expected hybrid structure, as can be seen by comparing Fig. 3 with the corresponding pure band types, *B* and *C*, of ethylene oxide. The low frequency maximum seems a little too intense, but it may have been strengthened by an accidental superposition of a weak band of type *C*. This view is supported by the doubling observed in this maximum. The surprising feature of this band is the low intensity of the type *C Q* branch, which means that the contribution of the type *C* structure is very small. If it were feasible to determine intensities in this region, the contribution of the two components could be determined with some accuracy, since the intensity distribution functions for the two pure band types involved could then be determined experimentally from the C−H bands of the very similar ethylene oxide molecule. If it were then possible to be certain that the change of electric moment took place along the line of the N−H bond, the angle between this bond and the plane of the ring could be calculated. The problem is a complicated one, but it surely appears that this angle is much smaller than the

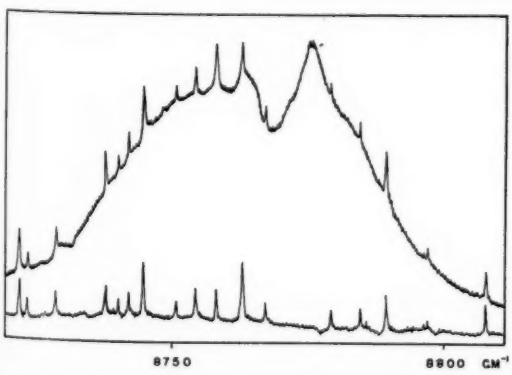

FIG. 2. Microphotometer trace of the strong type *B* band of ethylene sulfide. A trace of the water spectrum in this region is included.

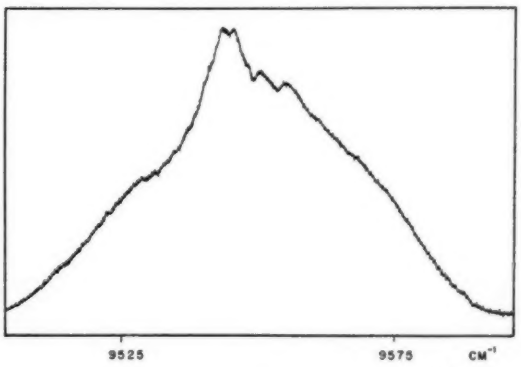

FIG. 3. Microphotometer trace of the hybrid N−H band of ethylene imine.

64° angle between one N−H bond in NH_3 and the plane of the other two bonds. The structure of N-methyl ethylene imine is being studied in these laboratories by Dr. H. A. Lévy, to see if the analogous angle in this compound can be determined with assurance.

It is of interest to observe that in all these molecules analogues of the 8720A (11465 cm^{-1}) band of ethylene[7] appear with considerable intensity. These bands in cyclopropane and ethylene oxide were photographed under high dispersion, and in both cases were found to be unresolved bands of considerable complexity, apparently the result of the superposition of a number of simple bands. Definite assignments of the components is not possible, since even in cyclopropane, which has been most carefully studied, the assignments of the C−H bending frequencies does not seem completely satisfactory. It is, however, probable that in all cases these bands are the result of the superposition of combination bands involving three C−H stretching and two C−H bending frequencies.

The other bands of Table II were too weak for high dispersion study, and many were visible only on the low dispersion plates.

The author is glad, in conclusion, to express his appreciation to Dr. E. R. Buchman and Mr. Herbert Sargent, Jr., of these laboratories, for their advice and assistance in the preparation of ethylene imine and ethylene sulfide, and to Professor R. M. Badger for much helpful assistance throughout the course of these investigations.

[7] Badger and Binder, Phys. Rev. **38**, 1442 (1931).

The Spectrum of Allene in the Photographic Infra-Red*

EUGENE H. EYSTER
University of Michigan, Ann Arbor, Michigan
(Received July 18, 1938)

The spectrum of allene between 7000 and 12,000A has been photographed under high dispersion, the observed bands being assigned as harmonics and combinations of fundamental frequencies of the molecule. Rotational analysis of the parallel band at 11,444A has given 97.0×10^{-40} g cm² as the large moment of inertia. The perpendicular band at 11,017A has been found to be unexpectedly complicated, but was too weak for detailed analysis. It has been concluded that the dimensions in ethylene and allene are:

C−H=1.087A, C=C=1.330A, H−C−H=116°.

INTRODUCTION

ALTHOUGH the rotational structure of the parallel type rotation-vibration bands of symmetric rotators is simple and well understood, that of the perpendicular bands may be complicated by strong rotation-vibration interactions which, although adequately understood in most cases, appear capable of producing complexities which, as in the 4.5μ band of SiH_4,[1] remain at present unexplained. Consequently it has seemed of interest to investigate the rotational structure of the bands of allene in the photographic infra-red under dispersion sufficient to resolve the fine structure of both the perpendicular and parallel types, comparing that of the former with the structure predicted by the first order theory of Teller,[2] and with the use of that of the latter to determine the large moment of inertia of the molecule. Since this moment is insensitive to reasonable changes in the carbon-hydrogen bond distance and the carbon-hydrogen bond angle, a knowledge of its value would determine with considerable accuracy the carbon-carbon double bond distance, a quantity of great interest in the theory of molecular structure.

EXPERIMENTAL

The allene employed in these investigations was a portion of a very pure sample sent from Harvard University by Dr. W. E. Vaughan to Professor Linus Pauling and Dr. L. O. Brockway for use in electron diffraction studies. A second sample for photographs at higher pressures was kindly sent by Dr. J. W. Linnett of Harvard University. A Pyrex absorption tube six meters in length and having a volume of one liter gave adequate absorption with relatively small gas samples. Exploration photographs taken at a pressure of one atmosphere on a Bausch and Lomb glass Littrow spectrograph revealed a rich spectrum in the region between 7000 and 12,000A, and all intense bands were then photographed in the first order of the 21-foot grating spectrograph of this laboratory, at pressures ranging from 40 mm to 1.5 atmospheres. Wavelength measurements on the prism spectrograms were made with respect to sodium, potassium, barium, and calcium lines, and on the grating spectrograms with respect to standard iron lines in the second and third orders. Eastman I-Z and 144-P plates, hypersensitized with ammonia, were used, and in every case visible radiation was removed with filters.

VIBRATIONAL STRUCTURE

In Fig. 1 are shown those three of the eleven allene symmetry coordinates which correspond to the modes of vibration most important in this region of the spectrum, namely those in which the motion consists chiefly of stretching of the C−H bonds, and also their distribution among the irreducible representations of the point group D_{2d}, which describes the symmetry of the molecule. The fundamental frequencies may, for clarity, be associated with these symmetry coordinates, which will in this case approximate the

* Contribution from the Gates and Crellin Laboratories of Chemistry, California Institute of Technology, No. 658.
[1] Steward and Nielsen, Phys. Rev. **47**, 828 (1935).
[2] E. Teller, *Hand- und Jahrbuch der Chemischen Physik* Vol. 9, No. 2 (1934), p. 125.

true normal coordinates with considerable accuracy. The symmetry selection rules are given in the usual fashion[3] by the transformation properties of the electric moment and polarizability tensor components. The irreducible representations of these components and of the harmonic and combination states are given in Table I. Raman investigations of liquid allene by Kopper and Pongratz[4] give values for two of the C−H frequencies, $\nu_1=2995$ and $\nu_3=3060$ cm^{-1}. Bonner and Hofstadter[5] report 3086 cm^{-1} as the position of the unresolved fundamentals ν_2 and ν_3. With the aid of these approximate frequencies, the analogous frequencies in ethylene, and the symmetry selection rules, the strong bands between 7000 and 12,000A may be assigned as harmonics and combinations of the three C−H stretching frequencies. In Table II are given the observed bands, their assignments, and the irreducible representations of the active components of the excited states, which are determinable from the observed band types. The unassigned bands, with the exception of the one at 8758A which will be mentioned later, were extremely weak and were observable only on the low dispersion plates. The photographic data for allene, in conjunction with similar data for ethylene,[6] whose fundamental frequencies are well known, lead one to the conclusion that the probable values of the C−H stretching frequencies in gaseous allene are:

$$\nu_1=3005, \qquad \nu_2=2981, \qquad \nu_3=3095.$$

TABLE I. *Selection rules for the group D_{2d}.*

COMBINATIONS						HARMONICS
	A_1	A_2	B_1	B_2	E	$[A_i^n]=\begin{cases}A_1, & n \text{ even}\\ A_i, & n \text{ odd}\end{cases}$
A_1	A_1	A_2	B_1	B_2	E	
A_2		A_1	B_2	B_1	E	$[B_i^n]=\begin{cases}A_1, & n \text{ even}\\ B_i, & n \text{ odd}\end{cases}$
B_1			A_1	A_2	E	
B_2				A_1	E	$[E^2]=A_1+A_2+B_2$
E				A_1+A_2		$[E^3]=2E$
				$+B_1+B_2$		$[E^4]=2A_1+A_2+B_1+B_2$
		$M_z\sim B_2$				$M_x\pm iM_y\sim E$
$\alpha_{xx}+\alpha_{yy}, \alpha_{zz}\sim A_1,$			$\alpha_{xx}-\alpha_{yy}, \alpha_{xy}\sim B_1,$			$\alpha_{yz}, \alpha_{zx}\sim E$

[3] L. Tisza, Zeits. f. Physik **82**, 48 (1933).
[4] Kopper and Pongratz, Weiner Berichte **B141**, 840 (1932).
[5] Bonner and Hofstadter, Phys. Rev. **52**, 248 (1937).
[6] Bonner, J. Am. Chem. Soc. **58**, 34 (1936).

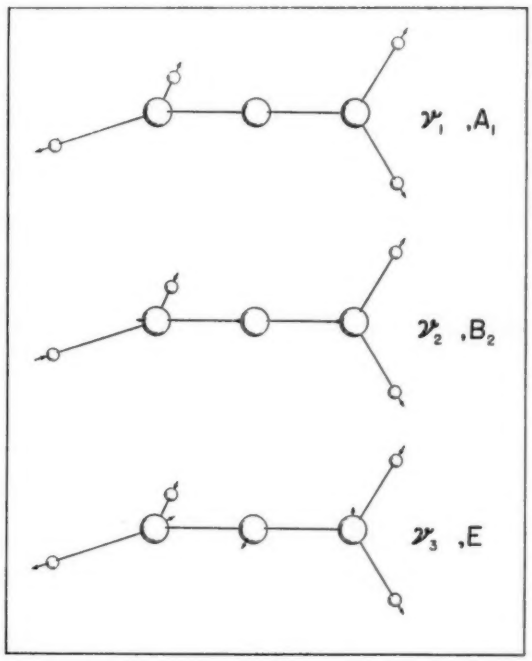

FIG. 1. C-H stretching symmetry coordinates for allene

ROTATIONAL STRUCTURE

Two of the bands, $3\nu_2$ and $2\nu_1+\nu_2$, show rotational structure of the usual parallel type. The lines, however, are incompletely resolved even at a pressure of 40 mm, and cannot be detected on the microphotometer trace shown in Fig. 2, though on the original plates a number of them are distinctly visible. By reversing the plates on Velox No. 5 with contrast developer, about twenty lines in $3\nu_2$ could be measured directly under the comparator with respect to the iron comparison spectrum on the same print. The other band, however, was so badly overlapped by

TABLE II. *Assignment of bands in the photographic infra-red.*

WAVE-LENGTH (A)	FREQUENCY (CM^{-1})	ASSIGNMENT	IRRED. REP.
11,444.32	8,738.96	$3\nu_2$	B_2
11,394.0	8,776.6	$2\nu_1+\nu_2$	B_2
11,205	8,722		B_2
11,139	8,978	$2\nu_3+\nu_2$	B_2
11,097	9,012	$2\nu_3+\nu_1$	B_2
11,017.2	9,076.7	$3\nu_3$	E
10,920	9,718		
9,602	10,420		
9,338	11,710		
8,758	11,418		B_2
7,192	13,904	$5\nu_2$	B_2

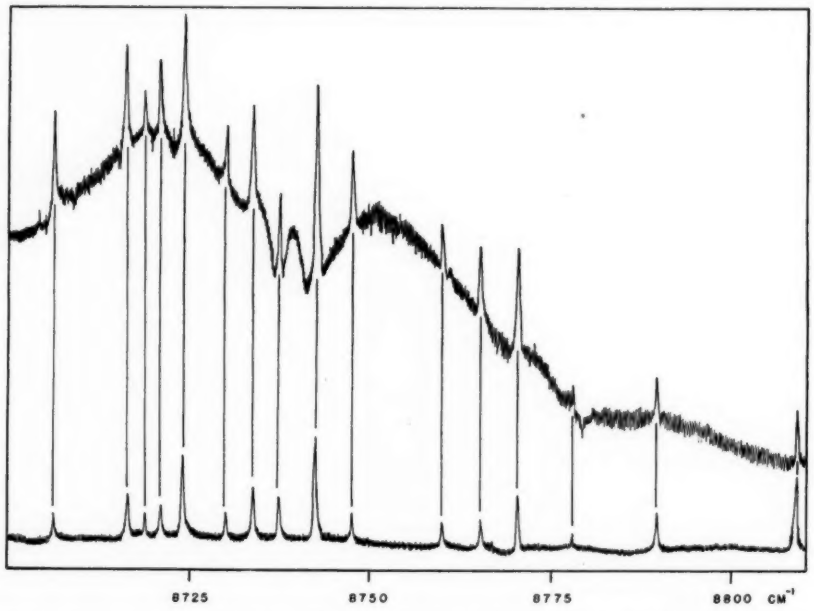

FIG. 2. Microphotometer trace of the 11,444 and 11,394A bands of allene; the lower trace shows the water lines in this region. The general trend in the background in the upper trace is not significant, and is absent in the lower trace only because the water plate was much more heavily exposed.

the much stronger $3\nu_2$ as to be quite useless for a determination of the rotational constant. Although it was impossible to measure the first few lines in either branch, the relative numbering of the lines in the P and R branches was easily made because the convergence was found to be extremely small. Furthermore, only one scheme of relative numbering produced a set of Δ''_2T's which showed a reasonable dependence on J. The absolute numbering, determined by the position of the Q branch, may be in error by one unit because this branch is rather weak and wide, but the error thus induced in the value of the rotational constant will be insignificant owing to the small convergence. The broadness of the band lines, the presence of strong water lines, and the overlapping, with $2\nu_1+\nu_2$ on the high frequency side made it impossible to obtain long branches or measurements of extreme accuracy. The usual combinations, shown in Table III, give a value of 97.0×10^{-40} g cm^2 for the large moment of inertia of the molecule.

The perpendicular band, $3\nu_3$ at 11,017.2A, was found to be extremely weak, and increasing the pressure above one atmosphere in the six meter tube served only to broaden the lines. A number of broad, rather widely spaced band lines could be distinguished on the original plates, and were even more clearly evident in twofold enlargements made on Velox No. 5. A microphotometer trace made with the microphotometer slightly out of focus to eliminate the effects of the coarse grain of the Eastman type I plates, is shown in Fig. 3. Careful comparison with the enlarged prints has shown that the maxima in the trace do indeed correspond to the band features observable visually, but it must be remembered

TABLE III. *Rotational lines and combinations in $3\nu_2$ at 11,444A.*

J	$R(J)$	$P(J)$	$\Delta''_2T(J)$	$\Delta''_2T(J)/2(2J+1)$
5	8741.488			
6	42.046			
7	42.680			
8	43.330		9.574	0.2816
9	43.911	8733.106	—	—
10	44.507	—	11.934	0.2841
11	—	31.977	13.117	0.2852
12	45.731	31.390	—	—
13	46.274	30.841	15.484	0.2867
14	46.817	30.294	16.576	0.2858
15		29.698	17.637	0.2845
16		29.180		
17		28.677		
18		28.090		

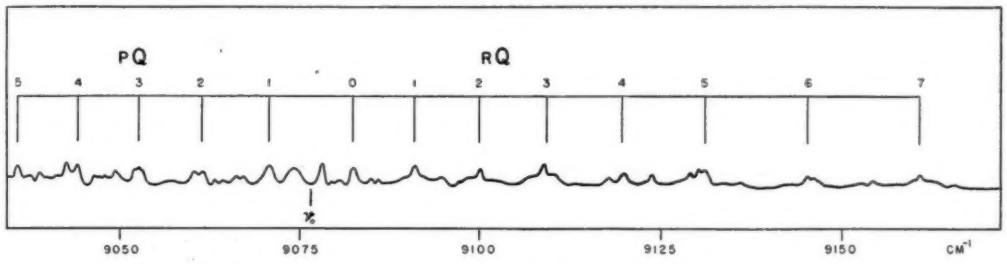

FIG. 3. Microphotometer trace of the perpendicular band of allene at 11,017A, smoothed and corrected for the change in background. Suggested numberings of the Q branches are given. The pQ branch only extends to the fifth line because the band overlaps the 11,100A bands beyond that point.

that many other weaker lines may have escaped detection. In spite of this fact, the rotational structure can be seen to deviate markedly from that predicted by Teller's theory, in that the spacings are not uniform, many of the Q branches are doubled or tripled, and a number of extra strong lines have made their appearance. It is, however, of interest to note that the small moment of inertia, calculated from the average spacing of the lines near the center of the band with the constant ζ in the Teller formula taken as zero, is 5.8×10^{-40}. One would expect the small moments of ethylene and allene to be very nearly equal, and this value does indeed agree very satisfactorily with the small moment 5.67×10^{-40}, determined by the fine structure of the 3.2μ and the 11.5μ bands of ethylene reported by Levin and Meyer.[7] Hence one is led experimentally to the conclusion, which also follows from a consideration of symmetry coordinates in the representation E, that the value of ζ, which is a measure of the vibration-rotation interaction, is not large. A satisfactory explanation of the rotational structure of this band must quantitatively account for the difference between the rotational levels associated with this $3\nu_3$ level of allene and those associated with the analogous $3\nu_\perp$[8] levels of the methyl halides, which appear to be in complete agreement with the Teller theory. The data are at present far too meager to permit a quantitative consideration of the problem, but it seems appropriate to point out two alternative explanations of the complex rotational structure of this band, and to suggest a possible method for distinguishing the correct one.

It is easy to show[3] that whereas the $3\nu_3$ level of allene will be split into two degenerate E levels by the anharmonicity, the $3\nu_\perp$ level in the methyl halides will be split into three levels, only one of which is of the type E and capable of giving perpendicular bands in absorption from the ground state. The remaining twofold degeneracy of the E states will only be removed by terms in the Hamiltonian such as the vibration rotation interaction, which do not possess the symmetry of the molecule. Since the magnitudes of these two types of perturbations which remove the degeneracy of the quadruply degenerate third harmonic state cannot be estimated with any certainty, the possibility that the rotational structure of the perpendicular allene band may be due to either of the following causes must be considered.

1. In case the degeneracy of the E levels has not been removed, and if, moreover, they have not been widely separated by the anharmonicity, the 11,017A band may be the result of transitions to the two E states, whose rotational levels have been so perturbed by interaction with the vibration that the resulting band cannot be simply decomposed into two ordinary perpendicular bands. In this case the difference between the allene and methyl halide third harmonics is easy to understand, and the fundamental perpendicular bands of the former might be expected to agree with the Teller theory.

2. Alternatively, it is possible that the two E levels of allene have been widely separated, and that the 11,017A band is the result of a transition to only one of these states, whose degeneracy has been removed by a strong interaction with the

[7] Levin and Meyer, J. Opt. Soc. Am. and Rev. Sci. Inst. **16**, 137 (1928).
[8] In the notation of H. Sponer, *Molekülspektren* Vol. I (1935), p. 84.

rotation, not present in the methyl halides, and not described by the first order Teller theory. In this case the fundamental perpendicular bands should show a similar structure.

The writer proposes to investigate the fundamentals of the degenerate frequencies of allene in the near future, in the hope of determining the true cause of this unusually complicated perpendicular band structure.

The band at 11,100A, shown in Fig. 4, presents the appearance of a superposition of two parallel bands, and seems to be the result of the approximate coincidence of the levels $2\nu_3+\nu_1$ and $2\nu_3+\nu_2$, which have the symmetry properties characterized, respectively, by the irreducible representations $A_1+A_2+B_2$ and $A_1+B_1+B_2$. The only infra-red transitions to this composite state are to the two B_2 components, which will produce two parallel bands. Fine structure similar to that observed in the 11,444A band could be faintly distinguished on the original plates, but not even the Q branches, which are, of course, rather weak in a molecule of this extreme spindle type, can be located with certainty on the microphotometer traces.

The band at 8758A, shown in Fig. 5, is of special interest as the analog of the ethylene band at 8720A,[9] whose anomalous intensity and complicated rotational structure have never been satisfactorily understood. The allene band appears to consist of a superposition of two parallel bands of unequal intensity, and the components may be assigned as $3\nu_2+2\nu_4$ and $3\nu_3+\nu_4+\nu_5$, where the new fundamental frequencies are:

$$\nu_4=1381\ (B_2), \qquad \nu_5=1031\ (E).$$

These frequencies, observed by Bonner and Hofstadter in the infra-red, are associated chiefly with the bending of C−H bonds. It is probable that the 8720A ethylene band is similarly a superposition of two or more combinations of C−H stretching and bending frequencies.

The remaining bands were too weak for high dispersion investigation, but the band at 7192A seems to be $5\nu_2$, and its doublet structure is clearly visible on the low dispersion plates.

Structures of Allene and Ethylene

Because of the importance of the carbon-carbon double bond distance in establishing the single-double bond resonance curve,[10] it seems of considerable interest to attempt to interpret the moments of inertia of ethylene and allene in terms of bond distances and angles. The C−H

[9] Badger and Binder, Phys. Rev. **38**, 1442 (1931).

[10] Pauling and Brockway, J. Am. Chem. Soc. **59**, 1223 (1937).

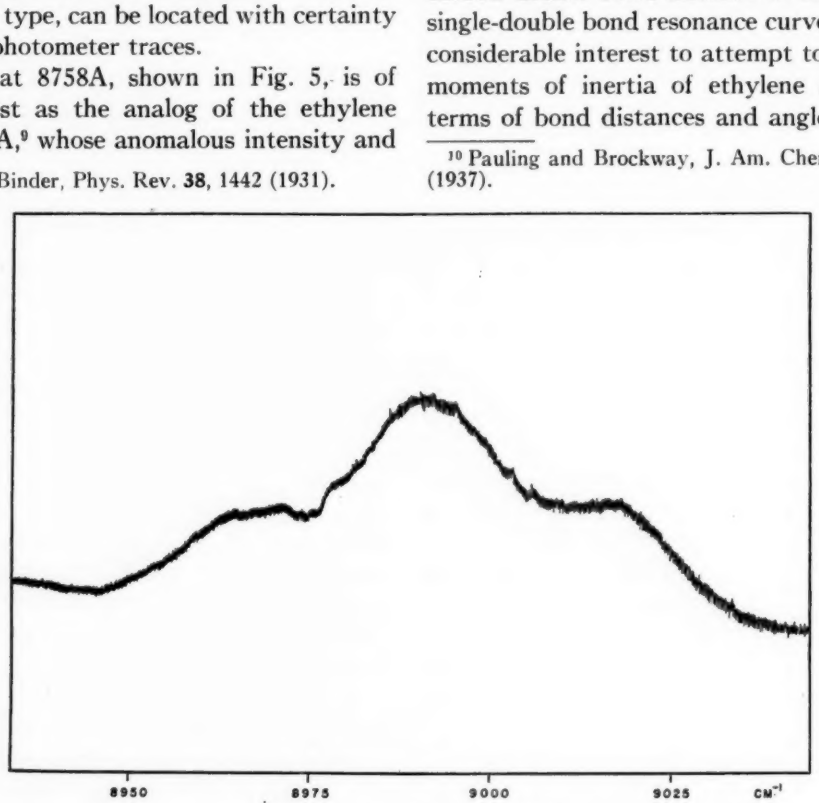

FIG. 4. Microphotometer trace of the 11,100A bands of allene.

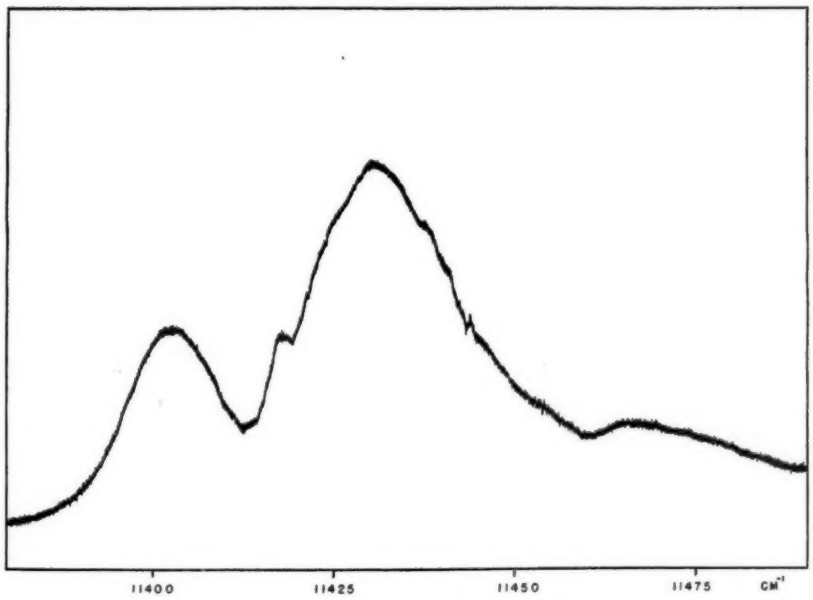

FIG. 5. Microphotometer trace of the 8758A bands of allene.

distance in these compounds can be obtained with some confidence by a consideration of the distances and force constants in a number of molecules containing the C−H group. When the C−H distances in C_2H_2, HCN, CH_4, and the ground state of CH are plotted against the inverse cube root of the C−H stretching force constant, following the procedure first suggested by Badger,[11] one obtains a very satisfactory straight line. The force constants of ethylene and allene may then be used to fix the C−H distance, which is thus found to be 1.087A in both compounds. This information then makes it possible to calculate the C−H bond angle in ethylene from the small moment of inertia, giving the angle H−C−H as 116°. Calculation of the C=C distance in ethylene and allene from their large moments of inertia, using the above parameters for both molecules, gives, respectively, 1.325 and 1.330A. The difference is probably insignificant, since the large moment of inertia of ethylene, calculated by Badger[12] from the rotational Raman band of Lewis and Houston, is probably not so accurate as the others, and none of the moments of inertia have been corrected to the vibrationless state.

In conclusion, the writer is pleased to express his appreciation to Professor R. M. Badger for his valuable advice and assistance during the course of this investigation.

[11] Badger, J. Chem. Phys. **2**, 128 (1934).

[12] Badger, Phys. Rev. **45**, 642 (1934).

The Raman Spectrum of Liquid Diborane

THOMAS F. ANDERSON, *Botany Department, University of Wisconsin, Madison, Wisconsin*

AND

ANTON B. BURG, *George Herbert Jones Chemical Laboratory, University of Chicago, Chicago, Illinois*

(Received July 5, 1938)

The Raman spectrum of $B_2H_6(l)$ is found to contain an isotopic triplet (ν_1) 793, 806, 821 cm^{-1}, a broad line (ν_2?) 1108 cm^{-1} and a very intense doublet (ν_3?) 2102, 2523 cm^{-1} as well as several weaker lines. Abnormally large values for the B−B, C−C, and Si−Si bond force constants in B_2H_6, C_2H_6, and Si_2H_6 suggest that these bonds are compressed in these molecules by forces which may be associated with those which restrict internal rotation. The value of 55.3±1.5 cal./deg. is calculated for the entropy of $B_2H_6(g)$ at 25°. Combined with the known heat of formation this value leads to a free energy of formation of −30,000±4000 cal. for $B_2H_6(g)$ at 25°. This large value does not truly indicate high stability, for diborane decomposes easily to form other boron hydrides.

THE x-ray[1] and electron diffraction[2] patterns of diborane (B_2H_6) show that its atomic arrangement is analogous to that in ethane. However, the formulation of its electronic structure is made difficult by the deficiency of two electrons.[3] In the hope of contributing toward the solution of this problem, we have obtained the Raman spectrum of diborane in the liquid condition.

Experimental Method

Preparation of the substance

Diborane was prepared by the method of Schlesinger and Burg,[4] and purified with great care. The vapor tensions of the first and last fractions corresponded to that previously recorded for the pure substance: 225 mm at −111.8°. The quantity employed was slightly more than three liters of the gas at standard conditions. The sample was completely condensed (by the aid of liquid nitrogen) in the Raman tube, which was sealed off and at once put to use.

Optical arrangements

The apparatus in which the diborane received and scattered the light from a mercury lamp, is shown in Fig. 1. The Raman tube was made from a 12.5 cm length of standard wall, 10 mm diameter Pyrex tubing, sealed at the lower end to a Wood light trap of black Pyrex glass, and at the upper end to a wider (18 mm) tube carrying a horizontal plane window and the side tube for introducing and removing the sample. This Raman tube was surrounded by a 19×4 cm copper cylinder, out of whose wall (2 mm thick) a 13×3 cm window had been cut. The piece cut out was soldered to the inner wall to make a well for receiving liquid nitrogen, by whose aid

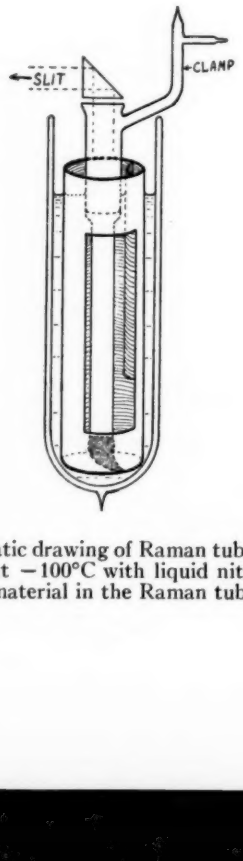

FIG. 1. Schematic drawing of Raman tube assembly. The alcohol is kept at −100°C with liquid nitrogen to liquify the low boiling material in the Raman tube.

[1] H. Mark and E. Pohland, Zeits. f. Krist. **62**, 103 (1925).
[2] S. H. Bauer, J. Am. Chem. Soc. **59**, 1096 (1937).
[3] A review of the literature on this subject is given by Wiberg, Ber. **69B**, 2816 (1936).
[4] Schlesinger and Burg, J. Am. Chem. Soc. **53**, 4321 (1931).

the required low temperature (in the neighborhood of $-100°$ or lower) could be maintained. The entire inner surface of the copper cylinder was silver plated to minimize the loss of light.

The Raman tube and reflecting cylinder were immersed in an alcohol bath, contained in a cylindrical Dewar vessel which had been silvered only around two-thirds of its circumference. As a safety device, in case of an accidental rise of temperature, solid carbon dioxide was placed in the space below the window of the copper cylinder.

The mercury vapor lamp used in this work was of the very convenient design shown in Fig. 2. In the use of this relatively simple type of lamp, the current passes through the Torricellian vacuum in the water-jacketed tube. The arc is struck by forcing the mercury to the top of the discharge tube, where it makes contact with the mercury in the closed end, and then releasing the pressure. The discharge tube has an internal diameter of 7.5 mm and the connecting "barometer" tube has a bore of 2.5 mm. Connected to a source of 110-volt direct current, through a six-ohm resistance, this lamp draws a current of 11 amperes, and produces mercury spectrum lines quite sufficiently sharp for accurate Raman studies.

TABLE I. *Observed frequencies in the Raman spectrum of* B_2H_6 *(l) with displacements from the exciting* Hg *lines* λ*3984(l),* λ*4047(k),* λ*4077(i),* λ*4339(g),* λ*4347.5(f), and* λ*4358(e), d=diffuse.*

I (ARB.)	ν (CM^{-1})	PROBABLE $\Delta\nu$ (CM^{-1})	ALTERNATE $\Delta\nu$ (CM^{-1})
9	22603.9	2101.5*k*	
3	22571.1	2527*l*	
3	22414.2	2101.9*i*	
10	22182.0	2523.4*k*	
5	22145.6	792.5*e*	
4	22131.9	806.2*e*	
3	22116.7	821.4*e*	
4	21993.2	2522.9*i*	
2*d*	21930.0	2775.4*k*	1008.1*e*
2	21757.7	1180.4*e*	2947.7*k*
3	20933.1	2106*g*	
1	20898	2101*f*	
10	20836.6	2101.5*e*	
0	20517	2522*g*	
0	20478	2521*f*	
3	20449.6	2488.5*e*	4255.8*k*
8	20416.2	2521.9*e*	
7	20155.3	2782.8*e*	Hg 4960.3A
2	20070.3	2867.8*e*	4635.1*k*
4	19818.4	3119.7*e*	4887.0*k*

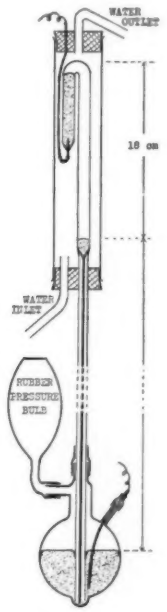

FIG. 2. Water-cooled mercury lamp. The arc is struck in the 18 cm long Torricellian vacuum.

This mercury lamp was placed against the window of the Dewar cylinder, and the two were wrapped with bright aluminum foil, in order to save as much of the light as was feasible. The scattered light was taken off through a right-angle prism into the slit of a three-prism Steinheil spectrograph, set for a dispersion of 18.7A per mm at a wave-length of 4350A. The instrument was in sharp focus between 4350A and 5100A. Three photographs were obtained: the first was exposed half an hour, the second, two hours, and the third, five hours, on Eastman DC *ortho* plates. The spectrum of an iron arc was photographed upon each plate for comparison; on the third plate the spectrum of the mercury lamp itself also was photographed, with an intensity of exposure almost the same as that of the scattered mercury spectrum.

EXPERIMENTAL RESULTS

Seven Raman lines were obtained with the half-hour exposure, sixteen with the two-hour exposure which had a low background, and sixteen or more with the five-hour exposure which gave a uniform background. In Table I are given the estimated intensity (I) and frequency (ν) of each of the observed lines together with

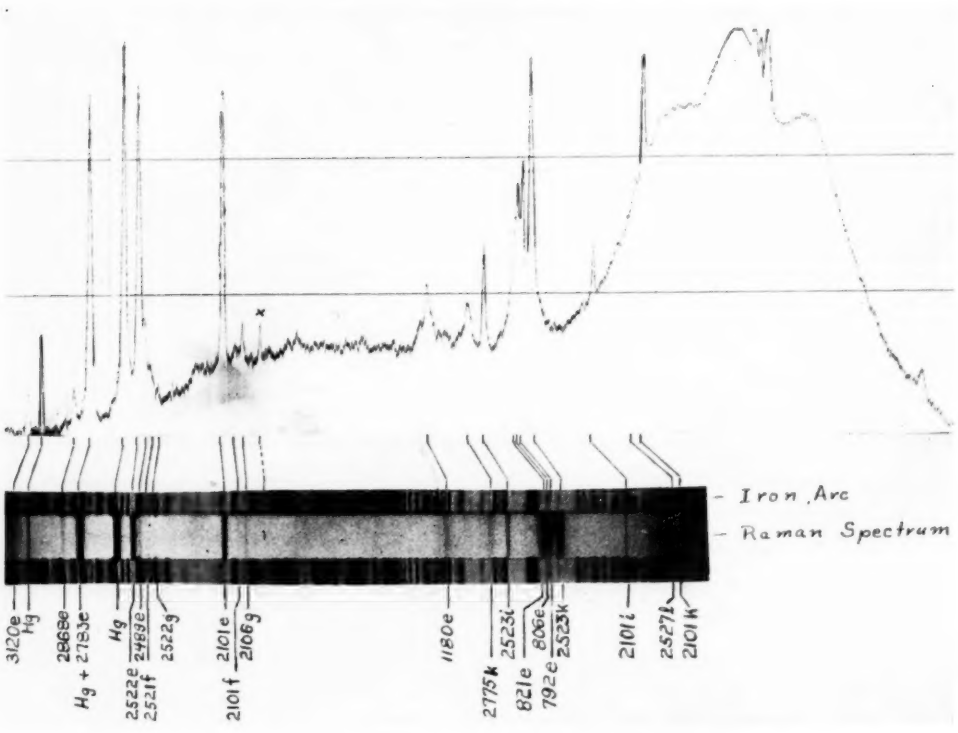

FIG. 3. The Raman spectrum of $B_2H_6(l)$ and its microphotometer tracing.

the displacements from the various exciting lines. In Fig. 3 the five-hour exposure is reproduced together with the iron comparison spectrum, the observed frequency shifts, and a microphotometer tracing of the Raman spectrum.

The lines 2101 k, e and 2523 k, e are most intense and exceedingly sharp; these frequencies have also been scattered from the Hg i, f, and g and the Hg l and i lines, respectively. The pair 792e and 806e are sharp and the former is considerably stronger than the latter. The line 821e is broad, however, and its integrated intensity is probably greater than that of 792e.

As indicated in Table I, in a number of cases it is uncertain whether the exciting line is λ4358 or λ4047. We feel, however, that λ4358 is responsible for most of these lines since if they were of higher frequency (i.e., scattered from λ4047) they should also be observed as scattered from λ4358. The broad line at 21,930 cm^{-1} may be an exception for if it were 2775k, 2775e would be obscured by the mercury line λ4960. The fuzzy appearance of the line Hg 4960 causes us to favor this latter possibility. Note that the apparently sharp line marked x on the microphotometer tracing is in reality only a dust mark on the plate.

ASSIGNMENT OF FREQUENCIES

Selection rules for this type of molecule have been given by Stitt and Yost.[5] They allow 6 frequencies for the D_{3d} configuration (center of symmetry), 9 for the D_{3h}' configuration (in which internal rotation is unrestricted) and 9 Raman active frequencies for the D_{3h} configuration (plane of symmetry perpendicular to the central bond). Howard[6] has worked out the normal coordinates using a three-constant valence-force potential function with restricted internal rotation.

The symmetrical stretching vibration ν_1,[6] for each of the three isotopic molecules containing

[5] Stitt and Yost, J. Chem. Phys. **5**, 90 (1937).

[6] J. B. Howard, J. Chem. Phys. **5**, 442 (1937). We have used the notation used in this paper to designate the frequencies. We are indebted to Dr. Howard for sending us the unpublished formulae for the ν_9, ν_{10}, and ν_{11} vibrations.

$B^{11}-B^{11}$, $B^{11}-B^{10}$, and $B^{10}-B^{10}$, are readily identified as the lines 793, 806, and 821 cm^{-1}, respectively. The calculated isotopic shifts in frequency agree within 1 cm^{-1} with the observed shifts, and the relative intensities are of an order of magnitude corresponding to the relative abundance, 4 to 1, of the boron isotopes except for the line 821 cm^{-1} which is more intense than corresponds to this ratio. It has been noted, however, that the line at 821 cm^{-1} is broad and therefore doubtless derives its principal intensity from another frequency, possibly ν_9.

A comparison of the spectrum of B_2H_6 with those of the analogous compounds C_2H_6 and Si_2H_6 aids in making further assignments. In Table II are listed our results together with those for $C_2H_6(l)$,[7] $C_2H_6(g)$,[8] and $Si_2H_6(g)$.[5] The frequency at 1180 cm^{-1} apparently corresponds to the 1463 cm^{-1} line for C_2H_6 and the 933 cm^{-1} band for Si_2H_6 which have been assigned to ν_2, associated with the symmetrical bending of the B−H, C−H, and Si−H bonds, respectively. Likewise the intense pair 2102, 2523 cm^{-1} would correspond to the pair 2884, 2941 cm^{-1} of $C_2H_6(l)$ and the line 2163 in $Si_2H_6(g)$ which have been assigned to ν_3, the frequency associated with the symmetrical stretching of the six bonds to the hydrogen atoms. These frequencies lie close to the B−H stretching frequency 2535 cm^{-1} in $B_3N_3H_6$.[9] In $C_2H_6(l)$ the 57 cm^{-1} split in the vibration is supposed to arise through coincidence and consequent resonance[10] of this mode with one of the overtones $2\nu_7$, or $2\nu_{10}$. It is difficult at this time to imagine another explanation for the appearance of such an intense pair of lines in this region; yet a resonance splitting of 421 cm^{-1} seems so abnormally large that we make this assignment only tentatively.

The frequency 2489 cm^{-1} might be tentatively assigned to ν_{11} in analogy with the assignment[11] of the line of $C_2H_6(g)$ at 2940 cm^{-1}; the latter assignment is confirmed by the appearance of the rotation lines associated with it which were observed by Lewis and Houston.[8] The meaning of the remaining frequencies is uncertain; a knowledge of the infra-red frequencies would probably help in assigning them.

[7] P. Daure, Ann. de physique **12**, 375 (1929); Glockler and Renfrew, J. Chem. Phys. **6**, 295 (1938).
[8] Bhagavantam, Ind. J. Phys. **6**, 596 (1931); Lewis and Houston, Phys. Rev. **44**, 903 (1933).
[9] B. L. Crawford, Jr. and J. T. Edsall, private communication of unpublished results.
[10] E. Fermi, Zeits. f. Physik **71**, 250 (1931).
[11] Bartholomé and Karweil, Zeits. f. physik. Chemie **B39**, 1 (1938).

The Force Constants

With the assignment of the three parallel frequencies ν_1, ν_2, ν_3, and Howard's formulae[6] for the normal modes of vibration derived from a valence force potential function it is possible to calculate the force constants of the molecule. We obtain 3.0×10^5 dynes/cm for K_1 associated with stretching the B−H bond, 0.26×10^5 dynes/cm for K_2 associated with bending the B−H bond and 3.6×10^5 dynes/cm for K_3 associated with stretching the B−B bond and determined principally by ν_1. The two B−H force constants are in satisfactory agreement with the B−H force constants in the triborine triamine molecule $B_3N_3H_6$ in which the B−H stretching constant is 3.42×10^5 dynes/cm and the B−H bending constants are 0.35 and 0.23×10^5 dynes/cm for the planar and out-of-plane bending, respectively.[9]

TABLE II. *Raman Frequencies of* B_2H_6, C_2H_6, *and* Si_2H_6.

$B_2H_6(l)$	$C_2H_6(l)$[7]	$C_2H_6(g)$[8]	$Si_2H_6(g)$[5]
792.5(5)			
806.2(4)	979(1)		
821.4(3)	994(10)	993(10)	435(7)
1180.4(2)	1463(5*d*)	1344(0)	910 to 955 (2)
		1460	
	2733(2)	2744(2)	
	2768(2)	2778(0)	
2102(10)	2884(10)	2899(10)	
2489(3)	2922(1*d*)	2940(1)	2163(10)
2523(10)	2941(10)	2955(10)	
2775(3)	2963(1*d*)	2969	
2868(2)		2979	
3120(2)		2989	
		2999	
		3009	

Intramolecular Forces in B_2H_6, C_2H_6, and Si_2H_6

A comparison of the internuclear distances for B_2H_6 and analogous molecules as calculated from the force constants and Badger's rule[12] with the

[12] *a*, R. M. Badger, J. Chem. Phys. **2**, 128 (1934); *b*, **3**, 710 (1935).

TABLE III. *Comparison of internuclear distances calculated from force constants and those observed by electron diffraction.*

COMPOUND	K_3 (DYNES/CM $\times 10^{-5}$)	R (CALC.) (A)	R (OBS.) (A)	R(OBS.) $-R$(CALC.) (A)	K_1 (DYNES/CM $\times 10^{-5}$)	r (CALC.) (A)	r (OBS.) (A)	r(OBS.) $-r$(CALC.) (A)
B_2H_6	3.57	1.48	1.86[2]	0.38	3.0	1.19	1.27[2]	0.08
C_2H_6	5.62	1.37	1.55[13]	0.18	4.79	1.06	1.09[13]	0.03
Si_2H_6	1.7	2.13	2.32[14]	0.19	—	—	—	—

internuclear distances as measured by electron diffraction, leads to interesting indications concerning intramolecular forces. In Table III are given in column II the values of the force constants K_3 for the B−B, C−C, and Si−Si bonds in the compounds B_2H_6, C_2H_6, and Si_2H_6 listed in column I. The corresponding internuclear distances R calculated from Badger's rule are given in column III for comparison with the values from electron diffraction given in column IV; differences between observed and calculated values are given in column V. Columns VI, VII, VIII, and IX contain the values for the B−H and C−H force constants K_1, the calculated distances r, the observed distances, and the differences between observed and calculated distances, respectively.

The fact that the calculated values of R are much smaller than the observed values for all three compounds strongly suggests that the bonds between the central atoms are compressed, in analogy with Badger's association[12b] of the apparent stretching of the bonds in tetrachlorides and hexafluorides by repulsion between halogen atoms. If the magnitude of the compressional forces indicated here depend upon the internal angle, internal rotation would be hindered.

The results for the central atom-hydrogen distances indicate that these bonds, too, are under compression. An effective attraction between hydrogen atoms of one CH_3 group in ethane with the C−H bonding orbitals of the other group possibly arising through consideration of the terms suggested by Penney[15] might give rise to just such compressional forces.

Any such attraction between hydrogen atoms would give the molecule a plane of symmetry perpendicular to the central bond (D_{3h}) rather than a center of symmetry (D_{3d}). In fact Bartholomé and Karweil[11] recently have obtained an infra-red spectrum for ethane which they could interpret using D_{3h} selection rules, but not with D_{3d} selection rules. They concluded that ethane has a plane of symmetry perpendicular to the C−C bond rather than a center of symmetry.

It is difficult at this time to make an estimate of the magnitude of the restricting potential,[16] or the magnitude of the dependence of the compressional forces on the internal angle.

THE STABILITY OF DIBORANE

Since the heat of formation is known[17] and it is now possible to calculate an approximate value for the entropy, it seems desirable to discuss the stability of diborane at this time. From electron diffraction results[2] the moments of inertia are calculated to be $A=B=55.2\pm2.0$ and $C=14.3\pm0.5\times10^{-40}$ g cm^2, on the assumption of tetrahedral distribution of bonds about boron atoms. The contribution of rotation and translation to the entropy of the gas at 25°C is thus 50.94 ± 0.1 cal./deg. including the symmetry term with the symmetry number equal to 18. The maximum contribution of internal rotation is 3.26 cal./deg. for no restricting potential, $V_0=0$, while for $V_0=3000$ cal. the contribution would be about 2.0 cal./deg.[18] A safe estimate of this contribution would probably be 2.4 ± 0.8 cal./deg. We have calculated the approximate values for the missing frequencies using Howard's formulae[6] and from them find

[13] Pauling and Brockway, J. Am. Chem. Soc. **59**, 1223 (1937).
[14] Brockway and Beach, J. Am. Chem. Soc. **60**, 1836 (1938).
[15] W. G. Penney, Proc. Roy. Soc. **A144**, 166 (1934).

[16] American authors favor a value of 3000 cal. in the case of ethane (see Kistiakowski, Lacher, and Stitt, J. Chem. Phys. **6**, 407 (1938) for references) while Eucken and coworkers estimate the height of the barrier to be about 350 cal. (W. Hunsmann, Zeits. f. physik. Chemie **B39**, 23 (1938)).
[17] Roth and Börger, Ber. **70**, 48 (1937).
[18] K. S. Pitzer, J. Chem. Phys. **5**, 469 (1937).

the contribution of vibration to the entropy to be only 1.9 ± 0.6 cal./deg., allowing a wide margin of uncertainty for the missing frequencies. We thus have the approximate value of 55.3 ± 1.5 cal./deg. for the entropy of $B_2H_6(g)$ at 25°.

The heat of formation of $B_2H_6(g)$ from the elements has recently been determined to be $44{,}000\pm3000$ cal.[17] We may make an estimate of the entropy of solid boron and write the following equations:

$$\begin{aligned} 2B(s)+3H_2(g) &= B_2H_6(g), \\ S^*_{298.1},\ H_2(g) &= 31.23 \text{ cal./deg.}, \\ S^*_{298.1},\ B(s) &= 4\pm1 \text{ cal./deg.}, \\ S^*_{298.1},\ B_2H_6(g) &= 55.3\pm1.5 \text{ cal./deg.}, \\ \Delta S^\circ_{298.1} &= -50.4\pm3.5 \text{ cal./deg.}, \\ \Delta H_{298} &= -44{,}000\pm3000 \text{ cal.}, \\ \Delta F^\circ_{298} &= -30{,}000\pm4000 \text{ cal.} \end{aligned}$$

The uncertainty in the entropy of diborane is indeed rather large, but it is to be pointed out that this uncertainty can at most lead to an error of only 1000 cal. in the standard free energy while the uncertainty in the measured heat of formation is estimated[17] to be 3000 cal. The total of 4000 cal. uncertainty in the free energy cannot possibly invalidate the following conclusions regarding the stability of diborane.

Namely, at room temperature diborane is stable with respect to decomposition into the elements and will not begin to decompose into the *elements* until about 500°C. Actually this process is not analytically complete short of 700°. It is well known, however, that diborane is unstable at room temperature and above, decomposing to form other hydrides in a complicated set of reactions:

$$\begin{aligned} B_2H_6(g) &\xrightarrow{25^\circ} B_4H_{10}+B_5H_{11}+B_6H_{10} \\ &\quad +B_8H_x+\cdots+H_2(g) \\ &\xrightarrow{100^\circ} \text{white solid}+\text{yellow solid}+\text{yellow oil} \\ &\quad +B_5H_9+B_{10}H_{14}+H_2 \\ &\xrightarrow{200^\circ} \text{brown solid}+H_2(g) \\ &\xrightarrow{700^\circ} B(s)+H_2(g). \end{aligned}$$

It will, of course, be impossible to relate the stability of diborane with respect to these products without a knowledge of their thermodynamic properties.

We are indebted to Professor H. I. Schlesinger for the use of large amounts of diborane prepared with his material aid. We are also grateful to members of the staff of the California Institute of Technology for the use of equipment to evaluate the plates.

The Variation of the Raman Spectrum of Nitrate Solutions with Cation

ELIZABETH R. LAIRD AND FRANCES M. PLESSET*
Department of Physics, Mount Holyoke College, South Hadley, Massachusetts

(Received July 29, 1938)

The strong Raman line from solutions of cadmium, silver and lead nitrates has been remeasured at varied concentrations, and the results of Grassmann confirmed, namely that the frequency shift diminishes with increasing concentration for lead and silver, and varies little for cadmium. A qualitative explanation of this behavior and that of sodium nitrate is suggested in the effect of the cations on the structure of water, and attention is drawn to the similar order of these nitrates in x-ray diffraction phenomena.

THE Raman effect in solutions of nitrate has been studied by a number of observers, and from various standpoints. One of these has been the question of the dependence of the magnitude of the frequency shift on concentration, cation, and temperature. Gerlach[1] found for $NaNO_3$ and $LiNO_3$ slight, barely measurable, increases in the frequency shift with concentration, but larger changes in various nitrate crystals. Grassmann[2] found variations in both directions, depending on the cation. Franklin[3] confirmed the increase in frequency shift for $NaNO_3$ solutions from 1048.0 ± 1 cm^{-1} at 1.25 N to 1050 cm^{-1} at 8 N and to 1068 cm^{-1} in the crystal. On the other hand, a change of 12.5 cm^{-1} reported by Embirikos[4] for solutions of magnesium sulphate was not confirmed by Woodward and Horner[5] nor by Coon.[6] It seemed, hence, worth while to repeat some of Grassmann's experiments, and for this the nitrates of silver, cadmium, and lead were chosen.

The source of illumination was a glass mercury arc, the spectrograph a Hilger D78, the Raman tube of the jacketed horn form, with the horn and the circle around the window painted black. It was placed under the arc, and so that the light scattered from the farthest portion would just fill the collimator lens of the spectrograph without use of lens between the tube and slit. Water was ordinarily used in the jacket, but for some of the long exposures a solution of praseodymium neodymium sulphate was used as filter. Times of exposure varied from three hours to thirty. The slit width was such as to give a slit image somewhat narrower than the Raman line. An iron arc comparison spectrum was put on most of the plates at the end of the exposure.

Measurements were made on a Hilger measuring micrometer. Earlier experience had shown that the use of a comparison iron arc in determining wave-lengths was unsatisfactory, as shifts between this spectrum and the unmodified Hg lines sometimes appeared. These were suspected to be due to changes in temperature or barometric pressure during exposure. The room temperature was controlled by a thermostat, and thermograph records showed a variation of less than 2°F, but there was no way of controlling the pressure. While the effect of variations in pressure and temperature on the mercury lines would be to broaden them, but not to shift the relative center of gravity by a measurable amount, the iron spectrum put on in a few seconds might be measurably shifted, and by different amounts at different parts of a plate. Hence it was decided to use the mercury lines only, with the Hartmann formula, in computing, and to make a correction curve for the Hartmann formula from some test plates where both the mercury and iron spectra were recorded with short exposures. Any slight error in determining this correction would affect all the measurements equally, and not alter comparative values. During the progress of the work the paper of Teal and MacWood[7] appeared giving data on the effect of changes in barometric pressure even

* Skinner Fellow in Physics, 1935–36.
[1] Gerlach, Ann. d. Physik **5**, 196 (1930).
[2] P. Grassmann, Zeits. f. Physik **77**, 616 (1932).
[3] Franklin and Laird, Phys. Rev. **45**, 738 (1934).
[4] Embirikos, Zeits. f. Physik **65**, 266 (1930).
[5] Woodward and Horner, Proc. Roy. Soc. **144**, 129 (1934).
[6] Coon and Laird, Phys. Rev. **47**, 889 (1935).
[7] Teal and MacWood, J. Chem. Phys. **3**, 760 (1935).

over a period of three hours. The mercury lines 4916.0A, 4339.23A, and either 4108.08A or 4077.83A were used as standards. The deviations of the other mercury lines measured as checks were of the order of 0.03A.

The results reduced to vacuum are shown in Table I; they have been computed from measurements on the strong Raman line excited by the Hg line 4358A. The corresponding line excited by 4047A was also measured but the accuracy was not so great. The dispersion in the neighborhood of 4566A is 25A/mm. The table of wave-number differences compiled by P. L. Bayley was used in checking. All but one of the silver nitrate plates were measured twice, and all but three of the lead plates, the $\frac{1}{2}N$ lead plates were measured four or more times on different days and at different points on the lines. The average was taken for each plate as the measurement of that plate, and the deviations shown are the deviations of these from the final average. In the case of lead nitrate there is also shown the average deviation of the separate measurements. The last column shows Grassmann's values.

It will be seen that in a general way the results are in agreement with those of Grassmann. His assumption that for silver nitrate the shift increases with dilution is confirmed, and it is shown that for cadmium nitrate the shift, if any, is very slight. For lead nitrate the variation found looks smaller than his, but the difference is within the sum of the estimated errors. Combining these results with those obtained earlier for sodium nitrate, one may arrange the four nitrates in the order sodium, cadmium, silver, lead, in that the effect of increasing concentration is with sodium to slightly increase the shift of the Raman line, with cadmium to change it very slightly if at all, and with silver and lead to diminish it, possibly more for the lead at the same concentration of the cation, also, the difference between the frequency shift in the crystal and in the dissolved state is larger for sodium nitrate than for cadmium nitrate, and for lead and silver is questionable.

In the observations of Prins[8] on x-ray diffraction by nitrate solutions a somewhat parallel order is found. Prins distinguishes the cases where a diffraction ring is found, the diameter of which increases with concentration, and inside of which, the diffraction diminishes as the angle approaches 0°, and the cases where the position of maximum diffraction does not change with concentration. He finds a mobile maximum in the case of cadmium nitrate but not for either lead or silver nitrates. He attributes the mobile ring to a kind of super-arrangement of the heavy ion, and the lack of it to an irregular gas-like distribution. Sodium is too light in comparison with the other atoms present for the method to be applied with success, and Prins found no small angle scattering of importance for sodium nitrate solution, but a pattern which he attributed to an arrangement that the water molecules assume in the electric field of the cations. As he notes that the phenomenon of super-arrangement decreases in the series K, Rb, Cs, one might infer that it would be large for sodium, although the experimental method does not show it directly.

Prins attributed the lack of superarrangement in the case of lead and silver to nondissociated molecules. One finds no support for this in the electrolytic conductivities of these nitrates, and measurements of the intensity of the Raman line at different concentrations by several observers has shown that for sodium, cadmium, and lead nitrates it is proportional to the concentration of the NO_3 ion. It has been argued that this is not an evidence of dissociation as the NO_3 constituent would be present in either case. But as in all cases the frequency shift in the crystal is different from that in the dilute solution, there should also be a difference for light scattered from associated

TABLE I.

SUBSTANCE	NORMALITY	NO. PLATES	$\Delta\nu$ IN CM^{-1}	$\Delta\nu$ IN CM^{-1} GRASSMANN
$Pb(NO_3)_2$	4	5	1044.1±0.4±0.6	1043.8±0.6
	2.7			1046.0
	2	5	1045.7±0.6±0.9	
	1	2	1045 ±1	
	0.5	3	1046.7±0.4±1.0	1048.0±1.0
Crystals		1	1044.3	1045
$AgNO_3$	7	2	1043.2±0.1	1042.3±0.8
	3	4	1045.4±0.4	
	1	2	1046.1±0.4	
Crystals				1045 (Gerlach)
$Cd(NO_3)_2$	8	4	1047.4±0.3	1047.4±0.4
	2	3	1047.7±0.3	
$Cd(NO_3)_2 \cdot 4H_2O$ Crystals		1	1052.2	

[8] Prins, J. Chem. Phys. **3**, 72 (1935); Physica **3**, 1016 (1935).

molecules. The photometric curves of the Raman lines from the concentrated solutions appear however those of single lines. If one concludes that dissociation is complete, one may still find in the ideas concerning the structure of water of Bernal and Fowler,[9] used also by Prins, a qualitative explanation of the difference with respect to Raman scattering between the behavior of the nitrates of sodium and cadmium on the one hand and silver and lead on the other. The sodium and silver ions are singly charged, but the sodium being smaller exerts a greater influence in maintaining or increasing a certain regularity in structure in the water. The cadmium and lead ions are doubly charged, so that although the cadmium ion is as large as silver it produces an effect more like that of sodium, but the still larger lead ion again has a smaller directing effect, and its presence may lead to a weakening of the structure. This might be tested in a study of the water bands of small frequency shift referred to by Hibben[10] as surely due to intermolecular interaction.

The NO_3 ion is considered to be plane, with the nitrogen at the center of an equilateral triangle, and the oxygen atoms at the corners. The Raman line studied here is ascribed to the radial vibration. The effect of the cations on this vibration would be indirect according to the point of view suggested here. Where there is a superarrangement of the cations, there are crystal-like groupings of molecules, and the symmetry makes for a higher vibration frequency, but if the water structure is weakened, and the cations are more at random, the central forces in the NO_3 ion may be weakened, and the frequency lowered.

Our thanks are due to Dorothy Franklin, who assisted considerably in measuring the plates.

[9] Bernal and Fowler, J. Chem. Phys. **1**, 515 (1933).

[10] Hibben, J. Chem. Phys. **5**, 166 (1937).

OCTOBER, 1938 JOURNAL OF CHEMICAL PHYSICS VOLUME 6

Temperature Scale and Thermionic Emission from Rhodium

H. B. WAHLIN AND L. V. WHITNEY
Department of Physics, University of Wisconsin, Madison, Wisconsin

(Received July 5, 1938)

When rhodium is heated to incandescence in an atmosphere of air or oxygen, a coating forms on its surface. This is shown by a change in the emissivity. When the temperature is increased sufficiently this coating suddenly disappears, and when the temperature is lowered it reappears. This coating is probably an activated adsorption of oxygen, or an oxide of rhodium. It is found experimentally that the temperature and partial oxygen pressure at which the coating disappears are related by the Clausius-Clapyron equation:

$$(d \log_e P)/dT = L/RT^2.$$

P is the partial oxygen pressure, T the absolute temperature, and L the heat of vaporization of the surface. The electron work function of a clean rhodium surface is found to be $\varphi = 4.80$ volts, and $A = 33$ amp./cm²/degree².

Emissivity and Temperature Scale

THE peculiarities of rhodium surfaces described below were first encountered when measurements of spectral emissivity were being taken.[1] A specimen of rhodium in the shape of a V wedge 6 cm long, 4 mm wide on a side, and about 0.04 mm thick was mounted inside a brass chamber which was evacuated to a pressure of $1\text{–}2\times10^{-6}$ mm. The true temperature was measured by an optical pyrometer sighted inside the wedge, and the apparent temperature by another pyrometer sighted on the outside surface.

A typical sequence of readings is shown in Fig. 1. When the temperature was first raised, a series of values shown by the lower curve was found. Upon lowering the temperature there was

[1] L. V. Whitney, Phys. Rev. **48**, 458 (1935).

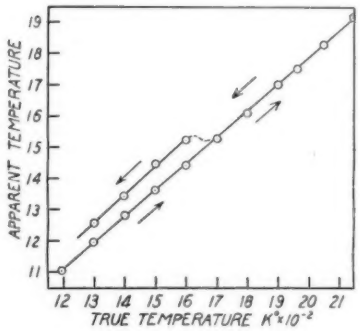

FIG. 1.

a sudden shift to the upper curve. The emissivity as calculated from points of the lower curve ranged from about 0.22 to 0.29 for $\lambda = 6698$A; that from points of the upper curve was about 0.60. High emissivities were always found with this chamber at low temperatures after the temperature had once been raised beyond the transition point, the initial low emissivities at low temperatures never being found again after the first set of readings. The change from one curve to the other was always abrupt. If the temperature were being raised slowly, a critical point would be reached at which the emissivity would change and the true temperature flash up 100 to 150 degrees. The sudden rise in temperature was due to the fact that a low emissivity surface replaced the high emissivity surface.

It was difficult to take readings in the neighborhood of the critical point, and a shorter wedge, about 13 mm long, was therefore substituted. Because of the steep temperature gradient along this wedge, it was possible to have the center hot enough to show a low emissivity while the extremities showed a high emissivity. Figs. 2 to 5 are photographs of this wedge at various temperatures.

Figure 2 shows the outer surface of the wedge below the critical point, after it had previously been conditioned above it. The apparent temperature at the center is about 1500°K, and the surface has a high emissivity. Fig. 3 shows the wedge when the apparent temperature at the center is about 1790°K; this center part has low emissivity, while high emissivities obtain nearer the ends. Fig. 4 shows the appearance of the wedge when the temperature was slightly lower than it was in Fig. 3; the central low emissivity region is shorter. Fig. 5 shows the inside of the wedge when the outside had the appearance of Figs. 3 and 4.

Figure 6 shows the same wedge after it had burned out. Five zones are distinguishable. The central zone had a blue appearance when cold, but at the time of burning out it had low emissivity characteristic of temperatures above the critical point. Zones adjacent to the center

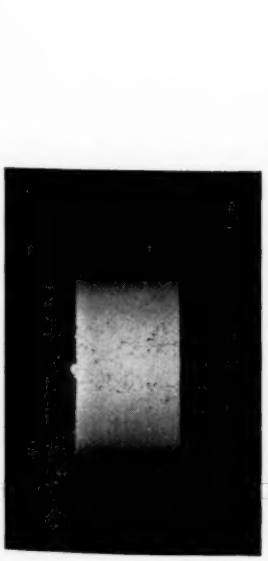

FIG. 2.

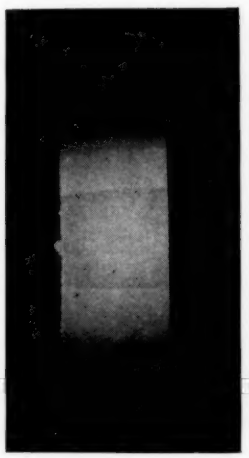

FIG. 3.

FIG. 4.

FIG. 5.

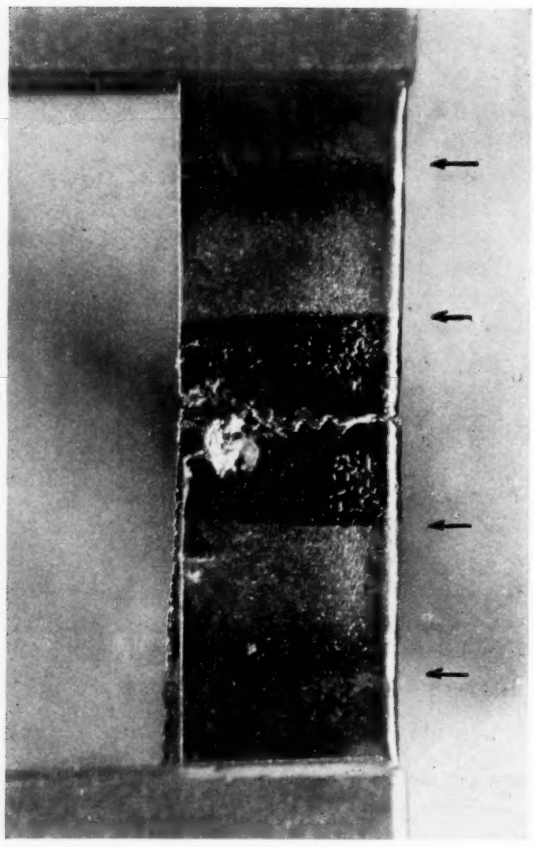

FIG. 6.

had high emissivity, and the top and bottom zones low emissivity. (These last zones are not as clearly marked as the others and are not visible in Figs. 3 and 4.) These end zones had never become hot enough to pass the critical point and thus had kept their initial low emissivity throughout the experiment. X-ray pictures taken of the high and low emissivity surfaces showed no crystalline differences in the metal.

Further investigation showed that prolonged outgassing affected the temperature of the critical point. This indicated a surface layer dependent on the temperature and pressure conditions. The brass chamber was therefore discarded and a study made of this effect in an all Pyrex system where better vacuum conditions could be obtained. At high vacua (2×10^{-8} mm) the effect disappeared entirely, and the low emissivity 0.242, corresponding presumably to the clean metal surface, was obtained at all temperatures. The temperature scale for this emissivity and for a wave-length of 6698A is given in Table I.

When air was introduced into the system the transition phenomenon immediately reappeared. This suggests very strongly that the high emissivity surface is covered by a surface layer which disappears at high temperature. Readings were taken of the temperatures of the critical point for various pressures of air, oxygen, nitrogen, and hydrogen. There was a marked difference between these results in Pyrex glass and those obtained in the brass chamber; the pressures necessary to obtain the transition in the all-Pyrex system were greater by a factor of 10^6 or more. Perhaps the wax, which was used in sealing the brass chamber together, saturated the atmosphere about the hot filament and acted similar to a catalytic agent. When wax was purposely introduced into the Pyrex system the layer formed at lower pressures, but it is questionable whether conditions duplicated those inside the brass chamber.

Figure 7 shows the transition temperatures obtained when gases were introduced into the Pyrex system. It is evident that the temperature of breakdown of what is apparently a surface layer is a function of the partial oxygen pressure, since the readings for air reduced to partial oxygen pressures fall on the curve found for pure oxygen. The readings for nitrogen indicate a small oxygen content, but the temperatures of the transition point were so low they could not be read accurately. No surface layer appeared when hydrogen was introduced into the system.

Figure 8 is a graph of the logarithm of the oxygen pressure to the base e plotted against the reciprocal of the transition temperature. The

TABLE I.

TRUE TEMPERATURE	APPARENT TEMPERATURE
1200°K	1111°K
1300	1197
1400	1282
1500	1365
1600	1447
1700	1528
1800	1609
1900	1689
2000	1768
2100	1847

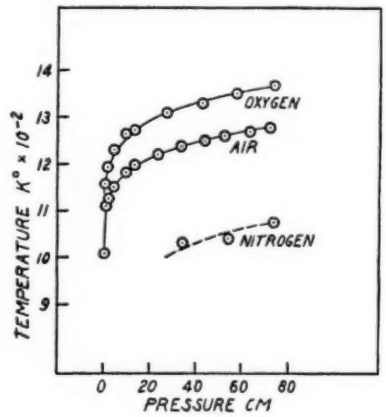

FIG. 7.

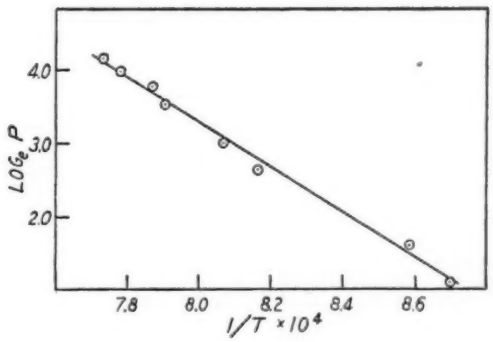

FIG. 8.

equation of this line is

$$\log_e P = -L/RT + b,$$

and the slope gives the value of L/R. The heat of vaporization of the surface, (L), was found from this graph to be 6.15×10^4 calories per g mole.

THERMIONIC EMISSION

A straight strip of rhodium 3 mm wide, 0.07 mm thick, and 10 cm long was mounted in a conventional type two-guard ring tube such as that described by Wahlin and Reynolds.[2] The tube was evacuated and the glass baked for 700 hours. During this baking the temperature of the filament was gradually raised to a value above the transition point. As soon as the furnaces were removed a thermionic determination was made. The Richardson plot showed a definite break at the transition point, the low temperature slope being the greater and corresponding to a work function higher by 3/10 volt. The high temperature portion of the plot gave a work function slightly greater than that of a clean surface. Continued heat treatment at a temperature above the transition point caused the break to disappear gradually and after 1100 hours the values $\varphi = 4.80$ volts, $A = 33$ amp./cm^2 degrees^2 were obtained. At this time a final pressure of 2×10^{-8} mm was reached. Additional heat treatment for 500 hours caused no further change. Two other specimens of rhodium gave the same values.

This value of the work function is not in agreement with that reported by Dixon.[3] He observed, however, an abnormal variation of the work function with temperature which can best be explained as due to incomplete outgassing. He also found definite changes in the thermionic properties of the metal at 1100°C, which he attributed to a change in the structure of the metal. In view of the x-ray findings reported here, such a conclusion seems untenable.

This project was supported in part by a grant-in-aid from the Wisconsin Alumni Research Foundation.

[2] H. B. Wahlin and J. A. Reynolds, Phys. Rev. **48**, 751 (1935).

[3] E. H. Dixon, Phys. Rev. **37**, 60 (1931).

The Diffusion of Hydrogen Through Nickel

C. B. Post, *The Carpenter Steel Company, Reading, Pennsylvania*

AND

W. R. Ham, *Department of Physics, The Pennsylvania State College, State College, Pennsylvania*

(Received July 20, 1938)

The diffusion of hydrogen through commercial and very pure anode nickel has been studied in a precision manner throughout the temperature interval 1100° to 150° Centigrade. It was found that the diffusion rates vary in a perfectly regular manner throughout this region, except for a discontinuity at the Curie point, namely near 360°C.

A very exact agreement with the formula $R=AT^{z}p^{y}\times\exp(-b/T)$ was found in all cases. After long heat treatment with hydrogen the value of y in the above equation for anode nickel becomes $+0.50\pm0.01$ with the possible exception of a region within 3° of the Curie point. All the nickel used had isotherms whose slope at the start of observations was a maximum in the Curie region and markedly greater than 0.5, but which approached 0.5 as the heat treatment, ordinarily considered as having a decarburizing effect, progressed.

The magnetic transition as shown by diffusion is abrupt, the isobars below the Curie region being quite as straight as above. There is always a sudden drop in the value of b as calculated from the simple equation $R=A\exp(-b/T)$ at the Curie point, the value changing in the purest nickel from 6600 to 5800 with rising temperature. No systematic breaks appear in the isobars at high temperatures, such as found in pure iron, but nevertheless the value of z indicates that the diffusing hydrogen possesses appreciable energy within the lattice.

The Curie region shows marked hysteresis, and is similar to the Curie region of pure iron in this respect.

Existing theories of ferromagnetism seem to require modification, inasmuch as the Curie transition in nickel appears to take place about as abruptly as the body-centered-face-centered transition in iron. The loss of magnetism at the Curie transition is essentially an atomic phenomenon and should not be associated primarily with conditions in aggregates of atoms or atomic domains. During the transformation for a finite time, there appears to be an additional electron in the valence shell of some nickel lattice points.

A possible description of the process of the change from the ferromagnetic to the paramagnetic condition in the transition elements is that an electron is moved from the $3d$ shell to one of the 4 levels, followed more or less quickly by a drop of another 4-level electron back to such a $3d$ level as to result in the pairing of electron spins in the $3d$ shell.

THE diffusion of hydrogen through metals at high temperatures has been studied quite extensively during the past several years in the Pennsylvania State College laboratories. The data for iron have been published,[1] and in view of the anomalies found in the diffusion rates of hydrogen through iron, it was felt that a precision study of the diffusion of hydrogen through nickel would be justified. This study would have the double purpose of showing whether such a series of breaks in the diffusion isobars as found in iron exists in the isobars for hydrogen through nickel (incidentally this would also show whether the series was due to peculiarities of the apparatus), and also show the applicability of the steady-state method (I) to a precision study of hydrogen through nickel. Several other sets of data on the diffusion of hydrogen through nickel are available from the Pennsylvania State College laboratories, namely Craninsky[2] and Ham.[3] The technique has been improved from that used to obtain these two sets of data, especially the temperature control, therefore we may expect an improvement in the data for nickel. In this precision study by both the trapping and steady-state[1] methods, we have used exactly the same apparatus, with the exception of the metal disk used for diffusion, as in I.

The diffusion rates were found to be very regular and to obey exactly the diffusion formula,[4]

$$D=AP^{\frac{1}{2}}T^{\frac{1}{2}}\exp(-b/T) \qquad (1)$$

where P is the pressure exerted by the gas on the ingoing side, T the temperature in absolute degrees, and b the so-called work function. A is a

[1] C. B. Post and W. R. Ham, J. Chem. Phys. **5**, 913 (1937), hereafter referred to as (I).

[2] Craninsky, Thesis for M.S. degree, Pennsylvania State College (1932). See also Fig. 4, this article.

[3] W. R. Ham, Am. Soc. Metals, **25**, 536–564 (1937).

[4] Richardson, Nicol, and Parnell, Phil. Mag. **8**, 1-29 (1904).

constant and D is the rate of hydrogen diffusion measured in cubic centimeters of hydrogen per square centimeter area per mm thickness at standard pressure and temperature.

The Curie point in nickel is easily recognized when the steady-state method (I) is used as a precision measure of the diffusion rates. Moreover the hydrogen diffusion rates obey the same sort of formula below the Curie point as above, consequently we can interpret the offset at the Curie point as an indication of demagnetization. The fact that the law governing the diffusion rates is the same below the Curie point as above indicates that the disappearance of magnetism is a relatively abrupt phenomenon when no field is present in the specimen and the effect is brought about entirely by temperature effects.

A marked hysteresis effect is noted at the Curie point when this transition is measured by hydrogen diffusion methods. This indicates that some of the transitions in the individual nickel atoms which are responsible for the loss of magnetism must be governed by some sort of "order-disorder" rearrangement as developed by Bragg and Williams[5] and extended by Fowler.[6] A possible mechanism for the demagnetization of nickel will be discussed in a later paragraph.

Isotherms were obtained above and below the Curie point. The variation of the slope of the isotherms was found to be regular above and below this point, that is, for commercial nickel the slopes varied from a value of 0.5 about 150° above the Curie point to a value of 0.56 at the Curie point (370°C) and decreased to 0.5 again about 50° below this point. A similar variation was observed with pure anode nickel except that prolonged treatment of this nickel by the diffusing hydrogen gas gradually eliminated the variation in slope from 0.5, except in a possible region within 3° of the Curie point (359.2°C). Such a variation is difficult to explain in terms of Smithells and Ransley's[7] application of the Langmuir absorption isotherm to deviations of the pressure exponent from $+\frac{1}{2}$, but can be explained from an extension of Ham's discussion of the effect of carbon in solution in iron.

[5] Bragg and Williams, Proc. Roy. Soc. **151A**, 540 (1935); **145A**, 699 (1934).
[6] R. H. Fowler, Proc. Roy. Soc. **149A**, 1 (1935); **151A**, 1 (1935).
[7] Smithells and Ransley, Proc. Roy. Soc. **150A**, 172 (1935).

Experimental Procedure

The apparatus used in this research has been previously reported in I, and is shown here in Fig. 1. Exactly the same procedure was used in studying the diffusion rates by use of the steady-state method as reported in I.

As explained in I, the steady-state method is characterized by having a stopcock barely open to the pumps on the vacuum side of the diffusing disk. This enables a small back pressure to be built up between this stopcock and the diffusing disk, which can be conveniently read on a McLeod gauge. As shown in I, this back pressure is directly proportional to the rate as determined by the trapping method (see Fig. 2, I). We must also mention the fact that the success of this method depends to a large extent upon having a system of very fast pumps to maintain a high vacuum on the pumping side of the stopcock.

The same temperature control was used as reported in I, *viz.*, a photoelectric cell relay.

The melting point of a pure silver bead furnished by the National Bureau of Standards was noted by means of a telescope, and the thermocouples standardized without disturbing their position. The silver bead holder was manipulated by magnets outside the apparatus.

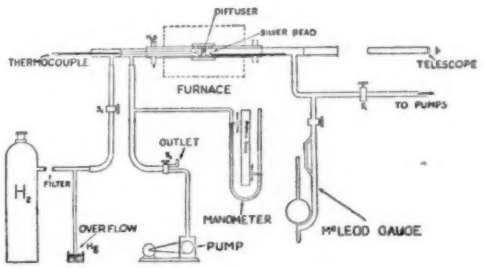

FIG. 1. Apparatus for measuring gas diffusion through metals.

Diffusers were prepared by welding the nickel diffusing disk to nickel tubes by atomic hydrogen welding as described in I.

Isotherms were obtained by operating the pump on the hydrogen inlet side of the diffuser. By manipulating the opening to this pump and the opening into the diffuser any convenient partial pressure of the hydrogen can be obtained from atmospheric down to 0.5 cm Hg. The logarithm of the rate was plotted against the log

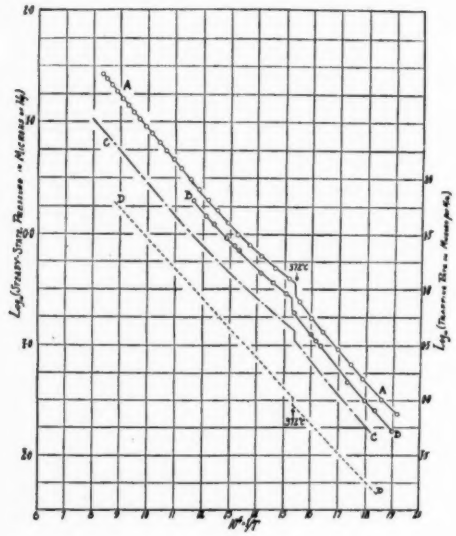

FIG. 2. Diffusion of hydrogen through commercial nickel. Sample XIII. 53 mil. AA, $\log_{10}$ (steady-state rate) *vs.* $1/T$; BB, $\log_{10}$ (trapping rate) *vs.* $1/T$; CC, $\log_{10}$ (steady-state rate) $-\frac{1}{2}\log_{10} T+1$ *vs.* $1/T$, DD, $\log_{10}$ (steady-state rate) $-\frac{1}{2}\log_{10} T-y\log_{10} P$ (in mm) $+1$ *vs.* $1/T$.

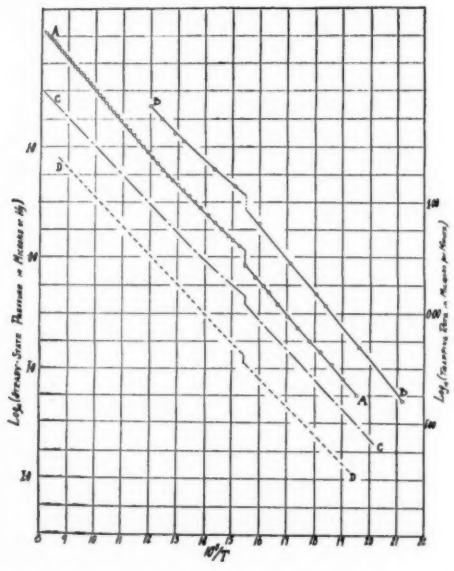

FIG. 3. Diffusion of hydrogen through commercial nickel. Sample XII. 38 mil. AA, $\log_{10}$ (steady-state rate) *vs.* $1/T$; BB, $\log_{10}$ (trapping rate) *vs.* $1/T$; CC, $\log_{10}$ (steady-state rate) $-\frac{1}{2}\log_{10} T+1$ *vs.* $1/T$; DD, $\log_{10}$ (steady-state rate) $-\frac{1}{2}\log_{10} T-y\log_{10} P$ (in mm) $+1$ *vs.* $1/T$.

of the pressure and the slope taken to determine the value which we designate as the "slope of the isotherm."

Trapping methods were also used to establish the value of the diffusion rate in cubic centimeters of hydrogen at standard pressure and temperature diffusing through the disk per square centimeter area per millimeter thickness. These trapping rates also served to establish the proportionality factor between these rates and the rates as determined by the steady-state readings.

EXPERIMENTAL RESULTS

Figures 2 and 3 show the diffusion rates of hydrogen through commercial nickel plotted as

$$\log_{10}(\text{steady-state rate}) \text{ vs. } 1/T, \tag{2}$$

$$\log_{10}(\text{trapping rate}) \text{ vs. } 1/T, \tag{3}$$

$$\log_{10}(\text{steady-state rate}) -\tfrac{1}{2}\log_{10} T \text{ vs. } 1/T, \tag{4}$$

$$\log_{10}(\text{steady-state rate}) -\tfrac{1}{2}\log_{10} T-y\log_{10} P \text{ (in mm)} +1 \text{ vs. } 1/T. \tag{5}$$

Note that the successive corrections applied by subtracting $\frac{1}{2}\log_{10} T$ and $\frac{1}{2}\log_{10} T+y\log_{10} P$ straighten out these curves in a surprising manner.

The various values of the constants used in several types of diffusion formulae are given in Table I for these two samples.

Figure 5 shows the logarithm of the diffusion rate of hydrogen through anode nickel* plotted against the reciprocal of the absolute temperature. Fig. 5 also shows the variation of the isotherm slope as a function of T before the sample has been completely purified by the diffusing hydrogen. Note that the maximum occurs at the Curie point within our experimental error. These slopes of the isotherms appear in the diffusion equation as P^y, where y is the value of the isotherm slope as described in experimental procedure. Table II shows the constants in several types of diffusion equations for anode nickel.

After several months running this sample of anode nickel showed that the variation of the isotherm slopes from 0.5 was not as great as that shown in Fig. 5. It was found that the slopes

* This anode nickel was kindly furnished by the International Nickel Co. According to information received from their laboratories this is the purest nickel they have been able to make up to the present time. Complete chemical analyses of this type of nickel are not available, but we have been assured that this metal is at least 99.99 percent pure.

remained 0.5 within 10° of the Curie point and then showed a slight variation to about 0.53 at the Curie point.

A new sample of anode nickel 42 mils in thickness was installed and after several months running with hydrogen diffusing through the sample it was found that the deviation of the isotherms from the 0.5 law (i.e., $R \propto P^{\frac{1}{2}}$) apparently occurs only near the Curie point and there is no variation from 0.5 except possibly within 3° above this point. Fig. 6 shows the log of the rates plotted against $1/T$ for this sample in the neighborhood of the Curie point. A small variation is apparent in the region directly above the temperature 360°C.

A very careful attempt has been made from the data obtained from the last diffuser (42 mil) to find if the plot of log R *vs.* $1/T$ is really linear between 360° to 1060°C. It has been found that the plot is not linear and $\log_{10} R - \frac{1}{2} \log_{10} T$ must be plotted against $1/T$ in order to obtain a linear relation. This is shown in Fig. 7. As mentioned before, this diffuser was in the system long enough so that the diffusion rates were completely reproducible and the variation of the isotherm

TABLE 1. *Diffusion constants for hydrogen through commercial nickel.**

EQUATION	ABOVE CURIE	BELOW CURIE
	SAMPLE NO. XIII	
$D=k_1 p^{\frac{1}{2}} \exp(-b/T)$	$b_1=6680$ $k_1=0.93\times10^{-2}$	$b_1=6780$ $k_1=1.02\times10^{-2}$
$D=k_2 P^{\frac{1}{2}} T^{\frac{1}{2}} \exp(-b/T)$	$b_2=6280$ $k_2=1.7\times10^{-4}$	$b_2=6440$ $k_2=2.42\times10^{-4}$
	SAMPLE NO. XII	
$D=k_1 P^{\frac{1}{2}} \exp(-b/T)$	$b_1=6650$ $K_1=2.0\times10^{-2}$	$b_1=6590$ $k_1=1.9\times10^{-2}$
$D=k_2 P^{\frac{1}{2}} T^{\frac{1}{2}} \exp(-b/T)$	$b_2=6200$ $k_2=4.0\times10^{-4}$	$b_2=6200$ $k_2=5.3\times10^{-4}$

* In all of the above equations, D is the rate of diffusion of hydrogen measured in cubic centimeters at N.T.P. per square cm area per millimeter thickness per second. P is the impressed pressure of the gas in millimeters of mercury.

slopes from +0.5 were at a minimum. This proves experimentally the complete diffusion equation, Eq. (1), above the Curie point and doubtless below that point also, but the lower temperature range is not sufficient to determine the exponent of T with certainty.

Figure 8 shows the experimental results of Craninsky[2] and Ham[3] obtained with relatively pure nickel obtained from Baker & Co. The existence of an offset at the Curie point in the diffusion isobars is clearly indicated by the results of these investigators.

The hysteresis at the Curie point for commercial nickel may be observed in Fig. 9. It should be noted that the rate obtained by the steady-state method enables one to follow this transformation under various conditions, and moreover, the method gives a clear insight into the behavior of this point when no magnetic field is present. The observations were taken for various speeds of heating through the transformation and it should be emphasized that even with very slow rates of heating (or cooling) a hysteresis is observed which can only be minimized by slowly working back and forth through the region until the transformation point is closed in between two temperatures. If readings are taken too fast the lower phase can be carried into the upper region for about 100° while the upper phase can only be brought for a much shorter distance into the lower, say about 25°. This latter effect is difficult to study because of the slow cooling rates of the furnace at these temperatures. The hysteresis for pure anode nickel seems to be considerably smaller than that shown in Fig. 9.

The possible effect of hydrogen concentration on the Curie point was studied by determining isobars at various pressures. No change in the position of the Curie point could be found for pressures from 1 atmosphere to 0.5 cm Hg.

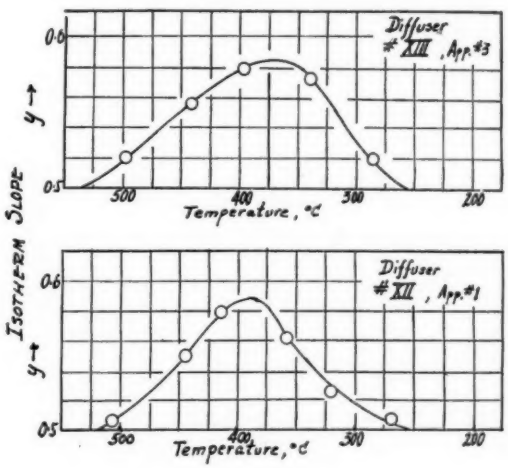

FIG. 4. Variation of isotherm slopes for commercial nickel. Samples XIII and XII.

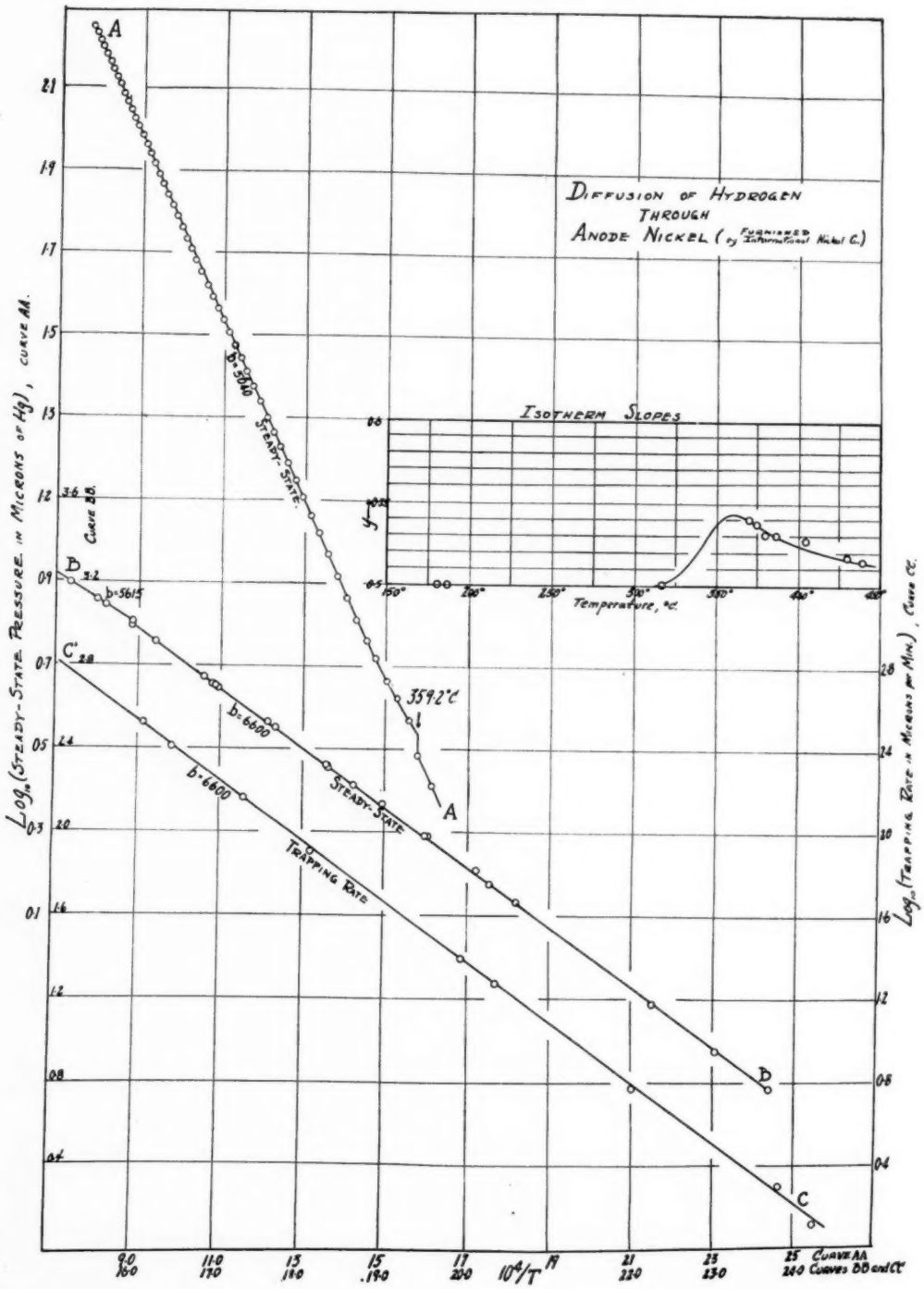

FIG. 5. Diffusion of hydrogen through anode nickel. 22 mil. *AA*, $\log_{10}$ (steady-state rate) *vs.* $1/T$; *BB*, $\log_{10}$ (steady-state rate) *vs.* $1/T$ for lower temperature runs; *CC*, $\log_{10}$ (trapping rate) *vs.* $1/T$ for low temperatures.

Discussion of Results

The first fact to be noted from this research on the diffusion of hydrogen through nickel is that a series of anomalies in the diffusion isobars as found in iron[1] do not exist in nickel. The same apparatus and technique as used in I was used here, consequently we must assume that the Rydberg series found in iron is truly characteristic for hydrogen diffusion through iron. While the constants given in Table I for the diffusion of hydrogen through commercial nickel are quite accurate they vary considerably with the different samples, and it has been found that these constants vary considerably with the life history of a particular sample.

The isotherms for hydrogen through nickel do not have a slope of 0.50 near the Curie point unless the nickel has been thoroughly decarburized by hydrogen diffusion. Information from the International Nickel Company indicates that minute quantities of carbon were present in the anode nickel at the start. All evidence in the data for both iron and nickel is that the explanation given by Smithells and Ransley[7] for a deviation from 0.5 of the slope for hydrogen diffusion isotherms for iron or nickel is completely erroneous, their explanation being that the variation is due to surface conditions. On the other hand, there is nothing that contradicts the opinion expressed by Ham[3] that this deviation from 0.5 is due to the simultaneous application of two or more mass action effects, or in simple terms that some of the diffusing hydrogen may be associated with an alloying element (often carbon) in the metal in pairs or ions (or as H_2+). This also appears to be the case if the metal is alloyed with N or O.

The proof of this is that isotherms for carbonyl irons are much above a 0.5 slope in the region of 500°C until the carbon is removed whereupon they approach 0.50. In the case of pure nickel, isotherms that were considerably above 0.50 are completely reduced to 0.50 by a process recognized as a decarburizing process. The material upon which Smithells and Ransley base their theory to explain the deviation of the isotherms from the $P^{\frac{1}{2}}$ law had not been decarburized. In all the ranges of temperature they discuss in the case of iron and nickel we have found almost

Table 2. *Diffusion constants for hydrogen through anode nickel.*

Equation	Above Curie	Below Curie
$D=k_1P^{\frac{1}{2}}\exp(-b/T)$	$b_1=5615$ $k_1=3.3\times10^{-2}$	$b_1=6600$ $k_1=0.17$

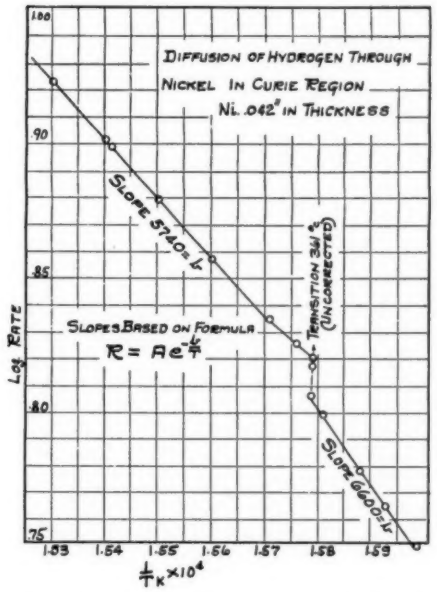

Fig. 6. Diffusion of hydrogen through nickel in the Curie region. 42 mil. Slopes based on Formula $R = A\exp(-b/T)$.

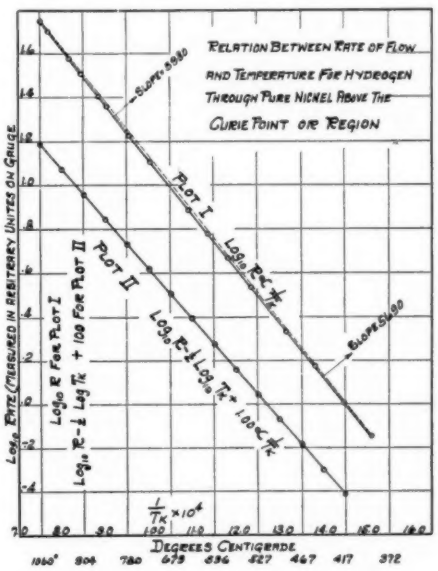
Relation Between Rate of Flow and Temperature For Hydrogen Through Pure Nickel Above The Curie Point or Region
Slope 5980
Plot I
Plot II
Slope 5480
Log Rate (Measured in Arbitrary Units on Grid)
Degrees Centigrade

Fig. 7. Relation between diffusion rates and temperature for hydrogen through pure anode nickel above the Curie point.

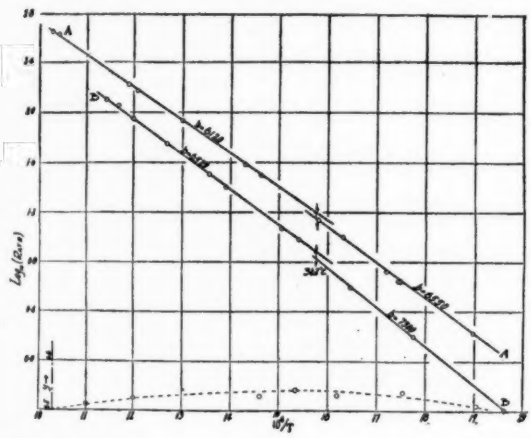

FIG. 8. Diffusion of hydrogen through Baker nickel, Craninsky[2] and Ham.[3]

perfect agreement in the variation of diffusion rate with the square root of pressure ($P^{\frac{1}{2}}$ law), provided the carbon is completely removed. Hence, the application of the Langmuir absorption formula which Smithells and Ransley employed is not necessary or justified.

The experimental fact that the exponent of T in the diffusion equation is $+\frac{1}{2}$ is an important theoretical point in connection with the energy of the hydrogen in the gas phase and in the metal. From this the hydrogen atoms appear to possess very nearly the same energy within the metal as without, and if the hydrogen is tightly bound to lattice points during most of its residence within the metal, because of the proton's light mass as compared to the metal atom of the lattice, but little energy of translation is allowed for the hydrogen. Its energy must be either vibrational or rotational or both. The reason that breaks indicating this rotation show in data on iron and do not in nickel may be because the latter has a relatively larger number of free electrons at any particular temperature as indicated by conductivity data, and the number of rotational states in which the hydrogen protons may exist at a particular temperature is correspondingly greater, thereby smoothing out the diffusion isobar.

The abrupt appearance of the offset at the Curie point as shown by hydrogen diffusion studies is surprising in view of the existing theories of ferromagnetism. It was for this reason that the lower portions of the curves below the Curie point were observed with great care to ascertain whether a small bowing of the curves below the Curie point existed. If the electronic shifts necessary to cause demagnetization are governed by a statistical distribution, the fact that we are able to detect the transition at the Curie point would lead one to expect that we should be able to follow any trend or shifting due to temperature below the Curie point. Such a trend has not been found and if it does exist the magnitude is almost negligible because we have found the rates below this point to follow the same kind of diffusion law as the rates above. Evidentally the intrinsic magnetism of the nickel atoms must be governed by forces which break suddenly. The above arguments, of course, refer only to demagnetization caused by temperature effects in the absence of a magnetic field.

To be specific, the theory of Slater[8] needs modification since this theory assumes a gradual rearrangement, as the metal is heated from absolute zero, of electrons in the third shell of the nickel atom, this rearrangement increasing rapidly as the Curie point is approached. The diffusion data indicate that such cannot be the

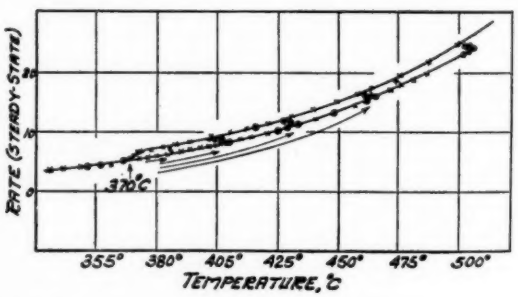

FIG. 9. Hysteresis at the Curie point in commercial nickel determined by steady-state methods.

case since the isobars are straight from 153° to 360°C.

A detailed picture of the nature of the Curie transformation is that certain atoms of the lattice must temporarily possess an additional valence electron during the transition, no doubt obtaining it from the 3*d* shell. This additional electron is necessary to interpret the behavior of the isotherms on pure anode nickel in the range

[8] J. C. Slater, Phys. Rev. **49**, 537 (1936); **49**, 931 (1936).

within 3° of the Curie point. However, this condition does not persist and evidently another valence electron drops back into the 3*d* shell and has such a spin that the electrons in the 3*d* level are now paired. When this has occurred the element may be considered as paramagnetic.

Conclusions

(*a*) The diffusion of hydrogen through nickel has been investigated from 1100° to 150°C with both commercial and pure anode nickel. Constants in the diffusion equations have been obtained.

(*b*) The Rydberg series found in iron has not been found in nickel. The same apparatus as used in I was used here.

(*c*) The isotherms are found to vary from 0.5 in the neighborhood of the Curie point for pure anode nickel. When this nickel has been fully decarburized by exposure to diffusing hydrogen for long periods this variation from 0.5 only occurs within 3° of the Curie point.

(*d*) The exponent of T in the diffusion equation $R=AT^{\frac{1}{2}}P^{\frac{1}{2}}\exp(-b/T)$ has been found to be $+\frac{1}{2}$ for the diffusion isobars from 360° to 1050°C.

(*e*) The magnetic transition of nickel as shown by diffusion is abrupt, the isobars below the Curie region being as straight as those above.

(*f*) There is always a sudden drop in the value of B, as calculated from the simple equation $R=A\exp(-b/T)$, at the Curie point, the value changing in the purest nickel from 6600 to 5800 with rising temperature.

(*g*) The Curie region shows marked hysteresis and is similar to the Curie region of pure iron in this respect.

(*h*) The explanation prepared by Slater to account for the effect of temperature on ferromagnetism seems to require serious modification inasmuch as the Curie transition for nickel appears to take place about as abruptly as the body-centered-face-centered transition in iron.

(*i*) A variation in hydrogen concentration in nickel near the Curie point does not change the position of the Curie point to a measurable amount.

(*j*) The loss of magnetism at the Curie transition is essentially an atomic phenomenon and should not be associated with conditions in aggregates of atoms or atomic domains.

(*k*) During the Curie transformation for a finite time there appears to be an additional electron in the valence shell of some nickel lattice points.

(*l*) A possible description of the process of the change from the ferromagnetic to the paramagnetic condition in the transition elements is that an electron is moved from the 3*d* shell to one of the 4-levels followed more or less quickly by the drop of another 4-level electron back to such a 3*d* shell as to result in pairing of electron spins in the 3*d* shell.

The Low Temperature Oxidation of Iron

H. R. NELSON
Battelle Memorial Institute, Columbus, Ohio

(Received July 20, 1938)

An electron diffraction study of the oxide films formed on abraded iron specimens by heating in air at temperatures ranging from 80° to 260°C has failed to detect structural effects due to a "critical temperature" in the neighborhood of 200°C. α-Fe_2O_3 was found on specimens which were oxidized at any temperature above about 130°C provided the period of oxidation exceeded a minimum value which depends upon the temperature. Thus 1 hour at 180°, 4 hr. at 165°, 13 hr. at 150° or 1000 hr. at 130° are just sufficient to produce an α-Fe_2O_3 film whose diffraction pattern is well defined. Lower oxidation temperatures or shorter times tend to strengthen the diffraction pattern due to the primary oxide film which is assumed to be γ-Fe_2O_3 (or Fe_3O_4) and is detectible immediately after the initial abrasive treatment. The strengthening of the primary oxide pattern is not accompanied by appreciable grain growth, however, and traces of iron are present in the pattern after oxidation periods as long as 1700 hr. at 120°C or below. Based on considerations of the presence of these iron rings it is estimated that the primary oxide film cannot be thicker than about 200A over some portions of the abraded surface. At 193°C and above the development of the first order blue interference color is characterized by the appearance of a new α-Fe_2O_3 film which is more coarsely crystalline and has a different type of preferred orientation than the first-formed α-Fe_2O_3 film. It is believed that this secondary film is formed by the outward diffusion of iron through the oxide layer. The axis of preferred orientation of the α-Fe_2O_3 is always symmetrical about the normal to the surface. This orientation cannot be attributed to pseudomorphism of the oxide crystals on the underlying iron as is the case with the primary oxide.

INTRODUCTION

THE nature and thickness of the air-formed oxide film formed on iron at various temperatures has been investigated by a number of workers[1] during the last few years. Many of the results indicate that the film composition or the mechanism of film formation or both depend upon whether the oxidation is effected at temperatures above or below 200°C. Vernon[2] found that when iron is heated in air at temperatures above 200°C interference colors develop which are characteristic of the oxide film thickness whereas at lower temperatures the color sequence does not appear even under prolonged heating. From gravimetric measurements he concluded that oxide films formed below 200°C were much thicker than indicated by the surface color. In addition he found by gravimetric methods that the oxidation *vs.* time curve is a parabola above 200°C but deviates therefrom at lower temperatures. Miley[3] confirmed the absence of interference colors below 200°C. Mehl and McCandless,[4] however, obtained interference colors on single iron crystals at temperatures as low as 140°C although their color *vs.* time curves at this temperature indicate that the color reaches a constant value which is unchanged on further heating.

Several electron diffraction investigations have shown that oxide formed on iron from room temperature up to some rather poorly defined temperature is cubic with a lattice constant of about 8.4A. Unfortunately both Fe_3O_4 and γ-Fe_2O_3 have a unit cell of this size and they are virtually indistinguishable by diffraction methods. Chemical considerations, however, have led Miley[3] and others[5] to conclude that the cubic oxide is γ-Fe_2O_3.[6] Preston and Bircumshaw[7] found the cubic oxide on specimens heated at 135°C and 175°C but rhombohedral α-Fe_2O_3 was present when the oxidation temperature was above 200°C. Their tests were made on small pieces cut from larger sheets which Vernon had used in his gravimetric work and for this reason were not well suited for the purpose.

[1] For recent reviews see: U. R. Evans, *Metallic Corrosion, Passivity and Protection* (London, 1937), Chapters II and III; W. H. J. Vernon, Chemistry and Industry **56**, 751 (1937).

[2] W. H. J. Vernon, Trans. Faraday Soc. **31**, 1668 (1935).

[3] H. A. Miley, Carnegie Scholarship Mem. **25**, 197 (1936).

[4] R. F. Mehl and E. L. McCandless, Trans. Am. Inst. Min. Met. Eng., Iron and Steel Div. **125**, 531 (1937).

[5] I. Iitaka, S. Miyake and T. Iimori, Nature **139**, 156 (1937).

[6] The conclusion of others that this primary oxide is γ-Fe_2O_3 has been accepted here for purposes of designating diffraction patterns but it must be emphasized that the experiments described herein do not distinguish between Fe_3O_4 and γ-Fe_2O_3.

[7] Reported by Vernon, Trans. Faraday Soc. **31**, 1677 (1935).

Since these investigations indicate a critical temperature in the neighborhood of 200°C it seemed desirable to find out what electron diffraction methods could determine about films formed in air at temperatures above and below 200°C. In some earlier work[8] it was demonstrated that the cubic crystals of the room-temperature air-formed film bear a definite orientation relationship with the underlying iron but no attempt was made to study films formed at higher temperatures.

Experimental

The specimens were small ($\frac{1}{2}''\times\frac{1}{2}''\times\frac{1}{4}''$) rectangular blocks cut from ingot iron (Armco) of the following analysis:

Carbon	0.02 percent
Manganese	0.03
Phosphorus	0.019
Sulphur	0.026
Copper	0.05

The initial surface treatment consisted of grinding all six surfaces on successively finer grades of emery paper ending with a very light abrasion on dry 4/0 paper. The resulting surface is in a finely abraded condition and gives a faint diffraction pattern due to γ-Fe_2O_3 overlying the stronger α-Fe pattern.[9]

The samples were heated in cylindrical electric furnaces equipped with automatic controls which maintained the temperature constant to within ±1°C. The ends of the furnaces were closed with loose fitting refractory plugs which permitted free access of air. Ordinary air without purification was used for oxidation. Some of the samples were placed in the furnace in small alundum boats; others were supported by the thermocouple wires used to measure the temperature of the sample.

The oxidation temperature was determined by means of a thermocouple the elements of which were wedged or peened into two small holes drilled in the sides of the specimen. Air temperatures near the test surface were sometimes measured by a second thermocouple or a mercury-in-glass thermometer placed close to but not touching the specimen. The temperature close to the sample as measured by this method was not appreciably different from that of the sample itself as determined by the attached couple.

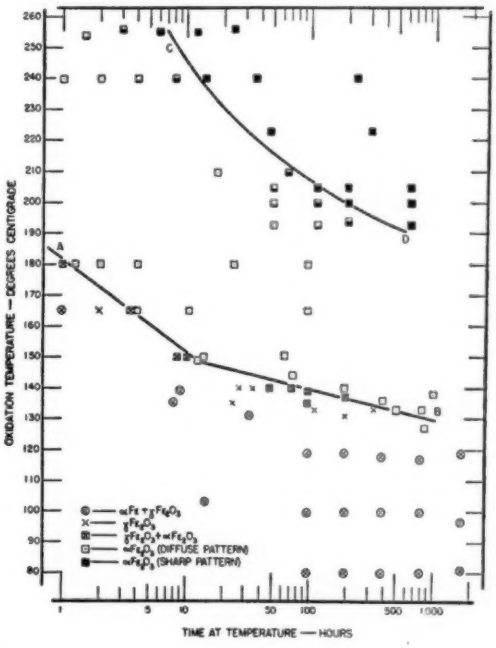

Fig. 1. Graphical representation of the results of heating iron specimens for various times at various temperatures.

The diffraction camera is similar to that described by Thomson and Fraser[10] with a hot cathode source of electrons. Constant accelerating potentials of 30 to 40 kv are provided by a transformer, rectifier and filter system. The grazing incidence or "reflection" method was used with a sample-to-plate distance of 40 cm.

Results

The results on abraded iron surfaces are summarized graphically in Fig. 1. Each point represents a single experiment in which a specimen was heated continuously at the indicated temperature for the time given on the

[8] H. R. Nelson, J. Chem. Phys. **5**, 252 (1937).

[9] Abraded surfaces were used partly because they most nearly represent a type of mechanically worked surface often met in practice. More important, however, is the fact that freshly abraded iron surfaces give an easily reproducible and interpretable pattern in which changes can readily be followed. Polished surfaces, on the other hand, give a poor pattern which, irrespective of its interpretation, is certainly not characteristic of metallic iron. With etched surfaces difficulty was experienced in removing the last traces of etching products which, it is reasonable to suppose, might profoundly affect the oxidation process.

[10] G. P. Thomson and C. G. Fraser, Proc. Roy. Soc. **A128**, 641 (1930).

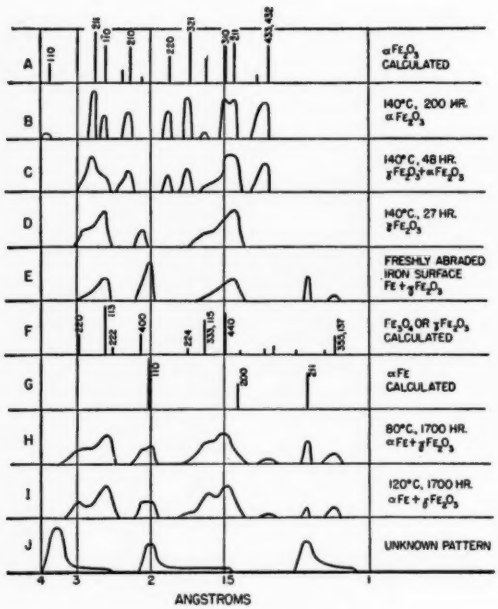

FIG. 2. Observed and calculated diffraction patterns. Heights of the curves represent estimated relative intensities.

logarithmic time scale after which the surface was examined in the diffraction camera. The character of the resulting diffraction pattern is indicated by the type of plotted point. A circle means that rings due to iron were present in the pattern. Crosses indicate the presence of the primary oxide γ-Fe_2O_3, while squares represent α-Fe_2O_3. The lines *AB* and *CD* are drawn simply to separate the time-at-temperature area into fields within which the indicated type of diffraction pattern was observed.

A freshly abraded iron sample gives a diffraction pattern consisting of broad diffuse rings and a few fairly sharp rings. As has been shown previously[8] this pattern is due to iron and the primary oxide. The latter is present in exceedingly small crystals as evidenced by the lack of resolution of the diffraction rings (cf. Fig. 2 *E*, *F*, and *G*). The iron rings are fairly sharp unless they happen to lie so close to oxide maxima as not to be resolved therefrom.

When such an abraded surface is heated in air at temperatures of 120°C or lower there is very little change in the pattern after heating periods as long as 1700 hours. (See Fig. 2, *H* and *I*.) In general the oxide pattern becomes slightly stronger with a slight tendency for the diffuse maxima to be resolved into their component rings. The resolution is never good even with the longest oxidation periods used and there was little difference in the patterns obtained from specimens heated at 80°C and 120°C for 1700 hr.

The presence or absence of iron was determined by the presence or absence of the strong (110), (211) and (321) reflections of iron in the pattern. The (110) ring was never completely resolved from the (400) ring of the oxide but the other two could be checked easily since they do not fall near oxide maxima. As can be seen in plots *H* and *I* of Fig. 2 iron was present after heating 1700 hr. at 120°C or below.

When an abraded iron specimen is heated at temperatures above about 130°C the observed patterns follow the sequence shown in plots *E*, *D*, *C*, *B* of Fig. 2. Rings due to iron disappear fairly rapidly in heating times which depend upon the temperature. The disappearance of the iron is accompanied by a strengthening of the primary oxide pattern but there is no appreciable sharpening of the diffuse rings before they begin to be replaced by new rings due to rhombohedral α-Fe_2O_3. After still longer heating periods the primary oxide is entirely replaced by α-Fe_2O_3, Figs. 3 and 2*B*. This sequence of patterns has been observed at temperatures as low as 133°C and as high as 210°C. At the higher temperatures these changes take place before the specimen has reached temperature equilibrium, consequently the time required for the various changes could not be determined accurately. These results show conclusively that abraded iron surfaces develop a film of α-Fe_2O_3 on heating in air at temperatures above about 130°C. The slope of the right-hand end of the line *AB* suggests that this oxide can be produced at even lower temperatures if sufficiently long oxidation periods are used. One specimen heated for 850 hr. at 127°C gave a well-developed α-Fe_2O_3 pattern. It is not known why this result falls so far out of line.

At higher temperatures the surface film of α-Fe_2O_3 undergoes a change characterized by a gradual replacement of the diffuse diffraction maxima by new, sharply defined rings due to the same oxide (see Figs. 4 and 5). There is also a change in the type of preferred orientation which is discussed later. The transition from the diffuse to the sharp α-Fe_2O_3 pattern is coincident with

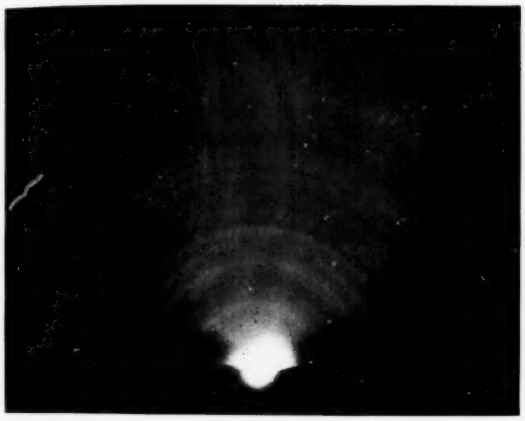

FIG. 3. α-Fe_2O_3 (diffuse pattern) from iron heated in air at 133°C for 800 hr.

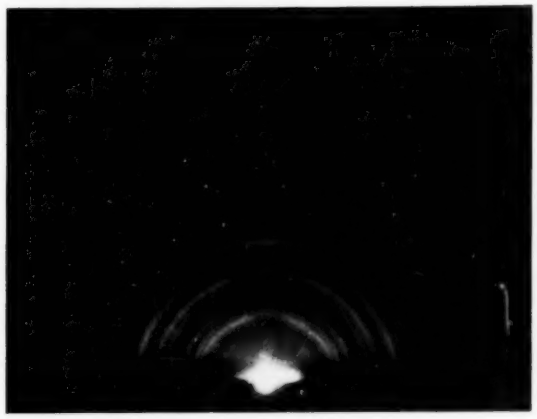

FIG. 4. α-Fe_2O_3 (diffuse pattern) from iron heated in air at 240°C for 4 hr.

FIG. 5. α-Fe_2O_3 (sharp pattern) from iron heated in air at 240°C for 14 hr.

the development of the first order blue interference color. Sharp diffraction rings begin to appear on the diffuse pattern when the surface reaches the purple stage. The diffuse maxima are entirely gone when the surface has become deep blue.

Above and to the right of *CD* in Fig. 1 only the sharp α-Fe_2O_3 pattern is obtained; below and to the left is a region in which the pattern due to this oxide is at least partly diffuse. It will be apparent from Fig. 1 that the data do not determine the shape of the curve *CD*. A straight line could be drawn to separate the fields nearly as well as the curve. The fact that at 193° this curve has not deviated sharply to the right indicates that the sharp α-Fe_2O_3 pattern characteristic of higher temperatures might be obtained from samples oxidized sufficiently long at temperatures well below 200°. Experimental data in the range 170° to 180° and 1000 to 10,000 hr. are necessary to test this point.

A diffraction pattern due to some unknown film was obtained in a number of experiments. (See Figs. 2*J* and 6.) The pattern is characterized by three strong diffuse rings which are rather sharply defined on the inside but poorly defined on the outside. The innermost ring which corresponds to a spacing of about 3.5A, is much stronger than the others. This pattern was always obtained when samples were heated at temperatures of 125°C or below in one of the several furnaces used for these tests. It could not be reproduced in any of five other furnaces which were used. Above 130°C this particular furnace gave results entirely consistent with those obtained in the other furnaces. The possibility that some unknown material from the walls of the furnace condensed on the surface and produced this pattern was tested by heating the test sample simultaneously with copper and nickel specimens placed beside it in the furnace. In every case the iron gave the diffuse ring pattern while the control surfaces did not. Moreover, the unknown pattern was obtained on a wide variety of iron surfaces, e.g. on electrodeposited iron films, on mirrors formed by vacuum evaporation and condensation of iron, and on etched and polished as well as abraded surfaces.

Attempts to analyze and explain this pattern have failed and at present it must be considered an anomalous result. It has not been included in

FIG. 6. Unknown diffuse ring pattern from iron heated in air at 122°C for 1850 hr.

the experimental results plotted in Fig. 1. The effect has been mentioned here, however, because it suggests the possibility that an amorphous oxide may be formed when iron is heated at temperatures below 125°C under certain special conditions which this experiment has failed to define.

A few experiments were performed on highly polished surfaces and various etched surfaces were tried. Although the results were similar to those obtained on abraded specimens there was evidence that the initial films left by such methods of preparation were too variable to give reproducible results (see footnote[9]).

In a previous paper[8] it was shown that the primary oxide crystals stand in a definite orientation relationship with the iron crystals on which they form. It follows, therefore, that on abraded iron surfaces in which the iron crystals are randomly oriented the primary oxide should also be randomly oriented. Such in fact was observed on all abraded surfaces irrespective of the temperature at which the specimens were heated. By similar reasoning we conclude that α-Fe_2O_3 crystals should be randomly oriented if they bear a definite orientation relationship to the primary oxide or to the underlying iron. Actually, however, the α-Fe_2O_3 patterns always show a low degree of preferred orientation. In the initial α-Fe_2O_3 (open squares in Fig. 1) the [111] directions of the rhombohedral crystals tend to be perpendicular to the surface. Referred to hexagonal axes this means that basal planes tend to lie parallel to the surface of the specimen.

The appearance of the sharp α-Fe_2O_3 pattern is accompanied by the development of a new type of preferred orientation characterized by a slight tendency for (211) rhombohedral planes to lie parallel to the surface. As can be seen in Fig. 5 this is a very low degree of orientation.

In order to determine the possible effect of orientation in the original iron surface the oxidation of electrodeposited surfaces was studied. The crystals formed when iron is plated onto polished or abraded iron tend to stand with [111] directions approximately perpendicular to the surface. The primary oxide film forms with an equally high degree of orientation because of the definite spacial relationship between it and the underlying iron. The preferred orientation exhibited by α-Fe_2O_3 films grown on such surfaces, however, was found to be exactly the same as was observed on abraded surfaces.

No careful attempts were made to determine the interference color of the specimens as a function of time and temperature. As has already been mentioned, however, the curve *CD* in Fig. 1 very nearly coincides with the appearance of the first order blue. The lowest temperature at which blue was obtained was 193°C. 1000 hr. at 138° gave a faint yellow similar to that observed after about 4 hr. at 180°. Specimens heated at 120° became perceptibly darker as the oxidation was prolonged. At 80° there was only a barely detectable darkening after 1700 hr.

DISCUSSION

During the course of this work Iimori[11] reported electron diffraction experiments in which he studied oxide films formed on etched iron surfaces heated in air at various pressures and temperatures. Below 340°C he found only the cubic oxide which he believes is γ-Fe_2O_3. At first sight this seems difficult to reconcile with the present results. However, Iimori reports only four experiments performed at atmospheric pressure and of these only two fall in the temperature range covered in Fig. 1. He finds γ-Fe_2O_3 after 1 hr. at 250°C or 24 hr. at 150°C. Both of these points fall within the region of diffuse α-Fe_2O_3 patterns obtained on abraded surfaces. The discrepancy is undoubtedly due to the different surface treat-

[11] T. Iimori, Sci. Papers, Inst. Phys. Chem. Research, Tokyo **34**, 60 (1937).

ment used in the two investigations and one is forced to the important conclusion that results on one type of surface cannot be applied to another. In fact Iimori states that on polished surfaces he obtained sharp α-Fe_2O_3 patterns as low as 250°C.

The real purpose of this investigation, *viz.*, to study the nature of a critical temperature near 200°C, has not been achieved. The results give no evidence of a critical temperature in this region. Long oxidation periods in the neighborhood of 180° might establish a lower temperature limit for the formation of the sharp α-Fe_2O_3 diffraction pattern. On the other hand comparatively short oxidation periods were sufficient for Vernon to show the existence of a critical temperature. It is apparent, therefore, that the difference between the oxidation mechanism above and below 200°C does not manifest itself in structural differences in the topmost layer of the oxide film.

The preferred orientations observed in the α-Fe_2O_3 films cannot be due to pseudomorphism on underlying crystals as is the case with the primary films. Since the axis of orientation is always normal to the surface with complete randomness in other directions it seems likely that the crystalline orientation is in some way associated with the diffusion of oxygen through the oxide film or, more probably, the diffusion of iron outward to form new layers of oxide at the outer surface of the film. Pfeil[12] has shown that iron diffuses outwards through thick layers of oxide when ferrous materials are heated at high temperatures. This suggests a possible reason for the appearance of the sharp α-Fe_2O_3 pattern with its new orientation at the higher temperatures. The sharp diffraction rings mean that the new oxide crystals are much larger than those which gave the diffuse pattern. Careful examination of plates showing the transition from the diffuse to the sharp pattern leads to the conclusion that this transition is not due to crystal growth or to a process resembling recrystallization. Instead it appears that new crystals with the new orientation grow on top of the old film. If this interpretation is correct, iron must diffuse through the oxide film to the surface. The curve *CD* in Fig. 1 may, therefore, be some sort of measure of the rate of diffusion of iron through the oxide layer and the curve's lower temperature limit, if there is such a limit, would determine the temperature at which the diffusion rate becomes negligible.

The presence of diffraction rings due to metallic iron after oxidation periods of 1700 hr. at 120°C and less is surprising. In the "reflection" method the electrons pass through jagged ridges and projections left by the abrasion process. In passing through such a projection an electron would pass first through an oxide film, then through the unoxidized core and finally emerge through the oxide film. In such a path the electron might be scattered in either the iron or the oxide. Since, however, electrons cannot penetrate more than several hundreds of angstroms of solid material without suffering multiple scattering or absorption, the presence of iron rings in the diffraction pattern fixes an upper limit of about 200A for the thickness of the oxide film.

[12] L. B. Pfeil, J. Iron and Steel Inst. **119**, 501 (1929).

The Diffusion of Helium and of Hydrogen Through Pyrex Chemically Resistant Glass

NELSON W. TAYLOR AND WILLIAM RAST
Department of Ceramics, The Pennsylvania State College, State College, Pennsylvania

(Received July 7, 1938)

The effects of temperature and of heat treatment on Pyrex chemically resistant glass have been studied by measuring the rate of diffusion of helium and of hydrogen through a tube of about one millimeter wall thickness. Measurements were made with helium between 180°C and 590°C, and with hydrogen at 512°C. The influence of gas pressure was determined and the diffusion rate was found to be directly proportional to the pressure for both helium and hydrogen.

The diffusion data throw light on the processes of molecular rearrangement involved in stabilization of the glass. Below 548°C the rates of diffusion (R) were increased about 10 percent by giving the glass sufficient heat treatment to assure "stabilization," i.e., equilibrium in the processes of dissociation and association. This increase occurred despite the fact that such heat treatment normally increases the density of the glass and therefore points to a chemical theory rather than a simple theory of holes governing the diffusion process.

The data also showed a continuous linear dependence for the stabilized glass of log R on $1/T$ from 440°C–590°C. This range extends into the region of a true viscous liquid and it follows that the properties of a stabilized glass are continuous with that of a viscous liquid and that there is no need to postulate a separate glassy state. The "transformation point" mentioned by some investigators is merely the temperature of rapid strain release of an unannealed sample.

At or near 440°C the log R *versus* $1/T$ curve takes a lesser slope (for lower temperatures) and this change is attributed to the loss of rotational or vibrational freedom in the silicate complex, analogous to that frequently found in dielectric studies on solids. Activation energies have been calculated for the two temperature ranges.

At 512°C the rate of helium diffusion is approximately 45 times that of hydrogen, and it is believed that chemical forces delay the progress of the hydrogen molecule through the silicate network.

The general conclusion is drawn that gas diffusion furnishes a highly sensitive method for studying the molecular condition of silicate glasses and similar materials.

THE principal feature distinguishing the glassy state from the ordinary liquid state is a very high viscosity which delays the establishment of equilibrium of molecular processes in glass. The result of this delay is that the properties of a glass depend to an important degree on its thermal history or heat treatment. Examples are expansion coefficient,[1] viscosity,[2] elastic properties such as Young's modulus,[3] electrical conductivity,[4] absorption spectrum,[5] and dielectric constant.[6] When the temperatures are sufficiently high equilibrium is very rapidly attained in a glass and it cannot be distinguished in its behavior from an ordinary viscous liquid.

The nature of the liquid state partakes in part the properties of crystals,[7] and in part the properties of a condensed gas, but its study has proven rather difficult. One may say that at present we have less knowledge of the structure of liquids than we have of either gases or crystalline solids. One of the difficulties lies in the fact that dynamic equilibrium is rapidly attained in ordinary liquids and that it is impossible to "freeze in" or preserve a certain molecular condition, for later study. In glasses this is not so. One may by quenching or rapid chilling preserve a high temperature structure down to low temperatures, or one may anneal a glass at any desired temperature and study the properties of the molecular configurations so developed. These characteristics of glass are utilized industrially in many ways.

There are various physical methods for investigation of the structure of glass. Several have

[1] M. E. Spaght and G. S. Parks, Glass VIII, "The Coefficient of Thermal Expansion of Boron Trioxide," J. Phys. Chem. **38**, 103–10 (1934).
[2] H. R. Lillie, "Viscosity-Time-Temperature Relations in Glass at Annealing Temperatures," J. Am. Cer. Soc. **16**, 619–631 (1933).
[3] N. W. Taylor, E. P. McNamara and J. Sherman, "A Study of the Elastico-Viscous Properties of a Soda-Lime-Silica Glass at Temperatures near the 'Transformation point,'" J. Soc. Glass Tech. **21**, 61–81 (1937).
[4] J. T. Littleton and W. L. Wetmore, "The Electrical Conductivity of Glass in the Annealing Zone as a Function of Time and Temperature," J. Am. Cer. Soc. **19**, 243–245 (1936).
[5] W. Weyl and E. Thümen, "The Constitution of Glass, II. Theoretical Basis of Glass Coloration," Glastech. Ber. **11**, 113–120 (1933).
[6] W. Weyl, personal communication.
[7] G. W. Stewart, "X-Ray Diffraction in Liquids," Rev. Modern Physics **2**, 116–122 (1930). "Molecular Structure as Interpreted by X-ray Diffraction Measurements in Liquids," Chem. Reviews **6**, 483–501 (1929).

been mentioned. X-ray analysis[8] has demonstrated a certain regularity of atomic or ionic arrangement. This technique, however, presents a statistical picture of average interatomic distances and does not show the result of heat treatments in much detail, i.e., it is not particularly sensitive to heat treatment of the glass.

A method which depends on individual atomic properties, or on the properties of small groups of atoms or ions, rather than on the whole complex, is the method of gas diffusion through the solid. The progress of the diffusing atom is delayed by its binding (electrical interaction) with neighboring host atoms and the rate of diffusion is proportional to a quantity $e^{-A/RT}$ where A is the activation energy necessary to overcome these atomic forces. Diffusion thus becomes a property subject to study and mathematical treatment by the usual procedures of chemical reaction kinetics, and precise data can be obtained which lead to rather direct interpretation in terms of atoms and molecules.

As an example of the success of the diffusion method in the study of solids we may mention the work of W. R. Ham,[9] on the diffusion of hydrogen through iron and nickel. It was found that "the magnetic changes at about 360° (Ni) and 750° (Fe) were clearly defined by diffusion data. In addition, iron exhibits changes in the isobars at 945°, 900° and at between 200° and 550°C. A definite difference in temperature is observed between Ar_3 and Ac_3, and this appears to be a true hysteresis. The other points are all ascribed to electronic changes of the iron atom and it is suggested that the well known maximum in the tensile value of iron at 200–350° is explained in part by one of these electronic shifts. The general conclusion is reached that the isobars from hydrogen diffusion tests furnish an accurate means of tracing phase or electronic changes in iron and nickel, and that the change in slope of the isotherms provides a means in some instances of determining small amounts of foreign elements in solution in the metals."

[8] B. E. Warren and J. Biscoe, "Fourier Analysis of X-ray Patterns of Soda-Silica Glass," J. Am. Cer. Soc. **20**, 259–65 (1938).

[9] W. R. Ham, "The Diffusion of Hydrogen Through Nickel and Iron," Trans. Am. Soc. Metals **25**, 536–64 (1937).

Chemical Theory of Diffusion

The simple physical picture of diffusion as a movement of atoms through open channels or cracks which are large compared to atomic diameters, does not offer an explanation for much of the most accurate and reliable experimental work in this field. On the other hand, several workers, notably Dushman and Langmuir,[10] and later Eyring,[11] have treated the diffusion process by the same methods as for chemical reaction rates. The fundamental assumption is made that the diffusing atom moves from lattice point to lattice point through the solid and is subjected to the influence of strong electrical fields of a periodic nature. In order for a diffusing atom to break away from its immediate environment and move to a new position of stability in the solid, it requires an amount of energy, E, to activate it. By application of the Boltzmann principle, the probability that a diffusing atom can cross this energy barrier is proportional to $e^{-E/kT}$, where k is the Boltzmann constant. For a gram molecular weight of diffusing atoms, since $R=Nk$ and $A=NE$ where N is the Avogadro number, the expression becomes $e^{-A/RT}$.

The quantity A is sometimes called the activation energy, the energy of transfer, or the heat of loosening per gram atomic weight. This is where the chemistry of diffusion may enter the theory, for obviously those atoms which can exert a strong attraction for the diffusing atom (large A value) will delay the progress of the diffusing atom through the solid. Thus for example at 500°C, helium has a rate of diffusion through silica glass about 22 times faster than has hydrogen, as shown by Williams and Ferguson[12] "Were it a case of effusion the ratio would be less than unity," that, is approximately $\sqrt{2}/4=0.7$, since the molecular weights of helium and hydrogen are 4 and 2 respectively.

This large difference is to be expected on the theory that H_2 forms temporary attachments to

[10] S. Dushman and I. Langmuir, "The Diffusion Coefficient in Solids and its Temperature Coefficient, "Phys. Rev. **20**, 113 (1922).

[11] H. Eyring, "Viscosity, Plasticity and Diffusion as Examples of Absolute Reaction Rates," J. Chem. Phys. **4**, 283–291 (1937).

[12] G. A. Williams and J. B. Ferguson, "The Diffusion of Hydrogen and Helium through Silica Glass and other Glasses," J. Am. Chem. Soc. **44**, 2160–2167 (1922).

the oxygen ions which are of greater stability than that which helium may form with these ions. The two gases have nearly the same diffusion velocities through rubber ($C_{10}H_{16}$) which has a low oxygen content.[13] In fact, because of the chemical inertness of the helium atom, it is probable that the only forces which tend to bind it to the ions of the glass are the so-called van der Waals forces which arise from the interaction of dipoles between the two kinds of atoms.

Our own experiments show that at 512°C the rate of helium diffusion through Pyrex glass is approximately 45 times as fast as that of hydrogen, and this despite the fact that the diameters of He and of H_2 are nearly the same, namely 4.00 and 3.94A, respectively. These values are computed from the densities of the two liquids, at $-271.5°$ for He and at $-258°$ for H_2.

The theory that weak bonds between diffusing atoms and host atoms lead to relatively rapid diffusion has been also emphasized in another paper by one of the authors,[14] in discussing the diffusion of gold, silver bismuth, thallium, and tin into lead, and the self-diffusion of lead. Further evidence that diffusion is essentially controlled by chemical factors has been given by W. R. Ham[9] who has shown that a mixture of N_2 and H_2 diffuses through metallic iron very much more rapidly than either gas alone. This effect may be explained by assuming that N_2 and H_2 together form a complex molecule, possibly of an amide type, which has less attraction for the iron atoms than have the two H atoms which form when N_2 is not present.

In connection with the problem of the glassy state there are several questions which might be clarified by gas-diffusion studies. The first question was concerned with the nature of the so-called "transformation point:" is it a true thermodynamic property of a glass or is it simply interpreted as such because of a confusion of rate effects with equilibrium properties? Most expansion measurements are dynamic, in the sense that the temperature is rising or falling at a finite rate. It was considered desirable to measure some property such as diffusion under constant temperature conditions, above and below the "transformation point." The second question is related to the first one and may be stated: "What influence does thorough annealing have on the permeability of glass to gas, and how shall the results be interpreted?"

Materials and Methods

Earlier work on gas diffusion through glass has shown that hydrogen and helium diffuse more easily than do other gases. For this reason, and because of the relative simplicity of atomic structure of these gases, they have been chosen for this study. For the glass, Pyrex chemically-resistant glass was chosen, primarily because it was easily made into a suitable shape for the diffusion sample and also because it could readily be sealed to the rest of the vacuum system. From the standpoint of theoretical interpretation a glass of simpler chemical composition, such as fused silica or boric oxide would have been better, but from the practical standpoint Pyrex is of greater interest.

Experimental Method

The diffusion sample was a 41.0 cc Pyrex test-tube, having 94.6 cm² effective diffusing area and 1.1 mm wall thickness, sealed into a larger Pyrex tube as in Fig. 1. It was placed in a wire wound cylindrical muffle furnace, whose temperature was maintained uniform to ± 0.25°C by three thermocouples, at ends and center, and by automatic control to ± 0.5°C. The temperature of the "sample" was read from a thermocouple placed inside the inner tube. The high pressure side connected with a manometer and gas supply, the low pressure side with a calibrated McLeod gauge and mercury diffusion pump and oil pump. Vacuum stopcocks (Hg seal) were used throughout. The apparatus was thoroughly tested for leaks, using air, before introduction of helium or hydrogen. These gases were from commercial sources and were purified before use, by contact with charcoal at liquid-air temperatures. This treatment probably removed water vapor or hydrocarbons, but would have no effect on any nitrogen which might be present. The speed of

[13] J. D. Edwards and S. F. Pickering, "Permeability of Rubber to Gases," U. S. Bureau of Standards, Scientific Paper 387 (1920).

[14] N. W. Taylor, "Reactions Between Solids in the Absence of a Liquid Phase," J. Am. Cer. Soc. **17**, 155–163 (1934).

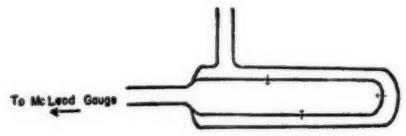

FIG. 1. Diffusion sample. Direction of diffusion indicated by arrows.

nitrogen diffusion through glass is extremely slow in comparison to that of helium, however.

The procedure consisted of trapping the diffused gas for definite intervals from 15 seconds to 30 minutes depending on the temperature, compressing this gas in the McLeod gauge and reading its volume at barometric pressure and room temperature which were of course known. At least 3 hours were devoted to each temperature, so that the glass had an opportunity to reach a steady state during that period. The diffusion data therefore represent essentially static conditions as compared with ordinary expansion studies.

PRESENTATION OF DATA

In view of the fact that the properties of a glass depend in part on the thermal history of the sample, the schedule of heat treatment will be given.

The rate measurements fall into five groups:

I. August 4–August 11, 1936. Temperature rising from 406°C to 590°C.
II. August 11–August 27. Temperatures falling from 590°C to 180°C.
III. August 28–September 11. Temperatures rising and falling between 352° and 570°C for 2½ cycles. This series will be described as "the isotherms."
IV. September 12–September 14. Temperatures rising from 187° to 367°C.
V. September 14–September 27. Glass held at 350° to 400°C. September 27–October 1. Temperatures rising from 242° to 544°C.

Group I. August 4–August 11. Temperature rising from 406° to 590°C (curve A)

After the whole vacuum system had been demonstrated to be free of leaks, measurements of diffusion rate for helium were begun at a temperature of 406°C. Since the glass sample had not been made strain-free by annealing at a temperature in the annealing range (approximately 545°C or above), the glass was really in a condition of strain. For this reason the rates of diffusion are less than those obtained later. The experimental points are plotted in Fig. 2, Curve *A*. It will be seen that at temperatures of 548°C or above the rates obtained on the strained glass are almost the same as those obtained later in the Group II series (Curve *B*) which presumably represents strainfree glass. Below 548°, however, i.e., between 406° and 548°C, the helium diffusion rates are about 10 percent less than those of Group II. Previous workers in the field of gas diffusion through glass have nearly always failed to remove the condition of strain in the glass before taking precise measurements, and it is therefore doubtful whether much of the published work on gas diffusion should be accepted in a quantitative sense.

Group II. August 11–August 27. Temperature falling from 590° to 180°C (curve B)

The data of Group II were taken over a period of 17 days, measurements made at 590, 584, 574, 567°C, etc., until a low point of 180°C had been reached. As in Group I and all other groups, each temperature was held constant for approximately 3 hours before the rate data were obtained. At all temperatures down to about 525° ample time was available to permit complete or nearly complete stabilization (molecular rearrangement) of the glass to a condition characteristic of that temperature. At or near 525°C there was a very slight change in direction of the log *R versus* $1/T$ curve which thereafter continued as a straight line down to about 440°C. Below 440°C the log *R versus* $1/T$ line was again straight, but had a somewhat lesser slope. Note that on Fig. 2 it diverges from the broken line which is a

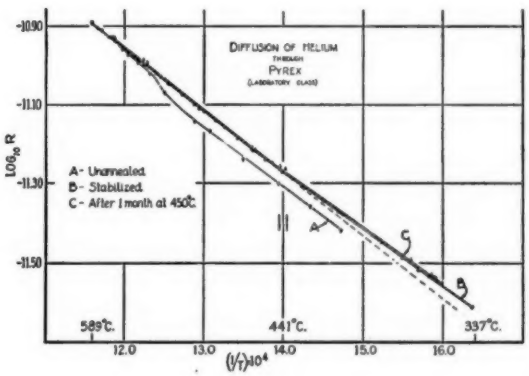

FIG. 2.

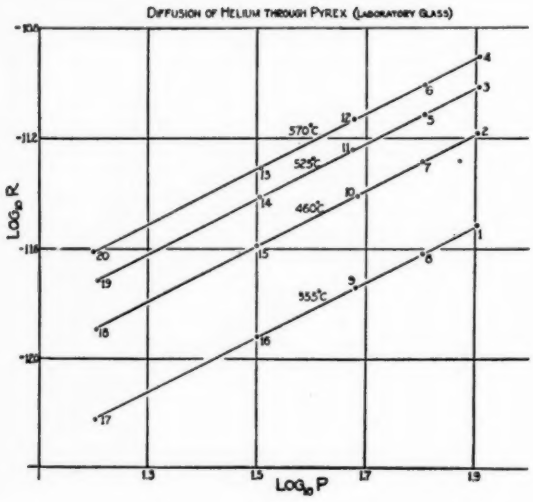

FIG. 3.

continuation of the upper slope. At about 225°C the line again changed direction, but as the rate measurements are less certain in this low temperature region, no emphasis will be laid on this effect, at present. The significance of the 525°C and 440°C breaks will be discussed later. Data below 337°C are not shown in Fig. 2.

Group III. The isotherms, August 28–September 11

The relation between diffusion rate and gas pressure was a subject of special interest, not only to permit reducing all rate data to a common pressure basis of 1 atmosphere, but also in connection with the more general problem as to the "molecular" state of the helium atom as it worked its way through the glass. For these reasons a series of isotherms were made at 5 different pressures, 16, 32, 48, 64 and 80 cm Hg. respectively, and at 4 different temperatures, 355°, 460°, 525° and 570°C. It was convenient to work at one helium pressure over the four temperatures, then to reduce its pressure and work back over the same four temperatures in reverse direction, etc. This resulted in heating the glass from 352 to 568, cooling to 355, heating to 570, cooling to 305 and finally heating to 571°C. The rate values are plotted in Fig. 3, and in Fig. 2, Curve *C*.

These cycles of alternate heating and cooling apparently produced no major effect on the diffusion rates except a slight increase, ca. 1 percent above 450°C and about $2\frac{1}{2}$ percent at or near 355°C. The "transformation point" at about 525 was wiped out, however, and its disappearance was confirmed by later tests, Group V.

The accuracy and reproducibility of the diffusion rates of Group III are shown by Fig. 2 where the plotted points fall nicely on the straight lines at each temperature.

Table I exhibits values of dm/dt for various values of p, and also shows values of R, the characteristic rate per atmosphere pressure gradient (g helium per cm² per sec. per mm wall thickness), calculated from the data of the two columns by means of the relation $R=76/p\ dm/dt$. The temperature is also shown. It will be seen that the values of R are practically constant, except for small shifts due to temperature.

In the range 440°–600°C, the data of Curve *C*, Fig. 2, may be satisfactorily expressed by the equation

$$-\log R=9.075+1562/T,$$

where R has the units already stated, and T is the absolute temperature, degrees Kelvin. This equation leads to rate values approximately 1 percent higher than those given in Table I, but is representative of the later data.

The linear relation between rate of diffusion and gas pressure is not surprising, since helium

TABLE I. *Rate of helium diffusion through stabilized Pyrex glass.*

TEMP. (°C)	PRESSURE (CM HG)	dm/dt	R
355	80.11	3.05×10^{-12}	2.82×10^{-12}
355.5	63.71	2.42×10^{-12}	2.89×10^{-12}
357	47.96	1.83×10^{-12}	2.94×10^{-12}
355	31.69	1.23×10^{-12}	2.88×10^{-12}
359	15.96	0.59×10^{-12}	2.90×10^{-12}
465	80.97	7.62×10^{-12}	6.29×10^{-12}
455.5	63.87	5.18×10^{-12}	5.96×10^{-12}
461	48.32	3.86×10^{-12}	6.15×10^{-12}
459	31.59	2.56×10^{-12}	6.12×10^{-12}
460.5	16.03	1.28×10^{-12}	6.10×10^{-12}
521.5	80.48	9.65×10^{-12}	8.92×10^{-12}
526	64.08	7.69×10^{-12}	9.15×10^{-12}
525	47.28	5.73×10^{-12}	9.21×10^{-12}
526	32.01	3.86×10^{-12}	9.20×10^{-12}
529	16.16	1.93×10^{-12}	9.27×10^{-12}
568	80.76	12.50×10^{-12}	11.62×10^{-12}
573	64.15	9.84×10^{-12}	11.84×10^{-12}
569	47.65	7.39×10^{-12}	11.70×10^{-12}
570	32.18	4.93×10^{-12}	11.66×10^{-12}
571	15.86	2.46×10^{-12}	11.83×10^{-12}

is normally monatomic. It may be mentioned that the solubility of helium in silica glass is in direct proportion to the pressure.[15]

Group IV. Temperatures rising from 187 to 367°C

Following the series of isotherms, a group of 5 determinations were made at temperatures between 187 and 367°C. They are consistent with Curve *C*, Fig. 2. This confirms the small increase in rate due to the heat treatment received by the glass sample in the 2½ weeks subsequent to August 27.

Group V. Temperature rising from 242 to 544°C following 2 weeks heat treatment at 400–350°C

After the series known as Group IV had been completed the sample stood one week at 400°C and one week at 350°C. Rate measurements were then made at approximately 244°, 440°, and 542°C. They indicate a further small increase, about 1–1.5 percent, over the rates in Group III and IV taken two weeks previously. They support the conclusion that further stabilization took place in the glass during this period. Secondly, they confirm the disappearance of the "transformation point." On the other hand, they appear to confirm the reality of a change in slope of the log R *versus* $1/T$ curve at or near 440°C.

Discussion

Interpretation of the energies of activation

The heats of activation computed from the log R *versus* $1/T$ curves for the temperature ranges 350°–440°C and 440°–600°C are *6480* and *7150* calories per mole respectively. For the unannealed glass it is *6920* calories (Temp. 400–500°C). These values may be compared with Van Voorhis'[16] value of 8700 cal. for helium through Pyrex (200° to 500°C), and W. D. Urry's[17] value of 5340 cal. for helium through unannealed Pyrex in the temperature range 81°–283°C.

Two possible factors may determine the magnitude of the activation energy barriers. One is the attraction of helium for the ions of the glass, which we believe to be small compared to the second which is the repulsive force acting on the helium atom as it moves from "hole" to "hole" in the molecular network. This quantity might be quite large in magnitude if the passages through which the helium has to move are very small. The term "hole" as used here indicates a space of about atomic dimensions which is not occupied by any of the ions constituting the glass. Just as a silicate crystal is formed of SiO_4 tetrahedra linked, by sharing of corners, into chains and rings and sheets, these larger units being joined through positive ions, so we believe a silicate glass to have a similar structure, the essential difference being that there is no repeating "unit cell" in the liquid, but only a random arrangement of SiO_4 tetrahedra in space, and secondly, that the centers of gravity about which the atoms oscillate or rotate, themselves move around in a kind of Brownian motion. This sort of structure provides small "open spaces" or "holes" of atomic size in which the diffusing helium atoms may easily stay. On the other hand, considerable energy may be required by a helium atom to allow it to squeeze past its nearest oxygen neighbors and find a similar "hole." The magnitude of the repulsive energy developed as the helium atom passes through a small molecular orifice will depend on an inverse 6th or 7th power law integrated over all the ions which act on a given helium atom as it moves from the center of its "hole" to the tightest point in the orifice. At present exact calculation of this energy from fundamental electrostatic or wave-mechanical theory cannot be made. Analogous calculations have, however, been made by Barrer,[18] who has

Table II.

Diameter of Square	Energy (cal/mole)
3.6A	13,920
3.8	8,393
4.0	4,250
4.2	2,183
4.4	1,078

[15] G. A. Williams and J. B. Ferguson, "The Solubility of Helium and Hydrogen in Heated Silica Glass and the Relation of this to the Permeability," J. Am. Chem. Soc. **46**, 635–639 (1924).

[16] C. C. Van Voorhis, "The Diffusion of Helium Through Several Widely Different Glasses," Phys. Rev. **A23**, 557 (1924).

[17] W. D. Urry, "Further Studies in the Rare Gases. I. The Permeability of Various Glasses to Helium," J. Am. Chem. Soc. **54**, 3887–3901 (1932).

[18] R. M. Barrer, "The Mechanism of Activated Diffusion Through Silica Glasses," J. Chem. Soc. (London) 378–86 (1934).

considered how the size of a hole between four helium atoms arranged at the corners of a square affects the energy required to bring in a fifth helium atom from an infinite distance normal to the square so that it finally rests in the center of the plane. Table II is taken from Barrer's article, page 385.

It will be seen that not only are the repulsive energies several thousand calories in magnitude and therefore comparable to those actually observed in the present work, but also they are quite sensitive to small changes in the size of the hole when the size is nearly the same as that of the atom which is being squeezed. This may partly explain why heat treatment of the glass changes the activation energy for helium diffusion.

Changes resulting from heat treatment

1. *The "transformation point."*—One question to which the diffusion data have given a clear answer is the nature of the "transformation point." The log R *versus* $1/T$ plot for the stabilized glass (Curve C) is exactly linear from about 440°C to 600°C and shows no discontinuity or change in direction at or near 550°C which is the approximate temperature at which the expansion coefficient shows large increase. Since each diffusion measurement was of several hours duration the data may be regarded as static, in contrast to the dynamic expansion measurements. The conclusions must be drawn that a viscous liquid and a stabilized glass are continuous with one another in properties and that the "transformation point" is purely a property of the unstabilized glass. It is merely a temperature at which the viscosity is low enough to permit rapid stabilization by molecular rearrangement, thus leading to equilibrium between the forces of association and dissociation. These views are in harmony with those of Lillie,[2] Littleton,[4] and Weyl[19] but contrary to those of Berger[20] and others.

2. *Strained and annealed glass.*—Various workers have noted that heat treatment affects the permeability of glass to gases. Tsai and Hogness[21] state "We find that silica glass when heated to a high temperature undergoes a permanent change which results in a noticeably greater permeability for helium. The permeability depends somewhat on the previous heat treatment of the glass." Other workers have recorded that various samples of the same glass, e.g. fused silica, gave different permeabilities, without ascribing any reason for it. An examination of Fig. 2 shows that the rate of diffusion of helium through the Pyrex glass after annealing (Group II) was about 10 percent greater than that through the unannealed Pyrex (Group I). This large increase occurs despite the fact that Pyrex glass becomes denser (of higher specific gravity), as a result of annealing. This is shown by the density values 2.236 (annealed) and 2.233 (chilled).[22]

These densities do not show the maximum spread which may be obtained under special conditions. On the other hand, they are in line with the usual experience that the chilled glass is less dense, and they fail to explain the lower permeability of this glass. The conclusion must follow that the chilled or unannealed glass is in a dissociated and unsaturated state which for some reason, either purely geometric or because of stronger chemical binding forces, delays the progress of the diffusing atoms. The idea of chemical unsaturation of the unannealed glass is in agreement with the views of W. Weyl based on absorption spectra. It has also been known for many years that unannealed glass is more susceptible to chemical attack then the annealed product.

The 440°C effect.—Figure 2, Curve C, shows two straight lines which meet at approximately 440°C. Above this temperature the rate of diffusion is expressed by

$$-\log R = 9.075 + 1562/T,$$

while below it, at least down to 350°C, the rate is given by

$$-\log R = 9.285 + 1415/T.$$

This change in slope occurs whether one approaches 440°C from above or below and with

[19] W. Weyl, "On The Constitution of Glasses," Glastech. Berichte **10**, 541 (1932).

[20] A. Klemm and E. Berger, "The Change in Transmission of Glasses with Temperature Above and Below the Transformation Point," Glastech. Berichte **14**, 194–206 (1936); E. Berger, "Contributions to the Theory of Glass Formation and the Glassy State," J. Am. Cer. Soc. **15**, 647–677 (1932).

[21] L. S. Tsai and T. R. Hogness, "Diffusion of Gases Through Fused Quartz," J. Phys. Chem. **36**, 2595–2600 (1932).

[22] H. R. Lillie, personal communication.

essentially static measurements (three hours per point).

Since there is no known pecularity in the properties of helium at 440°C it is believed that the effect is due to the Pyrex glass. The following hypothesis is tentatively advanced. The thermal energy of the glass at any temperature consists in atomic and molecular motion of translation, oscillation and rotation. It is possible that at or near 440°C a new degree of freedom is gained, i.e., above this temperature some molecule like SiO_4 may rotate about one axis with respect to the rest of the complex, while below 440°C it may not.

A recent paper by Smyth[23] presents evidence pertaining to rotation in crystal lattices. In NH_4NO_3 and $NaNO_3$ the NO_3 ion begins to rotate in the plane of its ions at 84°C and at 275° respectively. Similarly in NH_4Cl, NH_4Br and NH_4I rotation of the NH_4 ion sets in at $-30°$, $-38°$ and $-42°$, respectively. Many other examples are discussed by Smyth, who points out that the shape of the molecule is an important factor, and that symmetrical groups like NH_4, PH_4 (or SiO_4) rotate more easily than groups of lower symmetry.

No claim is made for great sharpness (small temperature range) of the "break" at 440°. As far as the experimental evidence is concerned it may actually extend over several degrees. In crystals the effect may be sudden or gradual. The writers have no data on dielectric constants for Pyrex in this temperature range, but such information would be useful to test this hypothesis. Since we regard glass as a highly viscous liquid, the following statement by Smyth is of interest. "From a molecular point of view, the essential difference between a solid with rotating molecules and a liquid is that the molecules of a solid are vibrating about points fixed in a lattice, while molecules of the liquid are vibrating about points which migrate slowly and irregularly through the liquid."

It is obvious that more glasses and in particular glasses of simple composition should be studied in order to get more light on this hypothesis. It seems highly probable that the increased loosening of the lattice because of a rotation (or an extra degree of vibrational freedom) would permit more rapid diffusion of helium, as observed.

It is also clear that exact specific heat or similar information on crystalline silicates on simple chemical composition would be of value in connection with the above mentioned hypothesis.

Diffusion of Hydrogen

Two determinations were made at 787.5°K (512.5°C) on the rate of diffusion of hydrogen. The first, with the hydrogen under a pressure of 78.04 cm Hg, led to a value $dm/dt = 1.908 \times 10^{-13}$, from which $R = dm/dt = 1.858 \times 10^{-13}$ when calculated for a pressure drop of 1 atmosphere (76 cm Hg). The second, with a measured hydrogen pressure of 41.44 cm, gave a value of $dm/dt = 1.017 \times 10^{-13}$ from which $R = dm/dt = 1.865 \times 10^{-13}$ when calculated for a pressure drop of 1 atmosphere.

The agreement between these two results shows that the rate of diffusion of hydrogen is directly proportional to the pressure, and not to the square root of the pressure as is the case when hydrogen diffuses through metals. It appears that the two hydrogen atoms diffuse through Pyrex glass in pairs, rather than as separate atoms.

A comparison of the rate of diffusion of hydrogen and helium at 787°K (512°C) indicates that the helium diffuses about 45 or 46 times as fast as does hydrogen at this temperature.

Even at 120°C the diffusion of hydrogen into glass is perceptible. W. Weyl[24] has produced fluorescence by reduction of dissolved Ag_2O to the free atoms by hydrogen at this temperature.

[23] C. P. Smyth, "The Dielectric Constants of Solids and Molecular Rotation," Chem. Review **19**, 329–361 (1936).

[24] W. Weyl, "Contribution to the Fluorescence of Glasses," Sprechsaal **70** (1937), No. 46.

Free Volumes and Free Angle Ratios of Molecules in Liquids

JOHN F. KINCAID[1] AND HENRY EYRING
Frick Chemical Laboratory, Princeton University, Princeton, New Jersey

(Received July 21, 1938)

The free volume is defined as the total integral over that part of the potential energy of the molecule in the liquid which is due to thermal displacements of the center of gravity of the molecule from its equilibrium position. The free angle is the corresponding integral over angular displacements of the molecule. The free volume, V_f is related to the velocity of sound, u, in the liquid by

$$u\ (\text{liquid}) = u\ (\text{gas})\ (V/V_f)^{\frac{1}{3}}.$$

This equation is used to derive a formula connecting the sound velocity in the liquid with its thermal conductivity. The quantity, $RT/p \exp(\Delta H/RT)$, gives the *product* of the free angle ratio and the free volume, rather than the free volume itself. Here p is the vapor pressure and ΔH is the heat of vaporization. The free volumes from sound velocities agree with those determined by independent methods. Specific heats, entropies of vaporization, the spectroscopic observations of Cartwright, and the differences between sound velocity, free volumes and the function $RT/p \times \exp(\Delta H/RT)$ are examined from the point of view of restricted rotation of the molecules in liquids. Lack of free rotation of molecules suffices to explain the abnormalities of the liquids examined. The dielectric constants of polar liquids are interpreted assuming restricted rotation and the following formula is derived:

$$\mu_l^2 \mu_g^{-2} = 1 - ((1 - \cos\theta_1)/2)^2,$$

where μ_l is the apparent dipole moment of the molecule in the liquid, μ_g is the dipole moment as determined from measurements in the gas phase, and θ_1, is the polar angle related to the free angle ratio, δ_2, by

$$\delta_2 = (1 - \cos\theta_1)/2.$$

The concept of restricted rotation of the molecules in the liquid accounts satisfactorily for the observed dielectric polarizations of water and methyl alcohol.

INTRODUCTION

IN the present paper certain kinetic theory formulae for gases are modified in such a way as to make them applicable to liquids. The point of view employed is to treat the molecule moving in its free volume in the liquid as equivalent to the molecule moving in the total volume in the gas phase. Using this notion it is possible to derive a new formula for the velocity of sound in liquids in terms of the velocity in the gas phase, the total volume and the free volume of the liquid. An equation very similar to that given by Bridgman[2] for the thermal conductivity of liquids also follows from such considerations.

The term, *free volume*, as employed here denotes the total integral over that part of the potential energy which is due to thermal displacements of the center of gravity of the molecule from its equilibrium position. The name, *free angle*, is introduced to refer to the corresponding integral over angular displacement of the molecule around its center of gravity. For linear molecules the *free angle ratio* is the free angle divided by 4π, and for nonlinear ones an analogous definition holds. The free angle ratio is a convenient quantity to employ since it is given by the ratio of the partition functions for the restricted rotation of the molecule in the liquid, and its free rotation in the gas phase. The free angle ratio thus extends from a lower value (greater than zero) to unity depending on whether the molecule is held tightly in its position or is allowed to turn freely about its axes. For linear molecules the free angle ratio includes two degrees of rotational freedom, and is designated by the symbol, δ_2. For more complicated molecules, three degrees of rotational freedom must be taken into account and the corresponding symbol is δ_3.

To a first approximation both the free volume and the free angle ratio may be thought of as regions in which completely free displacement occurs, the regions being surrounded by infinite potential walls. This is the hard spheres approximation previously employed by Eyring, Hirschfelder and Stevenson[3, 4] to yield the ex-

[1] Present address, University of Rochester, Rochester, New York.

[2] P. W. Bridgman, *The Physics of High Pressures* (Macmillan Co., 1931).

[3] H. Eyring and J. O. Hirschfelder, J. Phys. Chem. **41** 249 (1937).

[4] J. O. Hirschfelder, D. P. Stevenson and H. Eyring, J. Chem. Phys. **5**, 896 (1937).

pression for the free volume,

$$V_f=\frac{1}{V^{\frac{2}{3}}}\left[\frac{2RT}{P+(\partial E/\partial V)_T}\right]^3, \quad (1)$$

where V is the molal volume of the liquid, R is the gas constant per mole, T is the absolute temperature, and E is the thermodynamic energy. It is, however, not necessary to consider the molecules as hard spheres, and Kincaid and Eyring[5] have given a treatment of liquid mercury in which the size of the molecules is presumed to vary both with temperature and volume. The dynamic potential curve[6] in this case is a parabola with a flat bottom.

For monatomic liquids, the free volume is defined by,

$$V_f=RT/p \exp(\Delta H/RT), \quad (2)$$

where p is the vapor pressure of the liquid, and ΔH is the heat of vaporization. For liquids composed of polyatomic, nonspherical molecules, the expression on the right of Eq. (2) is equal to the product of the free volume, and the free angle ratio. When the molecules in the liquid do not rotate freely, this quantity will necessarily be smaller than the free volume.

The Use of Kinetic Theory Equations for Liquids

Velocity of sound in liquids

The velocity of sound, u, in any homogeneous medium is given by the general hydrodynamic formula:

$$u=(v/\beta_s)^{\frac{1}{2}}, \quad (3)$$

where v is the specific volume and β_s is the adiabatic compressibility defined by $\beta_s \equiv -1/v \times(\partial v/\partial P)_s$. For the special case of an ideal gas, (3) becomes

$$u=(RT\gamma/M)^{\frac{1}{2}},$$

where γ is the ratio of the specific heat at constant pressure to that at constant volume, and M is the molecular weight of the gas.

Equation (4) may be compared to that for $\bar{c}$, the average kinetic theory velocity of the molecules.

$$\bar{c}=(8RT/\pi M)^{\frac{1}{2}}. \quad (5)$$

It is seen that u is proportional to $\bar{c}$ but is slightly smaller since the factor $(8/\pi)^{\frac{1}{2}}$ is always greater than $\gamma^{\frac{1}{2}}$. This is what one might suppose since a wave propagated by matter would hardly be expected to travel faster than the molecules which carry it. However, when the velocity of sound in liquids is compared to the kinetic theory velocity of the molecules it is found that u for most liquids is greater than $\bar{c}$ by factors ranging from five to ten. For example for benzene at 25°C, $\bar{c}$ is 2.83×10^4, u(gas) is 1.88×10^4, while u(liquid) is 13.0×10^4 cm/sec. Fig. I illustrates the mechanism responsible for the fact that the velocity of sound in liquids can be so much greater than the kinetic theory velocity of the molecules. The wave front is assumed to travel from the edge of molecule A to the adjacent edge of molecule B with the velocity given by Eq. (4). As A collides with B, however, the signal is transmitted almost instantaneously to the opposite edge of molecule B. Since the ratio of the total distance to the free space between two points in a liquid is given by

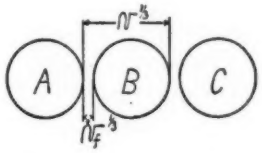

FIG. 1. Illustration of the mechanism which explains the observation that the velocity of sound in liquids is greater than the kinetic theory velocity of the molecules.

the ratio $(V/V_f)^{\frac{1}{3}}$, this leads at once to the equation,[7]

[5] John F. Kincaid and H. Eyring, J. Chem. Phys. **5**, 587 (1937).

[6] The *dynamic potential curve* is defined as the curve for which the corresponding partition function, when raised to the $3N$th power, is the translational partition function for the liquid as a whole aside from an exponential potential energy factor.

[7] Equation (1) of this paper is Eq. (13) of the paper by Eyring and Hirschfelder and was there derived from the expression $V_f^{\frac{1}{3}}=2(V^{\frac{1}{3}}-d)$ assuming $(\partial d/\partial V)_T$ equals zero, i.e., the hard sphere model. Eq. (1) is obtained by the same procedure from the expression $V_f=(V^{\frac{1}{3}}-d)$ provided $(\partial d/\partial V)_T$ has the appropriate negative value. This corresponds to getting more free volume from increasing $(V^{\frac{1}{3}}-d)$ than one would get if the sides of the free volume were flat faces. Since the sides of the free volume are spheres this sign of $(\partial d/\partial V)_T$ is obvious *a priori*. The necessity of going beyond the simplest hard sphere model has been encountered in two previous papers. See Eq. (22) of Kincaid and Eyring[4] and Eq. (21) of Hirschfelder, Stevenson and Eyring.[3] However, it is possible that Eq. (6) should be employed in the more general form, u(liquid) $=cu$(gas) $(V/V_f)^{\frac{1}{3}}$ when c is a proportionality constant not necessarily equal to unity.

$$u(\text{liquid}) = u(\text{gas})(V/V_f)^{\frac{1}{2}} = (RT\gamma/M)^{\frac{1}{2}}(V/V_f)^{\frac{1}{2}}. \quad (6)$$

Equation (6) may be employed either to find the velocity of sound in liquids if V_f is known from some other source, or to determine free volumes if sound velocity measurements have been made. A detailed comparison of free volumes computed by this and various other methods will be made in a later section.

Thermal conductivity of liquids

A straightforward application of the kinetic theory of gases gives the relation for the thermal conductivity K,

$$K(\text{gas}) = \tfrac{1}{3}(V/V_f)^{\frac{1}{2}}\bar{c}Lc_v, \quad (7)$$

where $(V/V_f)^{\frac{1}{2}}$ is the number of molecules per cc, L is the mean free path, and c_v is the specific heat per molecule. It is found, however, that Eq. (7) gives values which are too low for the thermal conductivity of gases, and Loeb[8] gives the correction factor $\frac{1}{4}(9\gamma'-5)$, where γ' is the ratio of c_p to c_v. Eq. (7) may now be rewritten,

$$K(\text{gas}) = \tfrac{1}{3}[\tfrac{1}{4}(9\gamma'-5)](V/V_f)^{\frac{1}{2}}\bar{c}Lc_v, \quad (8)$$

a relation which may be tested in the form,

$$K(\text{gas}) = \eta(c_v/m)\tfrac{1}{4}(9\gamma'-5), \quad (9)$$

since the viscosity, η, is given by $\frac{1}{3}(N/V)m\bar{c}L$. Eq. (9) has been observed to give excellent agreement with experiment.[8]

In order to convert Eq. (8) into a form applicable to liquids the following identifications may be made. (N/V) becomes the number of molecules per cc of liquid rather than per cc of gas. The average velocity $\bar{c}$ must be multiplied by the ratio, $(V/V_f)^{\frac{1}{2}}$, for the same reasons as are given above for justifying Eq. (6). The distance that the energy is carried is now $(V/N)^{\frac{1}{3}}$ rather than L, the mean free path for the gas. c_v for the gas is replaced by αc_v, where α is the accommodation coefficient which takes account of the number of degrees of freedom which come into equilibrium in the thermal conduction process. Making all these substitutions we have:

$$K(\text{liquid}) = 1/12(9\gamma'-5)(N/V)(8RT/\pi M)^{\frac{1}{2}} \times (V/V_f)^{\frac{1}{2}}(V/N)^{\frac{1}{3}}(\alpha c_v), \quad (10)$$

[8] Leonard B. Loeb, *Kinetic Theory of Gases* (McGraw-Hill Book Co., 1927).

TABLE I. *Comparison of the observed thermal conductivities of liquids at 30°C with those computed from Eq. (12).*

SUBSTANCE	K(OBS.)[9]	K(CALC.)[10]	$\frac{K(\text{OBS.})}{K(\text{CALC.})}$
Methyl Alcohol	21.1×10^3 c.g.s. Units	22.3	0.95
Ethyl Alcohol	18.0	19.2	.94
Propyl Alcohol	15.4	17.3	.89
Butyl Alcohol	16.7	13.3	1.26
Iso-Amyl Alcohol	14.8	14.1	1.05
Ether	13.7	10.9	1.26
Acetone	17.9	16.3	1.10
Carbon Bisulfide	15.9	16.1	0.99
Ethyl Bromide	12.0	12.8	.94
Ethyl Iodide	11.1	10.6	1.05
Water	60.1	51.7	1.16

a formula which reduces to

$$K(\text{liquid}) = 1/12(9\gamma'-5)(8/\pi\gamma)^{\frac{1}{2}} \times (NV)^{\frac{1}{3}}u(\alpha c_v). \quad (11)$$

Here u is the velocity of sound in the liquid, γ' is the effective value of the ratio of c_p to c_v for thermal conduction in the gas, and γ is the same quantity for the transmission of sound.

In order to have formula (11) reduce to the one successfully employed by Brdigman,[2] αc_v must be assigned the value $3k$ per molecule. For the polyatomic liquids which Bridgman studied, this is understandable if only the kinetic energy of translation and rotation transfer appreciable energy in the process of thermal conduction. Using a value of c_v equal to $3k$, γ' becomes 4/3 and (11) reduces to,

$$K(\text{liquid}) = 0.931(1/\gamma)^{\frac{1}{2}}3k(N/V)^{\frac{1}{3}}u. \quad (12)$$

This formula has the same form as that employed by Bridgman,[2] but the numerical coefficient is about 12 percent smaller, as a result of the factor $0.931/\gamma^{\frac{1}{2}}$ replacing unity in his expression.

Table I shows values for K at 30° for a number of liquids computed by (12) for comparison with Bridgman's experimental values. The agreement is somewhat better than Bridgman's earlier computations. Since carbon bisulfide is a linear molecule, the computation for this substance was made with a value of αc_v equal to $2.5k$, and a corresponding value of γ' of 1.40. The excellent agreement of the observed value with the one calculated in this way suggests that the liquid rare gases would be interesting substances with which to check the theory. A value for αc_v of

[9] P. W. Bridgman, Proc. Am. Acad. **59**, 109 (1923).

[10] γ values secured from K. Bennewitz, and W. Rossner, Zeits. f. physik. Chemie **B39**, 126 (1938). Sound velocity measurements from Bridgman[9] or Freyer, Hubbard and Andrews.[12]

about $3k$ would also be obtained from the translational contribution alone, if potential energy were included. Thus from data for the condensed rare gases, one will be able to determine whether or not potential as well as kinetic energy comes into equilibrium in the thermal conduction process in liquids.

Equation (12) not only works remarkably well for the variation of K from liquid to liquid at atmospheric pressure, but, as Bridgman has pointed out, it also gives approximately the temperature variation of K. It is therefore quite surprising that it does not predict the pressure effect correctly. Whereas most liquids increase their thermal conductivity by approximately a factor of 2 on going from atmospheric pressure to 12,000 atmospheres,[2] the formula predicts an increase by about a factor of 4. This is plausibly explained by a decrease in the value of α due to quantization of the mass motions of the molecules at high pressures. The effective heat capacity, αc_v, would have to become $1.5k$ in order to explain the observations at the highest pressures to which the experiments extend.

Debye[11] has treated the problem of the thermal conductivity of solids, with special reference to effects at low temperatures. The essential difference between his treatment and the one given above is that the identification of L with $(V/N)^{\frac{1}{3}}$ in the derivation of Eq. (12) is equivalent to assuming that each molecule acts independently while the essence of Debye's treatment lies in his assumption that the molecules are strongly coupled in such a way as to produce elastic waves of long wave-length. The effect of coupling, enabling the heat impulses to be transmitted by distances greater than the intermolecular distances without scattering is, however, important only at low temperatures. For most liquids it appears to be more satisfactory to treat the problem in essentially the manner indicated.

A comparison of values for free volumes of liquids computed by various methods

Since more complete data exist for benzene than for any other nonmetallic and nonpolar liquid, its free volume was computed by all available methods. The agreement between the various methods is seen by inspection of Table II to be very satisfactory. C_v for liquid benzene exceeds the gaseous value by 5 calories per mole per degree. This suggests lack of free rotation about two axes for the molecules in the liquid. On the other hand the sound velocity method gives a free volume only slightly greater than the product of free volume with free angle ratio as determined from vapor pressures, indicating a free angle ratio not greatly less than unity.

TABLE II. *The free volume of benzene as a function of temperature at atmospheric pressure.*

τ°C	V_f FROM[12, 13] Eq. (6) (Sound Velocity)	$\delta_3 V_f$ FROM[14] Eq. (2) (Vapor Pressure)	V_f FROM[15] Eq. (1) (Energy Volume Coefficient)
5°	0.193 cc		0.214 cc
25°	.272	0.238 cc	.288
50°	.411	.419	.423
75°		.727	.633
100°		1.24	.99

In general reliable values for heats of vaporization are not available over a sufficiently large temperature range to make possible a significant comparison of the absolute magnitude and temperature coefficients of the free volumes from vapor pressure with free volumes from sound velocity. However, although Eq. (1) is an approximate relation based on a very simple model, inspection of Table II reveals good agreement between values based on this relation and those calculated from vapor pressures. On the strength of this agreement, free volumes were computed by Eqs. (1) and (6) for a number of liquids for which the necessary data are given by Freyer, Hubbard and Andrews.[12] The results are shown in Table III. Although the computation of free volumes from vapor pressures and heats of vaporization is not a practical procedure for many liquids because of uncertainties in experimental heats of vaporization, the converse calcu-

[11] P. Debye, *Wolfskehl-Vorträge zu Göttingen* (Leipzig, 1914), Anhang p. 46. See also, Max Born, *Atomtheorie des Festen Zustandes* (B. G. Teubner, Leipzig, 1923), p. 707.

[12] Sound velocity data from E. B. Freyer, J. C. Hubbard and D. H. Andrews, J. Am. Chem. Soc. **51**, 759 (1929).

[13] Values of γ for computing μ for the gas were secured from the frequencies given by R. C. Lord and D. H. Andrews, J. Phys. Chem. **41**, 141 (1937).

[14] E. F. Frock, D. C. Ginnings and W. B. Holton, Nat. Bur. Stand. J. Research **6**, 881 (1931). δ_3 is the free angle ratio.

[15] Data from 25° to 65°C from R. E. Gibson and John F. Kincaid, J. Am. Chem. Soc. **60**, 511 (1938). Data at other temperatures extrapolated by a method to be published later.

TABLE III. *Values of the free volume for various liquids.*

SUBSTANCE	ACETONE		ETHER		CHLOROFORM		TOLUENE		CARBON TETRACHLORIDE		CARBON DISULFIDE	
t°C	V_f FROM EQ. (6)	V_f FROM EQ. (1)	V_f FROM EQ. (6)	V_f FROM EQ. (1)	V_f FROM EQ. (6)	V_f FROM EQ. (1)	V_f FROM EQ. (6)	V_f FROM EQ. (1)	V_f FROM EQ. (6)	V_f FROM EQ. (1)	V_f FROM EQ. (6)	V_f FROM EQ. (1)
0			0.48	0.47	0.21	0.25	0.16	0.16	0.16	0.21	0.23	0.45
10			.57	.55	.24	.29	.19	.19	.24	.26	.26	.52
20	0.45	0.54	.70	.65	.29	.34	.22	.22	.28	.31	.30	.58
30			.90	.79	.34	.40	.26	.26	.33	.37	.36	.66
40	.64	.63			.40	.47	.31	.31	.38	.43	.39	.75
50					.48		.36	.36	.45	.50	.47	.84

lation of heats of vaporization from vapor pressures and "sound velocity" free volumes appears to be a useful method.

In order to test the applicability of the sound velocity method of computing free volumes for a metallic liquid, free volumes of mercury as computed from Eq. (6) were compared with those given by the partition function previously published.[5] The expression for V_f is,

$$V_f = N\left[\frac{T/\Theta}{(2\pi mkT)^{\frac{1}{2}}/h} + 2\left(\frac{V}{N}\right)^{\frac{1}{3}} - 2\left(\frac{V_0}{N}\right)^{\frac{1}{3}}\right]^3. \quad (13)$$

Here Θ is the characteristic temperature of the liquid and V_0 is identified as the volume of the liquid at the melting point. Taking Θ equal to 79°, a value consistent with the experimental entropy of fusion, the free volumes shown in Table IV are obtained. It may be noted that the agreement between the values at both low and high pressures is quite satisfactory. This is of particular interest since the free volumes for mercury are of a different order of magnitude than those of the nonmetallic liquids discussed above. However, only a more exact investigation of mercury can establish how satisfactory these values really are.

In order to test the theory for another monatomic liquid, an attempt was made to utilize the somewhat inadequate data for liquid argon. The entropy of liquid argon at its melting point at atmospheric pressure, as computed from the data of Euken[16] is 12.5 E.U. The general formula for the entropy of a liquid is,[17]

$$S = 4R + R \ln (2\pi mkT)^{\frac{3}{2}} V_f / h^3 N \quad (14)$$

and this leads to a value of 0.15 cc for the free volume of liquid argon at its melting point. Taking the specific heats at constant volume and constant pressure given by Euken and Hauck,[18] and the volumes determined by Baly and Donnan,[19] we estimate β_s at the melting point to be 1.29×10^{-10} c.g.s. unit. This corresponds to a value of u equal to 0.74×10^5 cm/sec. and a free volume of 0.35 cc. The agreement to within a factor of two is considered satisfactory in view of the uncertainties in the data. The free volume for argon at its boiling point was determined from its heat of vaporization to be 1.25 cc. Since other methods yield much smaller values, it appears to us that the accepted figure for the heat of vaporization must be too low. A value of 1.65

TABLE IV. *Free volumes for liquid mercury at different temperatures and pressures.*

t°C	P(ATM.)	V_f FROM EQ. (6)	V_f FROM EQ. (13)
−39°	1		0.0081 cc
0	1	0.0120 cc	.0120
100°	1	.0220	.0256
200°	1		.0434
300°	1		.0718
357°	1		.0904
0°	1	.0120	.0120
0°	1000	.0117	.0116
0°	2000	.0114	.0114
0°	3000	.0111	.0111
0°	4000	.0107	.0109
0°	5000	.0104	.0107
0°	6000	.0101	.0105
0°	7000	.0098	.0103

[16] A. Euken, Verh. D. phys. Ges. **18**, 4 (1916).

[17] This formula in the exact form given depends on a contribution of R to the entropy of fusion resulting from the communal sharing of the free volume. It also is dependent on the assumption that each molecule moves on a parabolic dynamic energy curve, and on the vanishing of the derivative $(\partial E_s/\partial T)_T$, where E_s is the static energy previously defined (Ref. 5). It is believed that these simplifications do not lead to serious error in this case.

[18] A. Euken, and F. Hauck, Zeits. f. physik. Chemie **134**, 161 (1928).

[19] E. C. C. Baly, and F. G. Donnan, J. Chem. Soc. **81**, 907 (1902).

kcal./mole, 10 percent greater than that given in the *International Critical Tables*, is indicated by the theory.

Determination of free volumes from spectroscopy

The frequency of vibration of molecules in liquids is related to the free volume by the approximate relationship,

$$\frac{(2\pi mkT)^{\frac{1}{2}}}{h}\frac{V^{\frac{1}{3}}}{u}\left(\frac{RT\gamma}{M}\right)^{\frac{1}{2}}=N^{\frac{1}{3}}\frac{kT}{h\nu}$$

$$=\frac{(2\pi mkT)^{\frac{1}{2}}}{h}V_f^{\frac{1}{3}}, \quad (15)$$

which connects the velocity of sound in the liquid with the energy $h\nu$ for a translational degree of freedom. Thus one would expect the light scattered from liquids to show the familiar Stokes and anti-Stokes lines of the Raman spectrum corresponding to energies from 10 to 100 cm^{-1}. Such lines have been observed[20] and as Debye[21] has remarked they show the same correlation between frequency and sound velocity to be expected from Eq. (15). This method of arriving at free volumes will no doubt become of increasing importance.

Restricted Rotation of Molecules in Liquids

Heat capacity as a criterion of restricted rotation

Most of the available data for the quantity C_v(liquid) minus C_v(ideal gas) has been summarized in Table V. It is seen that in all cases the heat capacity at constant volume for the liquid is greater than the ideal gas value and that this inequality persists up to the critical point. Considering first the two examples of monatomic liquids which are given in the table, we note differences of 2.6 and 3.1 calories per mole per degree for argon and mercury respectively at their melting points. These are just the differences to be expected if three degrees of translational freedom for the molecule in the vapor have become vibrations in the liquid.

The data for liquids composed of more complex molecules can be interpreted in terms of hindered rotation of the molecules. If rotational degrees of freedom of the molecules in the vapor become librations[22] in the liquid we would expect a specific heat difference between liquid and ideal gas of about one calorie per mole per degree for each degree of freedom so affected. This may, of course, be modified by anharmonic terms in the

TABLE V. *Difference between the specific heats at constant volume for the ideal gas and the liquid for various substances at different temperatures.*[29]

Argon[23]		Mercury[5]		Carbon Disfulide[12, 24]		Carbon Tetrachloride[12, 26]		
T°K	C_v(LIQ) $-C_v$(IDEAL GAS)	T°K	C_v(LIQ) $-C_v$(IDEAL GAS)	T°K	C_v(LIQ) $-C_v$(IDEAL GAS)	T°K	C_v(LIQ) $-C_v$(IDEAL GAS)	
84°	(2.6)	234°	3.1	160°	(4.7)	250°	(4.0)	Melting Point
		370°	2.6	210°	(3.9)	280°	3.8	
		500°	2.4	265°	3.1	310°	3.4	
87°	2.5	630°	2.3	319°	2.3	349°	(3.0)	Boiling Point
156°	1.1							Critical Point

T Chloroform[12, 26]		Benzene[12, 27]		Ethylene[25, 25, 28]		
T°K	C_v(LIQ) $-C_v$(IDEAL GAS)	T°K	C_v(LIQ) $-C_v$(IDEAL GAS)	T°K	C_v(LIQ) $-C_v$(IDEAL GAS)	
203°	(6.7)	278°	5.3	104°	5.3	Melting Point
250°	(6.3)	300°	5.0	125°	5.3	
290°	5.3	325°	4.9	150°	5.3	
334°	4.7	353°	4.9	170°	5.3	Boiling Point
				283°	(4.2)	Critical Point

[20] E. Gross, and M. Vuks, Nature **135**, 998 (1935).
[21] P. Debye, Chem. Rev. **19**, 171 (1936).
[22] Libration is used here to mean restricted rotation.
[23] A. Euken and Hauck, Zeits. f. physik. Chemie **134**, 161 (1938).
[24] Paul C. Cross, J. Chem. Phys. **3**, 825 (1935).
[25] G. B. Kistiakowsky and Falih Nazmi, J. Chem. Phys. **6**, 18 (1938).
[26] Robert D. Vold, J. Am. Chem. Soc. **59**, 1192 (1935).
[27] R. C. Lord and D. H. Andrews, J. Phys. Chem. **41**, 149 (1937).
[28] Mathies E. Haas and Gebhart Stegeman, J. Phys. Chem. **36**, 2125 (1932).
[29] The data for specific heats at constant volume for the vapors are, in most cases, calculations from spectroscopic data. The references give either the computations or the necessary data for making them. Extrapolated values are given in parentheses.

potential functions. On this basis the difference of 5.3 calories per mole per degree shown by benzene and ethylene near their melting points is interpreted as being due to vibrations for five of the degrees of freedom and free rotation about the axis perpendicular to the plane of the molecule for the other. It is significant that carbon tetrachloride, a symmetrical molecule, has a smaller difference between the specific heats of liquid and vapor than chloroform, a relatively unsymmetrical one. The data indicate that even carbon disulfide does not rotate freely in the liquid, but the figures at the two lowest temperatures recorded must be interpreted with some caution since they represent long extrapolations. The same is true of the chloroform data. The high value of 4.2 calories per mole per degree for the difference between the observed and the ideal gas value for ethylene at the critical point may be due to a change with temperature of association into double and triple molecules, assuming, of course, that the data are correct. Any hypothesis of hindered rotation at such large volumes appears unlikely.

Since the data indicate that the effect of rising temperature, and thus of increasing volume, is to reduce the potential restricting rotation, it is of interest to examine the effect of volume changes alone on this potential. This can be done by examining the effect of pressure on the specific heat at constant volume of those liquids for which adequate data are available. Table VI shows values of C_v for liquid benzene at various pressures and temperatures. The contribution of the internal vibrations to the specific heat have been subtracted from the thermodynamic C_v. It is necessary to assume that this contribution is independent of pressure since no data are available on the effect of high pressures on the frequencies corresponding to the normal modes of vibration of molecules. Assuming that this effect will not change the qualitative aspects of the data we have the result that the heat capacity at constant volume is considerably greater at 1000 bars[31] than at low pressures. The fact that C_v rises to as high a value as 12.1 calories per mole per degree appears to indicate that at high pressures there is restricted rotation even about the axis perpendicular to the plane of the ring.

TABLE VI. *The heat capacity at constant volume of liquid benzene under pressure.*[30]

t°K	1 BAR	250 BARS	500 BARS	750 BARS	1000 BARS
298.1°	11.0	11.1	11.3	11.5	11.7
308.1°	10.9	11.0	11.2	11.5	11.7
318.1°	10.8	11.1	11.3	11.6	11.8
328.1°	10.8	11.2	11.4	11.7	11.9
338.1°	10.7	11.2	11.4	11.8	12.1

[30] The units are calories per mole per degree. The changes of specific heat with pressure were computed from the data of Gibson and Kincaid[15] using the thermodynamic equations,

$$dC_p/dP = -Td^2V/dT^2 \quad \text{and} \quad C_p - C_v = T\alpha^2 V/\beta,$$

where C_p is the specific heat at constant pressure, and α and β are defined as,

$$\alpha = 1/V(\partial V/\partial T)_p, \quad \beta = -1/V(\partial V/\partial P)_T.$$

The values for C_p at one bar are the weighted mean of the data given in Landolt-Börnstein, *Tabellen*. The contributions to the specific heat made by the internal vibrations were computed from the frequencies given by Lord and Andrews.[27]

The free angle ratio from spectroscopy

When the velocity of sound in liquid water is used to compute V_f at room temperature a value of about 0.4 cc is secured. On the other hand, the product $\delta_3 V_f$ as determined from heats of vaporization and vapor pressures at the same temperature is about 0.02 cc. A reasonable interpretation is to assign the discrepancy of a factor of about 20 to a small free angle ratio. A

TABLE VII. *Free volumes for liquid water.*

t°C	V_f FROM[32] EQ. (6) (SOUND VELOCITY)	$\delta_3 V_f$ FROM EQ. (2) (VAPOR PRESSURE)	$1/\delta_3$[33] (FROM SPECTROSCOPY)	$(\delta_3 V_f)1/\delta_3$
0	0.44 cc	0.0095 cc	26	0.25 cc
10	.43	.012	25	.36
20	.42	.014	25	.35
30	.42	.017	24	.41
40	.43	.021	24	.50
50		.025	24	.60
75		.040	24	.96
100		.062	24	1.5

[31] The bar, or metric atmosphere, is equal to 10^6 dynes per square centimeter. This is approximately one normal atmosphere.

[32] Sound velocity data from J. C. Hubbard and A. L. Loomis, Phil. Mag. **5**, 1177 (1928).

[33] $1/\delta_3$ computed from the relation

$$1/\delta_3 = \left[\frac{8\pi^2(8\pi^3(kT)^3ABC)^{\frac{1}{2}}}{h^3}\right]\left[\left(\frac{1}{1-\exp(-hc167/kT)}\right)^2 \times \left(\frac{1}{1-\exp(-hc500/kT)}\right)\right]^2$$

with a value of ABC, the products of the principal moments of inertia, equal to 6.1×10^{-120}.

check of this hypothesis is possible. Cartwright[34] has observed frequencies of 167 and 500 cm^{-1} in liquid water at room temperature. These frequencies were interpreted by him as arising from restricted rotation of the molecules. Since three degrees of rotational freedom must be accounted for, at least one of the rather broad absorption regions probably arises from two frequencies, and Stearn and Eyring[35] have employed a doubly degenerate frequency at 167 cm^{-1} to represent approximately this absorption band. Using this approximation we have the values for the free angle ratio shown in Table VII. These were secured by taking the ratio of the partition function for free rotation of the water molecule and the product of the Einstein function corresponding to frequencies of (2) 167 cm^{-1} and 500 cm^{-1}.

It may be seen that the free volume from the vapor pressure, the heat of vaporization, and the observed frequencies is almost exactly equal to the free volume from sound velocity at room temperature, the point at which the spectroscopic observations were made. The discrepancies at other temperatures indicate that the frequencies corresponding to restricted rotation should be greater than those observed at lower temperatures, and smaller at higher temperatures. Such a temperature drift will probably be difficult to observe spectroscopically because rising temperature simply makes the absorption bands broader and more diffuse, as has been observed.[36]

The dielectric constant as a criterion for restricted rotation

In order to have available a new tool for the determination and interpretation of restricted rotation of molecules in liquids, formulas connecting the free angle ratio with the dielectric constant are given. The importance of the free angle ratio in determining vapor pressures and boiling points of liquids may be seen by inspection of Fig. 2 where δ_2 is plotted as a function of the polar angle, θ_1, through which the molecule is free to turn. Here θ_1 is analogous to the angle of colatitude as measured on a globe from the north pole down to a given "parallel," and δ_2 is the corresponding solid angle divided by 4π. The two are connected by the equation,

$$\delta_2 = 1 - \cos\theta_1/2. \tag{15}$$

Here δ_2 is analogous to δ_2 previously defined for linear molecules, but differs from δ_3 for nonlinear ones since it does not take account of the restricted rotation of the molecule about the axis in which the dipole lies. If the potential curves for the rotation of the molecule about the three axes are symmetrical, then δ_2 is equal to the two-thirds power of δ_3. In some actual cases this relation is approximately correct as we shall see later.

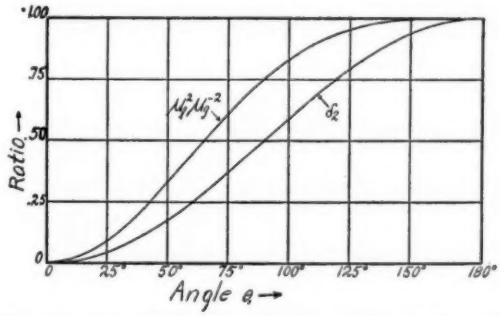

FIG. 2. $\mu_i^2\mu_g^{-2}$ plotted against the polar angle θ_1. This ratio is determined from equation (17) and the relation, $\bar{m}=\mu^2F/3kT$ which holds for the gas.

We next consider dipoles free to orient under the influence of the field in the region between the pole and colatitude θ_1, assuming the poles are distributed at random with respect to the field direction. The expression for the average moment $\bar{m}$, using classical statistics is then:

$$\bar{m}=\frac{1}{4\pi}\int_0^{2\pi}\int_0^{\pi}\left[\frac{\int_0^{2\pi}\int_0^{\theta_1}\exp\left(\frac{\mu F}{kT}\cos\theta_{12}\right)\mu\cos\theta_{12}\sin\theta_1 d\theta_1 d\varphi_1}{\int_0^{2\pi}\int_0^{\theta_1}\exp\left(\frac{\mu F}{kT}\cos\theta_{12}\right)\sin\theta_1 d\theta_1 d\varphi_1}\right]\sin\theta_2 d\theta_2 d\varphi_2. \tag{16}$$

Here θ_{12} is the angle between the dipole and the applied field, F, and μ is the dipole moment. θ_1 and φ_1 are the polar coordinates of the dipole

[34] C. H. Cartwright, Phys. Rev. **49**, 470 (1936).
[35] A. E. Stearn and Henry Eyring, J. Chem. Phys. **5**, 113 (1937).
[36] Paul C. Cross, John Burnham, and Philip A. Leighton, J. Am. Chem. Soc. **59**, 1134 (1937).

with respect to an axis chosen in such a way that the dipole can move with a potential energy which depends only on θ. This potential energy arises from interaction with neighbors. θ_2 and φ_2 give the direction of the applied electric field with respect to the same axis. The evaluation of $\bar{m}$ follows without difficulty using the expansion $\exp(x)=1+x+x^2/2+\cdots$ and the identity $\cos\theta_{12} \equiv \cos\theta_1 \cos\theta_2+\sin\theta_1 \sin\theta_2(\sin\varphi_1 \sin\varphi_2 +\cos\varphi_1 \cos\varphi_2)$. The result is

$$\bar{m}=\frac{\mu^2 F}{3kT}\left[1-\left(\frac{1+\cos\theta_1}{2}\right)^2\right]. \tag{17}$$

Higher powers of $\mu F/kT$ are readily calculable, but are in general negligible.

The values for δ_2 and $\mu_i^2\mu_g^{-2}$ as a function of θ_1 are tabulated in Table VIII and shown in Fig. 2. Here μ_g is the dipole moment which is calculated from measurements on the gas, while μ_i is the value calculated in the same way if the rotation is restricted to lie between the polar angles 0 to θ_1.

If in addition to moving freely between 0 and θ_1 an extra potential energy E permits the dipole to move between θ_1 and 180°, the equation corresponding to (16) gives,

$$\bar{m}=\frac{\mu^2 F}{3kT}\left[1-\left(\frac{\sin^2\theta_1(1-\exp(-E/RT))}{2(1-\cos\theta_1+(1+\cos\theta_1)\exp(-E/RT))}\right)^2\right]. \tag{18}$$

Finally if the potential energy for rotation between 0° and θ_1° is zero, between θ_1 and θ_2 is E, and between θ_2 and 180° is again zero, then the analog to (16) gives

$$\bar{m}=\frac{\mu^2 F}{3kT}\left[1-\tfrac{1}{4}\left(\frac{(\sin^2\theta_1-\sin^2\theta_2)(1-\exp(-E/RT))}{2+(\cos\theta_2-\cos\theta_1)(1-\exp(-E/RT))}\right)^2\right]. \tag{19}$$

Other cases can be obtained in a similar way but these will suffice for our purpose.

Consider first the application of the theory to a solution of a polar substance in a nonpolar solvent. If the solution is sufficiently dilute for interactions between the dipoles to be negligible, any restriction on the free rotation of the polar molecule is imposed by the nonpolar molecules around it. Under these conditions, the polar molecules can orient in the solution with almost exactly the same ease that they can do so in the gas phase, *provided the frequency of the applied field is well below the natural frequency of rotation of the solute molecules in the solution*. For small solute molecules in relatively nonviscous solvents, the frequencies at which derivations due to dispersion can be expected are well above the present experimental range.

In pure polar liquids, however, an entirely different situation exists. Under these conditions all the molecules are not free to orient in the field both because of dipole coupling and because of the size and shape of the molecules. As we have already seen for the case of water, spectroscopic considerations and the velocity of sound, in conjunction with the vapor pressures, agree in giving a value for δ_3 of about 0.04, corresponding to a δ_2 of $0.12(=0.04^{\frac{1}{3}})$. We use the familiar equations,

$$\frac{\epsilon-1}{\epsilon+2}V=\frac{4\pi}{3}N\left(\alpha+\frac{\mu^2}{3kT}\right) \tag{20}$$

TABLE VIII

θ_1	0°	10°	20°	30°	40°	50°	60°
$\mu_i^2\mu_g^{-2}$	0	.0153	.0594	.1296	.2202	.3252	.4374
δ_2	0	.0076	.0301	.0665	.1170	.1786	.2500

θ_1	70°	80°	90°	100°	110°	120°
$\mu_i^2\mu_g^{-2}$	.5508	.6555	.7500	.8292	.8919	.9375
δ_2	.3290	.4131	.5000	.5869	.6710	.7500

θ_1	130°	140°	150°	160°	170°	180°
$\mu_i^2\mu_g^{-2}$	.9681	.9864	.9954	.9990	1.0000	1.0000
δ_2	.8214	.8830	.9335	.9699	.9924	1.0000

and
$$\frac{n^2-1}{n^2+2}V=\frac{4\pi}{3}N\alpha. \tag{21}$$

At 20° and one atmosphere water has an index of refraction for sodium light of n equal to 1.3330, a molal volume, V, of 18.05 cc and a dielectric constant, ϵ, of 80. This leads to a value for $(4\pi/3)N\alpha$ of 3.7 cc and $(4\pi N/3)\mu^2/3kT=13.7$ cc for the liquid. For the gas $(4\pi N/3)\mu^2/3kT=71$ cc.[37] From Fig. 2 we see that this value of $\mu_l^2\mu_g^{-2}$ of 0.194 leads to a value of δ_2 of 0.10 to be compared to 0.12 found above.

The same calculations for methyl alcohol at 0°C yield the following results. $V_f\delta_3$ from vapor pressures and heats of vaporization is 0.026 cc, and V_f from sound velocity is 0.54 cc. The value of δ_3 from these results is 0.048, corresponding to δ_2 equal to 0.13. Utilizing the data of Åkerlöf[38] we obtain the value of 0.25 for δ_2 at the same temperature from the dielectric constant and dipole moment of the molecule.[39] It is of interest to observe that δ_2, as determined from dielectric constant, increases with the temperature being 0.34 to 60°C. Such a result is, of course, to be expected.

There is a tendency for δ_2 from the dielectric constant to be greater than $(\delta_3)^{\frac{1}{2}}$ determined from other sources. This might be interpreted as due to a restriction on rotation about the axis in which the electric moment of the molecule lies which is greater than that about the other two axes. This is probably a valid argument in the case of water since the higher of the two frequencies which were employed to account for restricted rotation undoubtedly corresponds to a mode of motion involving only the hydrogens, and thus is a libration about the axis in which the dipole lies. Computing this correction from the Einstein functions corresponding to these frequencies gives a value of δ_2 of 0.09 to be compared to 0.10 from the dielectric constant. It is not unreasonable that the discrepancy in the case of methyl alcohol might be accounted for on a similar basis, but the data for making such a computation are not at present available.

However, various factors which might cause deviations from the theory have been neglected. Thus, the coupling of dipoles in the liquid may operate in such a way as to either increase or reduce the apparent moment of the molecule in the liquid. Also the adequacy of equation (20) for pure polar liquids is by no means always conceded, even after account is taken of the restricted rotation of the molecules.[40]

However, it appears that any explanation of the deviations from (20) which is not compatible with restricted rotation of the molecules in many liquids is not in agreement with other lines of evidence. Fowler,[41] and Debye and Ramm[42] have also interpreted the dielectric properties of condensed phases from the point of view of restricted rotation.

Conclusion

The results of this work lead us to suggest that the abnormalities of the so-called associated liquids can be explained entirely from the standpoint of restricted rotation of the molecules. Thus although water and methyl alcohol are ordinarily classed as highly abnormal, their free volumes from sound velocity are not markedly different from those of other liquids. It is only the product, $V_f\delta_3$, rather than V_f itself, which is a different order of magnitude for "hydrogen bonded" as compared to normal liquids. The values recorded here for δ_3 for water and methyl alcohol thus account for their abnormally high entropies of vaporization.

[37] P. Debye, Chem. Rev. **19**, 171 (1936).
[38] Åkerlöf, J. Am. Chem. Soc. **54**, 4129 (1932).
[39] Trans. Faraday Soc. **30**, 905 (1934).

[40] Onsager, J. Am. Chem. Soc. **58**, 1486 (1936). Van Vleck, J. Chem. Phys. **5**, 556 (1937). J. Wyman, J. Am. Chem. Soc. **58**, 1482 (1936). R. H. Cole, J. Chem. Phys. **6**, 385 (1938). S. S. Kurtz, Jr., and A. L. Ward, J. Frank. Inst. **224**, 583 (1937).
[41] R. H. Fowler, Proc. Roy. Soc. **149A**, 1 (1935).
[42] P. Debye, Phys. Zeits. **36**, 193 (1935); P. Debye, and W. Ramm, Ann. d. Physik **28**, 28 (1937).

Order *Versus* Disorder in Ternary Structures Including Certain Spinels[1]

F. C. Blake
Ohio State University, Columbus, Ohio

(Received June 27, 1938)

The doubling process as the second alternative suggested by Professor M. v. Laue for mix-crystals is followed through in the case of lithium ferrite and it is shown in that case that all superlattice lines disappear when the lattice edge is eight times as large as the small disordered lattice found by Posnjak and Barth. It is shown that for this large (33A) lattice the *simple* space group, O_1^h, gives only face-centered lines on the powder photograph. The disappearance of the superlattice lines for this lattice may be said to be due to the coherence of the x-rays that cause the destructive interference involved.

1. Introduction

Professor W. L. Bragg in his Bakerian lecture, June 28, 1934, in conjunction with Dr. E. J. Williams,[2] discusses order *versus* disorder in alloys, and they call attention to some of the earlier work of others in this field. In general the effect of increasing temperature on alloys is to change an ordered lattice into a disordered one, and one may expect a sharp discontinuity in the specific heat of an alloy at the critical temperature as the temperature is lowered across it. With further lowering of the temperature the change in specific heat is more gradual as the degree of order is increased.

In his paper on the "Statistical Theory of Superlattices" Professor H. A. Bethe[3] extended Bragg and Williams' definition of order so as to include local order; thus he defines long range and short range order, and calculates these for the simple cubic lattice; but interaction between nearest neighbors is alone considered. Chang[4] has extended Bethe's theory to include interaction between next nearest neighbors and gets a better agreement with experiment.[5] He shows that with increasing interaction between second neighbors, the value of the specific heat at the critical temperature is very sensitive to the exact value chosen for this second neighbor interaction. He states, however, that it is not expected that his treatment should agree with experiment too well, for it leaves the higher interactions and the heat motions out of account. More recently Kirkwood[6] has presented "an alternative theory of order and disorder, essentially equivalent to Bethe's in its degree of approximation." Bethe in a later paper[7] adopts the method of Kirkwood.

Order-disorder problems in ternary alloys, or crystal structures, have, so far as the author is aware, received very little attention in the literature. In studying Posnjak and Barth's[8] so-called principle of "variate atom equipoints" the writer was aware of the two points of view concerning "mix-crystals" discussed by M. von Laue[9] in explanation of the results of Vegard and Schjelderup[10] for some mix-crystals of alkali halides. The two views are these. In a mix-crystal the two components, A and B say, are either distributed statistically (in a disordered fashion) or else there is perfect order, but the lattice is *much* larger. Vegard and Schjelderup chose the first alternative. It is well known that certain of the alkali halides form solid solutions in all proportions.[11] These alkali halide mix-crystals are ternary, not binary, structures, yet with regard to mixing they are binary. In KBr-KCl there is a common cation, K. In KI-NH_4I there is a common anion, I. Both of these mixes form solid solutions in all proportions.[11]

[1] Read before the American Physical Society, Indianapolis, Dec. 1937.
[2] Bragg and Williams, Proc. Roy. Soc. **A145**, 699 (1934). See also their second and third papers, Proc. Roy. Soc. **A151**, 540 and **A152**, 231 (1935). Many more references to earlier work are to be found in their second paper; the third paper is by Williams alone.
[3] Bethe, Proc. Roy. Soc. **A150**, 552 (1935).
[4] Chang, Proc. Roy. Soc. **A161**, 546 (1937); see also Bethe, J. App. Phys. **9**, 244 (1938).
[5] Sykes, Proc. Roy. Soc. **A148**, 443 (1935).
[6] Kirkwood, J. Chem. Phys. **6**, 70 (1938).
[7] Bethe, J. App. Phys. **9**, 244 (1938).
[8] Posnjak and Barth, Phys. Rev. **38**, 2234 (1931).
[9] Laue, Ann. d. Physik **56**, 497 (1918).
[10] Vegard and Schjelderup, Physik. Zeits. **18**, 93 (1917).
[11] E. g. Havighurst, Mack and Blake, J. Am. Chem. Soc. **47**, 29 (1925).

2. Superstructures

In binary alloys, when the degree of order is high, there is in general a tendency for superlattice lines to appear, because of the two superstructures present. The difference in scattering power for x-rays of the two components present results in extra reflections that are not present when the disorder is complete. This is well illustrated in the copper-gold alloy, Cu_3Au, studied by Sykes and Evans.[12] For a copper-gold wire heated to 425°C and quenched in water, only eight face-centered lines appeared on the powder photograph. After ordering by various methods of cooling, twelve extra superlattice lines appear, all of which are simple cubic. Techniques were developed by them for changing the character of the superlattice lines from fuzzy to sharp.

3. Second Alternative for Mixed Crystals

Since M. v. Laue[9] derived his expression for the structure factor of the mix-crystal K_2BrCl, most people have chosen the first (disordered) alternative in studying binary or ternary alloys, or structures, for oftentimes superlattice lines are absent, and such lines are at once eliminated by assuming disorder. Where possible, it is much more scientific to study specific heats of structures as a function of temperature, as well as to make an x-ray analysis of the structures. But superlattice lines can be eliminated by the second alternative, *viz.*, that of choosing a larger lattice. When properly done, it is possible, in some cases at least, to obtain the exact equivalent of the disordered lattice; and even though crystallographers and metallurgists might say that this large equivalent of the small disordered lattice could never be produced owing to an infinite time being needed for its formation, it is worthy of having attention called to it.

Table I.*

hkl for 4.14A Lattice	Observed Intensities		Calculated Intensities (33A Lattice)					
			$n\phi\lvert\Sigma SF\rvert^2$		$n\phi\lvert\Sigma SFe^{-M}\rvert^2$		$n\phi\lvert\Sigma SFe^{-M}\rvert^2 A$	
	Posnjak and Barth	Blake	Ionic	Atomic	Ionic	Atomic	Ionic	Atomic
111	40	27	15.3	22.1	15.5	23.5	15.5	23.4
200	100	100	100.0	100.0	100.0	100.0	100.0	100.0
220	90	60	58.5	61.0	55.7	58.1	56.0	58.5
311	30	12	10.3	12.5	10.6	12.8	10.7	12.9
222	40	18	18.1	19.3	16.5	18.5	16.7	18.7
400	20	6	7.7	8.2	6.7	7.2	6.8	7.3
331	10	5	4.5	5.5	4.5	5.5	4.6	5.6
420	50	14	19.9	20.4	16.7	17.2	17.0	17.5
422	40	9	13.6	14.3	11.0	11.6	11.3	11.9

*For an explanation of the symbols appearing in the intensity formulas see Blake, Rev. Mod. Phys. **5**, 169 (1933); also J. Chem Phys. **2**, 320 (1934).

[12] Sykes and Evans, J. Inst. Metals **58**, 255 (1936).

4. Low Temperature Modification of Lithium Ferrite

A couple of years ago I secured from Dr. Barth of the Geophysical Laboratory some of the powdered lithium ferrite and zinc stannate that he and Dr. Posnjak had used in their spinel studies[13] and that led them to announce their principle of "variate atom equipoints." Powder photographs of these two compounds were taken with molybdenum $K\alpha$-rays, and the photographs were densitometered. Proper[14] account was taken of all of the intensity factors and of the laws of photographic blackening for x-rays. The results for lithium ferrite are shown in Table I, together with the observed results of Barth and Posnjak. The chief differences between my results and theirs is due to their overestimation of the intensity for faces having large values of θ for fairly long times of exposure. When the exposure time is long (i.e., $S>0.6$ for the strongest line on the film) there is an exhaustion of silver for lines having θ small as against those having θ large, thus leading to errors.

In studying this second alternative a frontal attack was made on the problem by doubling the lithium ferrite lattice from 4.141A to 8.282A, care being used to increase the symmetry of the crystal if possible as the size was doubled. It is always possible in a crystal lattice to move the origin of coordinates without affecting intensity relations, though symmetry properties are thereby affected. In all cases I have chosen an oxygen atom as origin. Allowing no exchange between iron and lithium atoms, one is, of course, conscious in the 8.28A cell that neighboring 4.14A parts are not identical. Indeed, if one alternates lithium and iron in between the oxygen atoms in all directions parallel to the axes, he is conscious that when he has progressed along the

[13] (a) Barth and Posnjak, J. Wash. Acad. Sci. **21**, 255 (1931); (b) Posnjak and Barth, Phys. Rev. **38**, 2234 (1931); (c) Zeits. f. Krist. **82**, 325 (1932).

[14] Blake, Rev. Mod. Phys. **5**, 169 (1933).

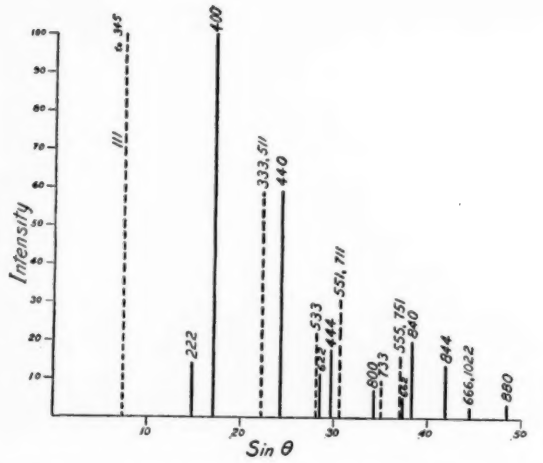

FIG. 1. Calculated intensities for 8.28A lattice.

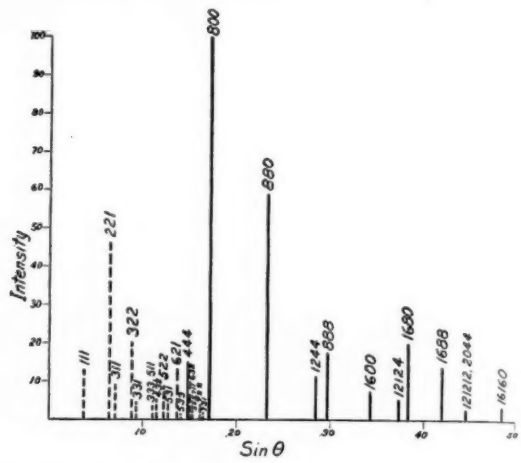

FIG. 2. Calculated intensities for 16.56A lattice.

cubical axes 8.28A the structure he has thus built up is only a piece of a cell, for at one corner he finds an oxygen atom with three iron atoms as nearest neighbors while at the opposite corner (that furthest removed) an oxygen atom is surrounded by three lithium atoms as nearest neighbors, the oxygen atoms at the other four corners having two lithium and one iron as nearest neighbors, or *vice versa*. Thus this 8.28A lattice is only one-eighth of a proper unit cell, and it is not surprising that when one plots intensity calculations against sin θ he gets a great overstressing of the superlattice (dotted) lines (faces), the full lines in Fig. 1 being the calculated face-centered lines that are observed, where for the calculations all intensity factors are taken into account except the temperature factor and the absorption factor. The *first legitimate* doubling of the lattice enlarges it at once to 16.56A. For, by inserting axial planes of symmetry, each oxygen atom at the corners of the enlarged lattice is surrounded by three iron atoms as nearest neighbors, while the oxygen atom at the center is surrounded by six lithium atoms as nearest neighbors. This fact determines the space-group of the lattice, *viz.*, simple cubic O^1_h. When the intensity relations are calculated and plotted (Fig. 2), it is noticed that the superlattice (dotted) lines are reduced in intensity, being largely crowded down into the region where θ is small. But since the powder photographs show their absence, another lattice doubling (the second legitimate one) is suggested. Thus the correct, *ordered* lattice, that is, the *exact* equivalent of the statistical averaging of Posnjak and Barth's 4.141A lithium ferrite lattice, has eight times the edge of that lattice, *viz.*, 33.13A. The result is shown in Fig. 3. The only superlattice line residue is for face 333, and it has an intensity less than 4 percent and hence could not be detected, for it occurs in the region of maximum general blackening. Moreover in Posnjak and Barth's observations no line is reported whose intensity is less than ten percent. In what I call the second legitimate doubling it should be borne in mind that care was used to preserve the axial planes of symmetry. This second doubling again gives the space-group as O^1_h. Thus an

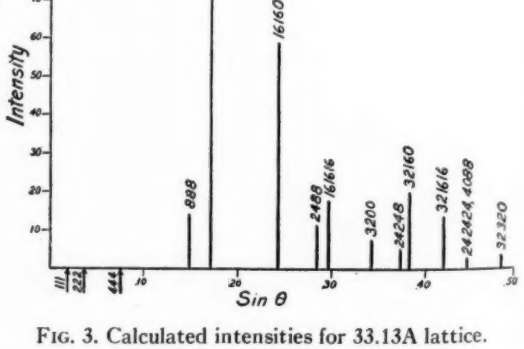

FIG. 3. Calculated intensities for 33.13A lattice.

TABLE II. *Coordinates of oxygen atoms.*

z \ x	0	1	2	3	4	5	6	7	$\bar{8}$	$\bar{7}$	$\bar{6}$	$\bar{5}$	$\bar{4}$	$\bar{3}$	$\bar{2}$	$\bar{1}$	0	x / z
0	0	1	0	1	0	1	0	1	0	1	0	1	0	1	0	1	0	0
1	1	0	1	0	1	0	1	0	1	0	1	0	1	0	1	0	1	1
2	0	1	0	1	0	1	0	1	0	1	0	1	0	1	0	1	0	2
3	1	0	1	0	1	0	1	0	1	0	1	0	1	0	1	0	1	3
4	0	1	0	1	0	1	0	1	0	1	0	1	0	1	0	1	0	4
5	1	0	1	0	1	0	1	0	1	0	1	0	1	0	1	0	1	5
6	0	1	0	1	0	1	0	1	0	1	0	1	0	1	0	1	0	6
7	1	0	1	0	1	0	1	0	1	0	1	0	1	0	1	0	1	7
$\bar{8}$	0	1	0	1	0	1	0	1	0	1	0	1	0	1	0	1	0	$\bar{8}$
$\bar{7}$	1	0	1	0	1	0	1	0	1	0	1	0	1	0	1	0	1	$\bar{7}$
$\bar{6}$	0	1	0	1	0	1	0	1	0	1	0	1	0	1	0	1	0	$\bar{6}$
$\bar{5}$	1	0	1	0	1	0	1	0	1	0	1	0	1	0	1	0	1	$\bar{5}$
$\bar{4}$	0	1	0	1	0	1	0	1	0	1	0	1	0	1	0	1	0	$\bar{4}$
$\bar{3}$	1	0	1	0	1	0	1	0	1	0	1	0	1	0	1	0	1	$\bar{3}$
$\bar{2}$	0	1	0	1	0	1	0	1	0	1	0	1	0	1	0	1	0	$\bar{2}$
$\bar{1}$	1	0	1	0	1	0	1	0	1	0	1	0	1	0	1	0	1	$\bar{1}$
0	0	1	0	1	0	1	0	1	0	1	0	1	0	1	0	1	0	0
z / x	0	1	2	3	4	5	6	7	$\bar{8}$	$\bar{7}$	$\bar{6}$	$\bar{5}$	$\bar{4}$	$\bar{3}$	$\bar{2}$	$\bar{1}$	0	z / x

TABLE III. *Coordinates of iron atoms.*

z \ x	0	1	2	3	4	5	6	7	$\bar{8}$	$\bar{7}$	$\bar{6}$	$\bar{5}$	$\bar{4}$	$\bar{3}$	$\bar{2}$	$\bar{1}$	0	x / z
0	1	0	3	2	1	0	3	2	1	2	3	0	1	2	3	0	1	0
1	0	3	2	1	0	3	2	1	0	1	2	3	0	1	2	3	0	1
2	3	2	1	0	3	2	1	0	3	0	1	2	3	0	1	2	3	2
3	2	1	0	3	2	1	0	3	2	3	0	1	2	3	0	1	2	3
4	1	0	3	2	1	0	3	2	1	2	3	0	1	2	3	0	1	4
5	0	3	2	1	0	3	2	1	0	1	2	3	0	1	2	3	0	5
6	3	2	1	0	3	2	1	0	3	0	1	2	3	0	1	2	3	6
7	2	1	0	3	2	1	0	3	2	3	0	1	2	3	0	1	2	7
$\bar{8}$	1	0	3	2	1	0	3	2	1	2	3	0	1	2	3	0	1	$\bar{8}$
$\bar{7}$	2	1	0	3	2	1	0	3	2	3	0	1	2	3	0	1	2	$\bar{7}$
$\bar{6}$	3	2	1	0	3	2	1	0	3	0	1	2	3	0	1	2	3	$\bar{6}$
$\bar{5}$	0	3	2	1	0	3	2	1	0	1	2	3	0	1	2	3	0	$\bar{5}$
$\bar{4}$	1	0	3	2	1	0	3	2	1	2	3	0	1	2	3	0	1	$\bar{4}$
$\bar{3}$	2	1	0	3	2	1	0	3	2	3	0	1	2	3	0	1	2	$\bar{3}$
$\bar{2}$	3	2	1	0	3	2	1	0	3	0	1	2	3	0	1	2	3	$\bar{2}$
$\bar{1}$	0	3	2	1	0	3	2	1	0	1	2	3	0	1	2	3	0	$\bar{1}$
0	1	0	3	2	1	0	3	2	1	2	3	0	1	2	3	0	1	0
z / x	0	1	2	3	4	5	6	7	$\bar{8}$	$\bar{7}$	$\bar{6}$	$\bar{5}$	$\bar{4}$	$\bar{3}$	$\bar{2}$	$\bar{1}$	0	z / x

ordered simple cubic lattice, of edge 33.13A, containing 512 molecules of $Li_2Fe_2O_4$, with cations differing in scattering power as 23 to 2 (or as 26 to 3 if neutral atoms) gives only face-centered reflection intensities. I invite the attention of the crystallographers to this fact. I think this gives the answer also to the question implied in this sentence of Posnjak and Barth's paper on lithium ferrite, "Taking into consideration not too small a portion of the crystal, an equal number of points is occupied by iron and by lithium." The "not too small a portion" is a cube of 33A edge.

In order that others who care to may study this 33A lattice for themselves, I give in Tables II, III and IV the atomic positions of the oxygen, iron and lithium atoms, respectively, with certain necessary explanations. In Table II the figures 0 and 1 occur while in Tables III and IV the figures 0, 1, 2, 3 occur. Let any figure in any of the three tables represent the numerator of a fraction of which the denominator is 16. To illustrate, choose the figure 3, then 3/16 is the y coordinate of an atom whose x and z coordinates are given (also as numerators of fractions having the denominator 16) at the top and side of each table, where it is understood that $\bar{7}/16$ is the same as 9/16, because the unit angle chosen for the revolving radius vector[15] is $2\pi/16 = 22.5$ degrees. Thus the least count in stating the exact position of an atom along any of the three axes is 1/16 of the lattice edge. One interprets the tables correctly thus.

Since there are 16 units along the x and z axes, there must be 16 units along the y axis. In Table II only two such units are given by the figures 0 and 1 as numerators of y for positions occupied by 256 oxygen atoms. To obtain positions of another 256 of the total 2048 oxygen atoms in the unit cell, it is necessary to substitute 2 for 0, and 3 for 1, in the y values of Table II. Similar substitutions of 4, 6, $\bar{8}$, $\bar{6}$, $\bar{4}$, and $\bar{2}$ for 0, and of 5, 7, $\bar{7}$, $\bar{5}$, $\bar{3}$, and $\bar{1}$, for 1, give the coordinates of the remaining oxygen atoms. Table III gives the coordinates of 256 iron atoms. The remaining iron atom positions, which total 1024 in the unit cell, are obtained by substitutions of 4, $\bar{8}$, and $\bar{4}$ for 0, of 5, $\bar{5}$, and $\bar{1}$ for 1, of 6, $\bar{6}$, and $\bar{2}$ for 2, and of 7, $\bar{7}$ and $\bar{3}$ for 3, in the y values of Table III. The same substitutions made in Table IV

[15] See Blake, J. Chem. Phys. **2**, 320 (1934).

TABLE IV. *Coordinates of lithium atoms.*

z \ x	0	1	2	3	4	5	6	7	$\bar{8}$	$\bar{7}$	$\bar{6}$	$\bar{5}$	$\bar{4}$	$\bar{3}$	$\bar{2}$	$\bar{1}$	0	x / z
0	3	2	1	0	3	2	1	0	3	0	1	2	3	0	1	2	3	0
1	2	1	0	3	2	1	0	3	2	3	0	1	2	3	0	1	2	1
2	1	0	3	2	1	0	3	2	1	2	3	0	1	2	3	0	1	2
3	0	3	2	1	0	3	2	1	0	1	2	3	0	1	2	3	0	3
4	3	2	1	0	3	2	1	0	3	0	1	2	3	0	1	2	3	4
5	2	1	0	3	2	1	0	3	2	3	0	1	2	3	0	1	2	5
6	1	0	3	2	1	0	3	2	1	2	3	0	1	2	3	0	1	6
7	0	3	2	1	0	3	2	1	0	1	2	3	0	1	2	3	0	7
$\bar{8}$	3	2	1	0	3	2	1	0	3	0	1	2	3	0	1	2	3	$\bar{8}$
$\bar{7}$	0	3	2	1	0	3	2	1	0	1	2	3	0	1	2	3	0	$\bar{7}$
$\bar{6}$	1	0	3	2	1	0	3	2	1	2	3	0	1	2	3	0	1	$\bar{6}$
$\bar{5}$	2	1	0	3	2	1	0	3	2	3	0	1	2	3	0	1	2	$\bar{5}$
$\bar{4}$	3	2	1	0	3	2	1	0	3	0	1	2	3	0	1	2	3	$\bar{4}$
$\bar{3}$	0	3	2	1	0	3	2	1	0	1	2	3	0	1	2	3	0	$\bar{3}$
$\bar{2}$	1	0	3	2	1	0	3	2	1	2	3	0	1	2	3	0	1	$\bar{2}$
$\bar{1}$	2	1	0	3	2	1	0	3	2	3	0	1	2	3	0	1	2	$\bar{1}$
0	3	2	1	0	3	2	1	0	3	0	1	2	3	0	1	2	3	0
z / x	0	1	2	3	4	5	6	7	$\bar{8}$	$\bar{7}$	$\bar{6}$	$\bar{5}$	$\bar{4}$	$\bar{3}$	$\bar{2}$	$\bar{1}$	0	z \ x

obviously give the positions of the 1024 lithium atoms in the unit cell. To obtain the positions of all atoms in any one plane of the unit cell, e.g. $y=1/16$, take the positions of the figures 1 in Table II as the positions of oxygen atoms in the plane $y=1/16$, the positions of figures 1 in Table III as the positions of iron atoms in that plane, and the positions of the figures 1 in Table IV as the positions of lithium atoms in the same plane.

A few words as to the space group, O^1_h or *Pm3m*. In calculating the structure factor the general formulas give $A=\Sigma \cos 2\pi hx[\cos 2\pi ky \cdot \cos 2\pi lz+\cos 2\pi ly \cdot \cos 2\pi kz]$, and $B=0$. But I have found it no easier to use these formulas than to summarize by the revolving vector method.[15] As already stated, assuming that for the spinels the absorption and temperature factors pretty well cancel each other, the correct intensity relations are given in Fig. 3 and these agree well enough with the lithium ferrite observations of Table I. The atomic form factors for lithium, iron and oxygen used are those of the *International Tables for the Determination of Crystal Structures*, the crystal being taken as ionic or atomic as indicated in Table I.

In the case of zinc stannate, I have tried the doubling process on the 8.61A disordered lattice given by Barth and Posnjak[13c] to see if I could get the large lattice equivalent; but I haven't completed the study for the reason that if it is also true in this case that the lattice edge should be enlarged eight times, the labor involved becomes quite burdensome, for the cell would then have an edge 68.88A. The 34.44A cell containing 512 molecules of Zn_2SnO_4 goes to zero for the fourth order of 311, no matter what value is used for the oxygen parameter. This indicates another doubling, or some sort of reorganization of the cell. I intend to study the doubling process further in the case of zinc stannate.

5. Large-Sized Lattices and Molecules

It is becoming more fashionable to speak of large-sized lattices, even if in some cases there is apparently but one molecule per unit cell. The recent series of papers in *Nature*,[16] "Crystal Structure of the Proteins," gives a tetragonal lattice, $a=b=63.5$A, $c=145$A, and an orthorhombic lattice, $a=49.6$A, $b=67.8$A, $c=66.5$A. Bernal, Fankuchen and Perutz stating that "the proteins fall into two groups, pseudo-hexagonal and pseudo-cubic, in both cases with a side of 60–75A." Long needle-like structures up to a length of 6000A seem to have been prepared by Astbury and Bell.[17] What is the distinction in building blocks between the spinels and these organic compounds that would prevent 33A cubes for the lithium ferrite? In Sykes and Evans' paper, "The Transformation in the Copper-Gold Alloy, Cu_3Au,"[12] the authors conclude that when this alloy was cooled at 30°C per hour it consisted of small "nuclei" within the individual crystals; so they distinguish between two different states of the alloy, one with nuclei, the other without. Each nucleus could be said to have 100 percent local order but an aggregation of nuclei could lack long range order. It seems to me that the 33A lithium ferrite lattice discussed in this paper shows 100 percent local order and 100 percent long range order, that is, the nuclei are properly fitted together. A recent remark of Professor H.

[16] Crowfoot and Riley; Crowfoot and Fankuchen; Bernal, Fankuchen and Perutz; Nature **141**, 521–524 (1938).

[17] Astbury and Bell, Nature **141**, 747 (1938).

A. Bethe to the writer, that there ought to be more than one way in which all superlattice lines could be eliminated for a lattice as large as 33A, leads me to admit the possibility, but not the probability, of this unless the local order is in a nucleus as small as 4.14A, when the long range disorder is 100 percent. It should be borne in mind that if one turns the 33A lattice inside out, as it were, that means nothing but an interchange throughout the lattice of iron and lithium atoms, thus giving the same, not a different, solution.

Granted that this 33A, ordered lithium ferrite, according to present notions concerning alloys, could not be produced in the laboratory because of the inordinate amount of time required to set it up, it nevertheless remains as the low temperature form of the disordered 4.14A lattice of lithium ferrite. Further studies on rates of cooling of alloys with specific heat measurements and with the possible use of "stabilizing agents" may help to clarify the knotty problems involved in *order versus disorder* studies. Bragg and Williams[2] in their first study in this field remark as their concluding sentence, "Maxima and minima in physical properties at certain relative proportions (e.g. Fe_3Al and Cu_3Au) are statistical effects, and do not imply the existence of corresponding compounds." It seems conceivable to the writer that an ordered solution of such binary alloys could be found, in which case it would be a fair question to ask whether a single ordered-lattice alloy is not a definite compound. It has been shown that proper ordering causes superlattice lines to disappear, that a large (33A) lattice of lithium ferrite is the exact equivalent of the small (4.14A) disordered lattice, that a simple cubic lattice of edge 8 times the disordered face-centered cubic lattice gives only face-centered lines on the powder photograph in the case of lithium ferrite.

OCTOBER, 1938 JOURNAL OF CHEMICAL PHYSICS VOLUME 6

The Dipole Moments of Molecules Containing Two Movable Dipoles

J. Y. Beach* and D. P. Stevenson
Frick Chemical Laboratory, Princeton University, Princeton, New Jersey

(Received June 20, 1938)

The average dipole moment of a molecule containing two movable dipoles has been calculated as a function of temperature and restriction to internal rotation for three different potential functions. The potential functions used are: $(V_0/2)(\cos\phi+1)$, $(V_0/\pi)(\pi-\phi)$ and $V_0/\pi^2(\pi-\phi)^2$, where V_0 is the difference in potential energy between the *cis* and *trans* forms of the molecule and ϕ is the angle between the planes containing the dipoles and the axis of rotation. Values of the integral $\int_0^\pi \cos x \exp(-bx^2)dx$ are tabulated for values of b ranging from 0 to 2 at intervals of 0.1. The dipole moments of *s*-dichloro-ethane, 1,2-bromo-chloro-ethane and *s*-dibromo-ethane as a function of temperature are used with the three potential functions to determine values of V_0. The values thus obtained are compared with the values obtained by other methods.

Introduction

THERE have recently been several attempts to determine the magnitude of the potential barrier restricting internal rotation around single carbon-carbon bonds. Most of these attempts have been made on ethane.[1] In attacking the problem from the standpoint of dipole moments it is necessary to substitute for symmetrically located hydrogen atoms, polar groups whose relative orientations will have a large effect on the resultant dipole moment of the molecule. In order to treat successfully the dipole moment data of such molecules as the 1,2,di-substituted ethanes it is necessary to derive expressions relating the observed dipole moment to the height and shape of the potential barrier and the individual bond moments. We have de-

* National Research Fellow in Chemistry.

[1] Kemp and Pitzer, J. Chem. Phys. **4**, 749 (1936); J. Am. Chem. Soc. **59**, 276 (1937). Howard, Phys. Rev. **51**, 53 (1937). Kistiakowsky and Nazmi, J. Chem. Phys. **6**, 18 (1935). Bartholomé and Karweil, Zeits. f. physik. Chemie **39**, 1 (1938). Hunsman, Zeits. f. physik. Chemie **39**, 23 (1938).

rived such expressions for the cases of cosine, linear and parabolic potential functions. To find the average dipole moment it is necessary to calculate the average value of the square of the dipole moment, averaging over all possible configurations of the molecule and weighting each configuration with a Boltzmann factor taken from the assumed potential function. The square of the moment rather than the moment itself, is averaged because the Debye[2] equation applied to each molecular species gives the square of the moment, rather than the first power of the moment, as a function of the dielectric constant and the refractivity.

Calculations

The square of the dipole moment of a molecule containing two dipoles capable of relative motion to the extent of rotating about an axis in the molecule is:

$$\mu(\phi)=A+B\cos\phi, \tag{1}$$

where $A=m_1^2+m_2^2-2m_1m_2\cos\alpha_1\cos\alpha_2$, and $B=2m_1m_2\sin\alpha_1\sin\alpha_2$. m_1 and m_2 are the magnitudes of the two movable dipoles. α_1 and α_2 are the angles made by the dipoles with the axis of rotation. ϕ is the angle between the plane containing one dipole and the axis of rotation and the plane containing the other dipole and the axis of rotation. For α_1 and α_2 tetrahedral and $m_1=m_2=m$, A and B each become $16/9\ m^2$.

The observed, or average dipole moment for the molecule is

$$\mu^2=\overline{\mu^2(\phi)}=\frac{\int_0^\pi \mu^2(\phi)\exp\left(-V(\phi)/RT\right)d\phi}{\int_0^\pi \exp\left(-V(\phi)/RT\right)d\phi}. \tag{2}$$

Table I. *ρ for linear and cosine potential functions.*

a	$-\rho$ (linear)	$-\rho$ (cosine)	a	$-\rho$ (linear)	$-\rho$ (cosine)
0.0	0.000	0.000	4.0	0.868	0.863
0.5	0.199	0.242	4.5	0.892	0.880
1.0	0.378	0.446	5.0	0.910	0.892
1.5	0.527	0.596	6.0	0.935	0.912
2.0	0.640	0.698	7.0	0.952	0.927
2.5	0.727	0.765	8.0	0.963	0.935
3.0	0.788	0.808	9.0	0.970	0.944
3.5	0.835	0.841	10.0	0.977	0.954

[2] Debye, *Polar Molecules.*

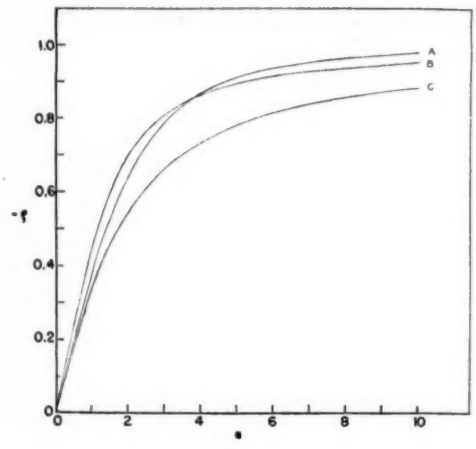

Fig. 1.

The effect of the angle ϕ on the moments of inertia and thus the entropy of the various configurations is negligible except for small ϕ,[3] and will be neglected. Integrating ϕ from 0 to π is equivalent to integrating from 0 to 2π. $V(\phi)$ is only required to represent the potential function when ϕ is between 0 and π. Substituting Eq. (1) into Eq. (2) we obtain

$$\mu^2=A+B\rho \tag{3}$$

where $$\rho=\frac{\int_0^\pi \cos\phi\exp\left(-V(\phi)/RT\right)d\phi}{\int_0^\pi \exp\left(-V(\phi)/RT\right)d\phi}.$$

We shall first evaluate ρ for the linear potential function

$$V(\phi)=(V_0/\pi)(\pi-\phi).$$

V_0 is the difference in potential energy between the *cis* and *trans* configurations of the molecule. In this case

$$\rho=\frac{\int_0^\pi \cos\phi\exp\left(-V_0(\pi-\phi)/\pi RT\right)d\phi}{\int_0^\pi \exp\left(-V_0(\pi-\phi)/\pi RT\right)d\phi}$$
$$=-\left(a^2/(a^2+\pi^2/4)\right)\coth a,$$

where $a=V_0/2RT$. $\rho=0$ when $a=0$ and ap-

[3] Altar, J. Chem. Phys. **3**, 460 (1935).

proaches -1 as a becomes large. When a is large and $\rho=-1$, the dipole moment $\mu=(A-B)^{\frac{1}{2}}$, which is the moment of the *trans* molecule. When a is small, the moment approaches $A^{\frac{1}{2}}$ the value for free rotation. ρ is tabulated in Table I and plotted in Fig. 1, curve A, as a function of a.

The integrals arising when the potential function $V=(V_0/2)(\cos\phi+1)$ is used have been evaluated by Mizushima and Higasi.[4] In this case

$$\rho=\frac{\int_0^\pi \cos\phi \exp(-V_0(\cos\phi+1)/2RT)d\phi}{\int_0^\pi \exp(-V_0(\cos\phi+1)/2RT)d\phi}$$

$$=\frac{\int_0^\pi \cos\phi \exp(-a\cos\phi)d\phi}{\int_0^\pi \exp(-a\cos\phi)d\phi}$$

$$=iJ_1(ia)/J_0(ia). \quad a=V_0/2RT.$$

Numerator and denominator are Bessel functions which are tabulated.[5] In this case too $\rho=0$ for $a=0$ and -1 for a large. ρ is tabulated in Table I and plotted in Fig. 1, curve B.

In calculating the average moment for the parabolic potential function $V=(V_0/\pi^2)(\pi-\phi)^2$,

$$\rho=\frac{\int_0^\pi \cos\phi \exp(-V_0(\pi-\phi)^2/\pi^2RT)d\phi}{\int_0^\pi \exp(-V_0(\pi-\phi)^2/\pi^2RT)d\phi}.$$

Let $b=V_0/\pi^2RT$ and $\pi-\phi=x$, then

$$\rho=-\frac{\int_0^\pi \cos x \exp(-bx^2)dx}{\int_0^\pi \exp(-bx^2)dx}=-\frac{S(b)}{B(b)}.$$

The integral $B(b)$ can easily be transformed into an error integral. The result is $B(b)=(\frac{1}{2})\times(\pi/b)^{\frac{1}{2}}\Phi(b^{\frac{1}{2}}\pi)$. $\Phi(b^{\frac{1}{2}}\pi)$ is the normalized error integral and is tabulated.[5]

The integral $S(b)$ does not become integrable by simple transformations, nor is it tabulated. We found it necessary to expand both $\cos x$ and $\exp(-bx^2)$ in powers of x and integrate term by term. The result is the following double series:

$$S(b)=\sum_{n=0}^{\infty}c_nb^n, \quad c_n=\frac{1}{n!}\sum_{l=n}^{\infty}\frac{(-1)^l\pi^{2l+1}}{(2l+1)(2l-2n)!}.$$

This series converges fairly rapidly for small values of b and was used for calculating S(b) when $b=0.5$ or less. When b is large $S(b)$ can be approximated to by the integral

$$\int_0^\infty \cos x \exp(-bx^2)dx=\tfrac{1}{2}(\pi/b)^{\frac{1}{2}}\exp(-\tfrac{1}{4}b).$$

We can test the error made by this approximation in the following way. The error is less than the error which would be made by making the same approximation for $B(b)$ because $\cos x$ is always less than 1. The error in $B(b)$ is found, from the error function table, to be 0.1 percent at $b=0.55$, and to decrease rapidly as b increases. For calculating $S(b)$ when $b=0.6$ or larger the approximate formula was used. $S(b)$ and ρ are tabulated in Table II. In Fig. 1, curve C ρ is plotted as a function of a. ρ varies from 0 to -1 as b (or a) varies from 0 to ∞.

TABLE II. *S(b) and ρ for the parabolic potential function.*

b	a	$S(b)$	$-\rho$
0.00	0.000	0.0000	0.0000
0.05	0.247	0.2606	0.0968
0.1	0.495	0.4373	0.1858
0.2	0.988	0.6367	0.3371
0.3	1.48	0.7238	0.4541
0.4	1.97	0.7563	0.5425
0.5	2.47	0.7622	0.6097
0.6	2.96	0.754	0.659
0.7	3.46	0.741	0.700
0.8	3.95	0.724	0.731
0.9	4.45	0.707	0.757
1.0	4.95	0.690	0.779
1.1	5.43	0.673	0.796
1.2	5.92	0.658	0.813
1.3	6.42	0.641	0.825
1.4	6.91	0.626	0.836
1.5	7.40	0.612	0.846
1.6	7.90	0.600	0.855
1.7	8.39	0.587	0.863
1.8	8.88	0.575	0.870
1.9	9.38	0.563	0.876
2.0	9.88	0.552	0.881

[4] Mizushima and Higasi, Proc. Imp. Acad. **8**, 482 (1932).
[5] Jahnke and Einde, *Tables*.

TABLE III. *Potential barrier, V_0.*

T°K	$\mu\times10^{+18}$	POTENTIAL FUNCTION COSINE V_0 KCAL./MOLE	LINEAR V_0 KCAL./MOLE	PARABOLIC V_0 KCAL./MOLE
		$C_2H_4Cl_2$		
305	1.12	4.02	4.17	7.97
341	1.24	3.78	4.15	7.11
376	1.32	3.71	4.46	6.85
419	1.40	3.71	4.26	6.63
457	1.45	3.80	4.41	6.66
480	1.48	3.81	4.52	6.66
485	1.48	3.85	4.57	6.73
544	1.54	4.02	4.80	6.85
		C_2H_4BrCl		
339	1.09	4.65	4.77	9.32
368	1.14	4.67	4.90	9.22
405	1.20	4.74	5.12	9.10
436	1.28	4.54	5.05	8.46
		$C_2H_4Br_2$		
339	0.94	6.00	5.66	12.87
368	0.99	5.92	5.74	12.20
405	1.03	6.12	6.04	12.56
436	1.10	5.85	5.92	11.69

Moment of $CH_2Cl=2.03$[7]
Moment of $CH_2Br=2.02$[7]
The moments of $C_2H_4Cl_2$, C_2H_4BrCl and $C_2H_4Br_2$ from Zahn[6]

DISCUSSION

If one of the potential functions described above is assumed to be the actual one, V_0 can be found from the value of the dipole moment at a single temperature. Substituting in Eq. (3) values for the group moments, bond angles and the observed moment of the molecule, a value of ρ is obtained. From the graph of the relation between ρ and a, a value of a is obtained which, with the temperature at which the dipole moment was measured gives a value of V_0. If values of the dipole moment have been determined for several temperatures several values of V_0 can be obtained. These values should be consistent if the assumed potential function is a good one.

We have taken the dipole moment data for *s*-dichloro-ethane, 1,2,bromo-chloro-ethane and *s*-dibromo-ethane[6] and calculated values for V_0 for each of the potential functions. We assumed that $\alpha_1=\alpha_2=109°\ 28'$ for all three molecules. For the group moments we have used the gas values of the moments of ethyl chloride and bromide.[7] The ethyl rather than the methyl compounds were used to obtain the group moments in order that the inductive effects should be approximately the same as in the disubstituted ethanes. Gas values of the dipole moments were used for the three disubstituted ethanes. The values of V_0 calculated by the above method are tabulated in Table III. Professor C. P. Smyth has suggested to us that perhaps the group moments should be obtained from the methyl rather than the ethyl compounds. If this is done, the values in Table III are all lowered by about 1 kcal./mole. The arguments in favor of either procedure are not conclusive.

The values of V_0 calculated from the cosine potential function are more consistent than the values obtained from the linear or parabolic potential functions. They are also generally lower. In estimating a probable value for V_0 we shall accordingly give them more weight. From these results the probable values of V_0 for *s*-dichloro-ethane, 1,2,bromo-chloro-ethane and *s*-dibromo-ethane are 4, 5, and 6 kcal./mole, respectively. When values of the dipole moments obtained in solution are used somewhat lower values of V_0 are obtained. Lennard-Jones and Pike[8] have treated dichloro-ethane using the cosine potential function. They find that lower values of V_0 are obtained, 2.0 to 3.2 kcal./mole, if a variation of the group moments with ϕ is considered. Altar[3] has treated the dichloroethane dipole moment data using a two-term Fourier series to represent the potential function. This potential curve extended smoothly to small values of ϕ gives a value of V_0 of about 5 kcal./mole. An extrapolation to $\phi=0$ is necessary as his potential function does not represent the actual potential function at small values of ϕ. The determination of the potential curve near $\phi=0$ by any experimental method is doubtful because of the small numbers of molecules in those configurations. The shape of the curve when ϕ is greater than 90° (say) is of much more significance.

The values of V_0 obtained in this paper are in fairly good agreement with electron diffraction results on these compounds.[9]

[6] Zahn, Phys. Rev. **40**, 291 (1932); **38**, 521 (1931).
[7] Smyth and McAlpine, J. Chem. Phys. **2**, 499 (1934).
[8] Lennard-Jones and Pike, Trans. Faraday Soc. **30**, 830 (1934).
[9] Beach and Palmer, in publication; Beach and Turkevich, to be published.

Internal Rotation in Ethylene Chloride*

J. Y. Beach† and K. J. Palmer
Princeton University and California Institute of Technology

(Received July 1, 1938)

The electron diffraction method of investigation has been used to determine the nature of the potential barrier restricting the rotation about the carbon-carbon single bond in ethylene chloride (CH_2Cl-CH_2Cl). Assuming that the shape of the barrier is given by a cosine function, the height of the barrier is between 5 kcal./mole and infinity. This potential barrier is compared with the barrier resulting from the exchange repulsions and the electrostatic repulsions of the two ends of the molecule. Eyring's method was used for calculating the exchange repulsions. The repulsions between the chlorine atoms must be calculated differently from the repulsions between hydrogen and chlorine atoms in order to obtain agreement between theory and experiment. Duplicate experiments were done at Princeton and at Pasadena.

THE electron diffraction photographs of ethylene chloride vapor from which these results are deduced were taken at Pasadena and at Princeton. Both compounds were Eastman products, fractionally distilled in three-foot columns on which the reflux ratio could be controlled. The first photographs were taken by both of us at Pasadena. The Pasadena apparatus has been described by Brockway.[1] The Princeton apparatus is similar to the Pasadena apparatus and has been used previously.[2] The Pasadena and Princeton photographs were made with electrons having wave-lengths of 0.0611A and 0.0590A, respectively. The two sets of photographs, which are identical except for the effect of electron wave-length, and lead to identical results, will not be discussed separately.

We did not attempt to determine by electron diffraction all the bond distances and bond angles in the molecule in addition to the shape of the potential barrier. The carbon-hydrogen distance was assumed to be 1.09A, the carbon-hydrogen distance in methane.[3] The carbon-carbon distance was assumed to be 1.54A, the carbon-carbon distance in diamond[4] and a large number of saturated hydrocarbons.[5] All the bond angles on the carbon atoms were assumed to be tetrahedral. This assumption is made reasonable by the fact that in methylene chloride and chloroform, where the chlorine-chlorine distances are only about 2.90A, the bond angles are but slightly (about 3°) distorted from the tetrahedral value.[6]

The observed values of $s(s_{obs}=(4\pi \sin \theta/2)/\lambda)$ for the maxima and minima and the intensities of the maxima of the electron diffraction photographs are tabulated in Table I. The heavier photographs show up to nine maxima. The last two cannot be measured with much accuracy. The first three maxima are of approximately equal intensity. The fourth and fifth are much weaker. The sixth is strong. The seventh, eighth and ninth are progressively weaker.

The data have been treated by the radial distribution method[7] and by the modified radial distribution method.[8] Both radial distribution curves are shown in Fig. 1. The modified radial distribution curve differs from the ordinary radial distribution curve in that the peaks are sharper. The positions of the maxima are practically identical. The average positions of the maxima on the two curves are 1.73A, 2.70A and 4.29A. The first two peaks represent carbon-chlorine distances, and the third peak represents the chlorine-chlorine distance. 4.29A is just the value of the chlorine-chlorine distance for the *trans*-configuration of the molecule if the carbon-

* Part of these results were presented to the American Physical Society at New York City, February, 1938.
† National Research Fellow in Chemistry.
[1] Brockway, Rev. Mod. Phys. **8**, 231 (1936).
[2] Beach and Stevenson, J. Am. Chem. Soc. **60**, 475 (1938); J. Chem. Phys. **6**, 75 (1938).
[3] Ginsburg and Barker, J. Chem. Phys. **3**, 668 (1935).
[4] *Strukturbericht.*
[5] Pauling and Brockway, J. Am. Chem. Soc. **59**, 1223 (1937).
[6] Sutton and Brockway, J. Am. Chem. Soc. **57**, 473 (1935).
[7] Pauling and Brockway, J. Am. Chem. Soc. **57**, 2684 (1935).
[8] Schomaker, to be published.

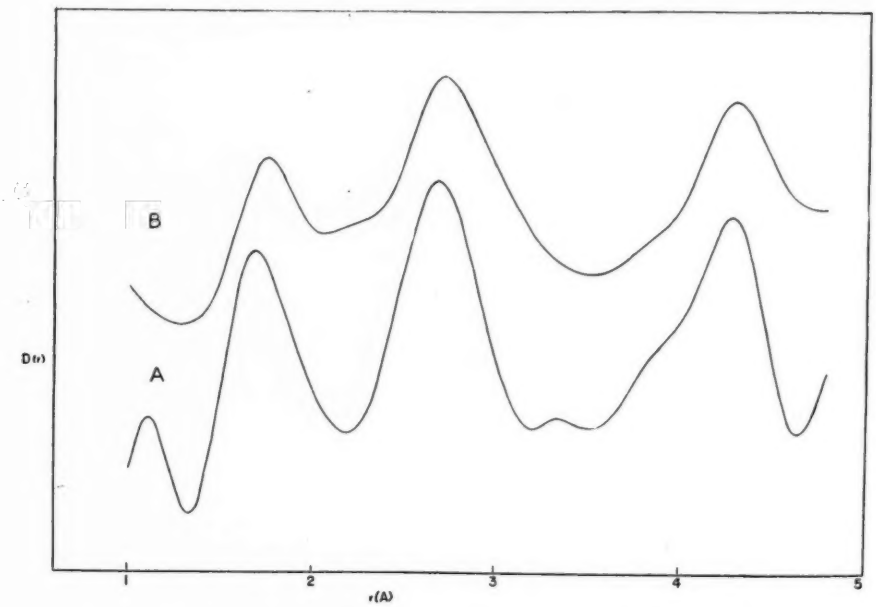

FIG. 1. Curve *A*, modified radial distribution function. Curve *B*, ordinary radial distribution function.

chlorine distance is assumed to be 1.76A, the radius table value[9] for the carbon-chlorine single bond distance. The dissymmetry in the chlorine-chlorine peak on the modified radial distribution curve indicates that some of the molecules are oscillating from the *trans*-configuration to intermediate configurations having shorter chlorine-chlorine distances. While doubtless such motion occurs, the radial distribution function is not sufficiently accurate to make a quantitative estimate of the extent of the motion possible.

TABLE I. *Ethylene chloride.**

Max.	Min.	I	s_{obs}	s_a	s_a/s_{obs}	s_b	s_b/s_{obs}
1		12	3.160	3.26	1.032	3.31	1.047
	2		4.136	3.97	0.960	4.01	0.970
2		15	4.936	4.84	0.981	4.87	0.987
	3		6.668	6.68	1.002		
3		13	7.679	7.72	1.005	7.79	1.014
	4		8.594	8.58	0.998	8.70	1.012
4		4	9.194	9.14	0.994	9.23	1.004
	5		9.964	9.98	1.002	10.09	1.013
5		3	10.591	10.78	1.018		
	6		11.302	11.12	0.984		
6		8	12.041	12.02	0.998	12.10	1.005
	7		13.183	13.02	0.988	13.14	0.997
7		4	14.815	14.95	1.009	14.90	1.006
					Av. 0.998		Av. 1.005
				C−Cl=1.76		C−Cl=1.77	

Final results C−Cl=1.76±0.02A.
5 kcal./mole=≤V_0≤infinity.

* (a) From *trans* curve. (b) From 6 kcal./mole curve. The first maximum and the second minimum were omitted in the averaging.

To arrive at more definite results regarding the oscillation about the *trans*-configuration the electron diffraction data have been treated by the visual method.[10] The relation $V=V_0(\cos\phi+1)$ is assumed to represent the potential barrier to internal rotation. ϕ is the angle between the plane containing one chlorine atom and the two carbon atoms and the plane containing the other chlorine atom and the two carbon atoms. V_0 is the height of the barrier and limits will be placed on its value from the electron diffraction data. This form for the potential function has been shown to be a fairly satisfactory approximation to the actual potential function by a study of the consistency of the V_0 values obtained from dipole moments using different potential functions.[11]

The formula for the intensity of scattered electrons is

$$I=\sum_i\sum_j Z_iZ_j\frac{\sin sl_{ij}}{sl_{ij}}.$$

[9] Pauling and Huggins, Zeits. f. Krist. **87A**, 205 (1934).

[10] Pauling and Brockway, J. Chem. Phys. **2**, 867 (1934).
[11] Beach and Stevenson, J. Chem. Phys. **6**, 635 (1938).

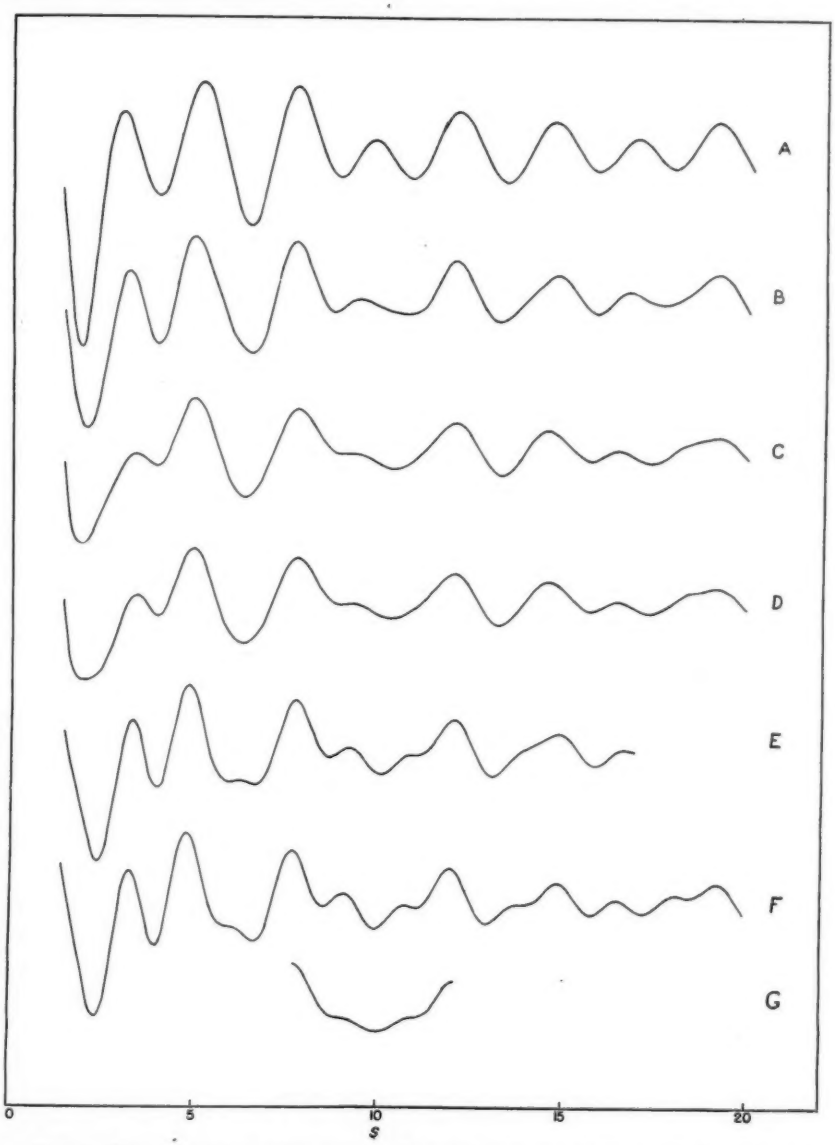

FIG. 2. Theoretical intensity curves. Curve *A*, *cis* model. Curve *B*, half-*cis* and half-*trans*. Curve *C*, free rotation. Curve *D*, $V_0=0.6$ kcal./mole. Curve *E*, $V_0=6.0$ kcal./mole. Curve *F*, $V_0=$infinity, *trans* model. Curve *G*, segment of curve for potential function shown in Fig. 4, Curve *A*.

l_{ij} is the distance from the ith to the jth atom; Z is atomic number. Intensity curves were calculated for ethylene chloride for values of V_0 ranging from zero to infinity. When V_0 equals infinity all the molecules are in the *trans*-position. When V_0 equals zero all the molecules rotate freely, and there are equal numbers of molecules in all configurations. For intermediate values of V_0 the number of molecules possessing a given configuration is found from the Boltzmann factor, $\exp(-V(\phi)/RT)$. The electron diffraction curves are calculated by adding the intensity formulas for molecules having values of $\phi=0°$, $30°$, $\cdots$ $180°$ weighted by the appropriate Boltzmann factor. The Boltzmann factors and the final curves are determined by the value given to V_0.

It has been shown by Altar[12] that this procedure is not rigorously correct. The weighting

[12] Altar, J. Chem. Phys. **3**, 460 (1935).

factors are not exactly equal to the Boltzmann factors. The entropy of the molecule varies with ϕ and the statistical weights are not constant when V_0 equals zero. This is true for this type of molecule even if the product of inertia is independent of ϕ. However, these effects are small at all angles near 180°, which is the region occupied by most of the molecules, and will be neglected.

The electron diffraction intensity curves are plotted in Fig. 2. The *trans*-curve corresponds most closely to the photographs. The 6 kcal./mole curve is less satisfactory because the fifth maximum on it is not sufficiently prominent. The other curves are unsatisfactory from a qualitative inspection, none of them showing the fourth and fifth maxima correctly. Quantitative comparisons of the photographs with curves *E* and *F* are made in Table I. The curves in Fig. 2 are all calculated for molecular models having a carbon-chlorine distance of 1.76A. This does not predetermine the carbon-chlorine distance because if the value had been incorrect a value for the carbon-carbon distance different from the assumed 1.54A would have been obtained when quantitative comparisons of curves and photographs were made. The final results are: C−Cl $=1.76\pm0.02$A and 5 kcal./mole$\leq V_0\leq$infinity.

Wierl,[13] from electron diffraction photographs showing only three maxima, reported that the chlorine-chlorine distance in ethylene chloride is 4.5A. He also stated that ethylene chloride could be an approximately equimolal mixture of *cis* and *trans*-molecules. The theoretical intensity curve for this mixture is curve *B*, Fig. 2. It is unsatisfactory because it possesses only one maximum between the prominent third and sixth maxima, Wierl assumed a carbon-chlorine bond distance of 1.82A. Debye[14] reported a chlorine-chlorine distance of 4.4A from x-ray photographs.

TABLE II. *Repulsions in ethylene chloride, kcal./mole.*

ϕ	0°	30°	60°	90°	120°	150°	180°
Electrostatic interactions	1.80	1.46	0.85	0.18	−0.29	−0.59	−0.65
Exchange repulsions	14.03	13.30	12.83	13.83	14.58	14.38	13.75
Total	15.83	14.76	13.68	14.01	14.29	13.79	13.10
$E(\phi)-E(\pi)$	2.73	1.66	0.58	0.91	1.77	0.69	0.0
Corrected exchange repulsions	17.37	15.82	14.22	14.45	14.87	14.56	13.89
Corrected exchange plus electrostatic	19.17	17.28	15.07	14.63	14.58	13.97	13.24
$E(\phi)-E(\pi)$	5.93	4.04	1.83	1.39	1.34	0.73	0.0

[13] Wierl, Ann. d. Physik **13**, 453 (1932).

Discussion

There are several contributions to the potential barrier to internal rotation, the more important ones being the exchange steric repulsion between all atoms not bonded to each other, the electrostatic interaction of the bond dipoles, and the interaction between the bond orbitals on the carbon atoms. The magnitude of this last effect in H_2O_2 has been calculated by Penney and Sutherland.[15] They find that the potential energy of the molecule due to this interaction has maxima of about 2 kcal./mole in the *cis*- and *trans*-positions and minima when ϕ is $\pm90°$. This effect in ethane or ethylene chloride would lead to three approximately equal potential minima at angles of 120°. The depth of the minima should be less for several reasons. The carbon atoms are separated by a greater distance than the oxygen atoms. The orbitals on the carbon atoms make a larger angle (109° 28′) with the carbon-carbon bond than the oxygen orbitals make with the oxygen-oxygen bond (90°). The potential humps are separated by only 120° instead of 180° and the nine repulsions will tend to cancel. To show how this might occur we have calculated the exchange repulsions[16] between hydrogen atoms for the hypothetical molecule H_2OOH_2. The H_2OO groups are assumed to be planar and the H−O−O angles tetrahedral. The hydrogen atoms are located approximately on the loops of the oxygen orbitals, the interaction between which has been calculated by Penney and Sutherland. Taking 0.94A and 1.32A for the hydrogen-oxygen and oxygen-oxygen distances, the steric repulsions between hydrogen atoms is greater by 1.9 kcal./mole when $\phi=0°$ than for the configuration with $\phi=90°$. Comparing this with the steric repulsion potential barrier of 0.3 kcal./mole, obtained by Eyring[16] for ethane, it is seen that the nine interactions tend to cancel out. If an analogy exists between orbital interactions and steric

[14] Debye, Physik. Zeits. **31**, 142 (1930).
[15] Penney and Sutherland, J. Chem. Phys. **2**, 492 (1934).
[16] Eyring, J. Am. Chem. Soc. **54**, 3191 (1932).

repulsions, which does not seem unreasonable, the orbital interaction in ethane, ethylene chloride, etc., would be expected to give rise to a small potential barrier, 0.3 or 0.4 kcal./mole.

The dipole interaction of the two CH_2Cl groups has been calculated by Smyth, Dornte and Wilson.[17] They used the formula for the interaction of dipoles at large distances, placing the dipole at a point along the carbon-chlorine bond. Changing the position of the dipole on the carbon-chlorine bond altered the shape of the potential curve but did not change the difference in energy between the *cis*- and *trans*-configurations. We have repeated the calculations assuming that the dipoles are due to charges located at the center of the atoms. This is true insofar as the charge distributions on the atoms are spherically symmetric. The magnitudes of the charges are found by dividing the bond moments[18] by the interatomic distances. Summing the nine electrostatic interactions gives a slightly higher potential barrier, 2.4 kcal./mole. This potential curve is tabulated in Table II and is shown in Fig. 3, curve *A*.

The van der Waals attractions have not been calculated as the present methods of calculating them yield abnormally large interaction at small interatomic distances.

The largest interactions between the two CH_2Cl groups are the exchange repulsions. These can be calculated by the method of Eyring.[16] We have calculated and summed the nine repulsions as a function of the angle ϕ. The Morse curve was assumed to be 20 percent coulombic. The sum is tabulated in Table II and is shown in Fig. 3, curve *B*. The exchange plus the electrostatic interactions are tabulated in Table II and shown in Fig. 4, curve *A*.

To see if this potential curve is compatible with the electron diffraction data we have calculated the theoretical intensity formula for it. A segment of it is shown in Fig. 2, curve *G*. It is unsatisfactory in the region shown. It does not show the fourth and fifth maxima. If the potential curve *A*, Fig. 4, were correct the radial distribution function would show a peak at 3.2A roughly equal in height to the one at 4.29A.

[17] Smyth, Dornte and Wilson, J. Am. Chem. Soc. **53**, 4242 (1931).
[18] Smyth, J. Phys. Chem. **41**, 209 (1937).

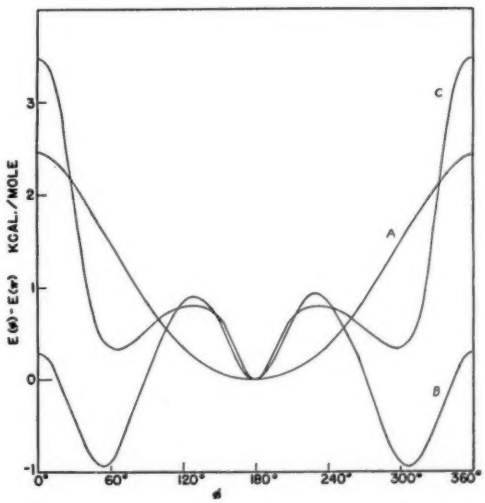

FIG. 3. Curve *A*, electrostatic interaction. Curve *B*, exchange repulsion. Curve *C*, corrected exchange repulsion.

That this peak is not present is easily seen in Fig. 1. If the repulsions between the chlorine atoms were greater at the *cis*-position by about 2.5 kcal./mole, the theoretical potential curve would be brought into agreement with the electron diffraction data.

Professor Eyring has suggested to us that because of the large number of nonbonding electrons in Cl_2 a deeper Morse curve than the actual one should be used in calculating the exchange repulsions. We have adopted the following procedure for doing this. The Morse curve for Cl_2 is multiplied by 14/8, the ratio of the total number of valence electrons to the number of electrons on the valence shell of one atom. This will not affect the Morse curve of a bond involving a hydrogen atom. Assuming that 20 percent of this Morse curve is coulombic and calculating the chlorine-chlorine repulsions leads to the corrected repulsions. When these repulsions are used the potential barrier becomes higher. It is tabulated in Table II and plotted in Fig. 4, curve *B*. The electron scattering curve calculated for this potential barrier is identical with the one calculated for $V_0=6.0$ kcal./mole, curve *E*, Fig. 2. The agreement between theoretical and experimental potential barriers requires that the chlorine-chlorine repulsions be calculated by this or some analogous method. The same results can be reached by assuming

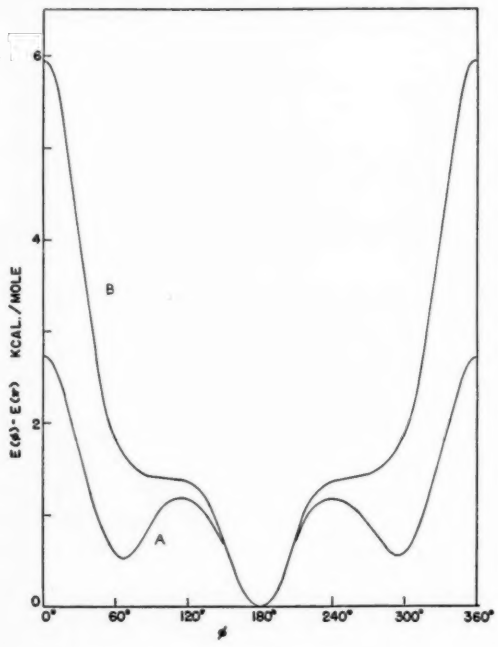

FIG. 4. Curve *A*, exchange repulsion plus electrostatic interaction. Curve *B*, corrected exchange repulsion plus electrostatic interaction.

that the coulombic part of the Cl_2 Morse curve is different (smaller) from the 20 percent used for the other calculations of exchange repulsions. The procedure above seems to us more justifiable.

The strongest justification for the above procedure is that it leads to results in agreement with the electron diffraction data on ethylene chloride. This calculation does not change the values previously calculated for the hydrogen-hydrogen repulsion in ethane. Our estimate of the orbital interaction when added to the hydrogen-hydrogen repulsions gives a value of about 0.6 kcal./mole for the potential barrier in ethane. The methods we find satisfactory for calculating the barrier in ethylene chloride do not lead to the high barrier (3 kcal./mole) which has been reported for ethane. It is possible that the analogy on which our estimate of the orbital interaction is based is not sufficiently good. However, it is difficult to understand why it should be as bad as is indicated by the existing data on ethane.

Altar[12] has obtained a potential barrier for ethylene chloride from the temperature variation of the dipole moment. The theoretical intensity curve from Altar's potential function is identical with curve *E*, Fig. 2, for which V_0 is 6 kcal./mole. The shape of his curve near the *trans*-position is the same as the shape of a cosine curve having an amplitude of 5 kcal./mole. The difference between the two potential curves at small values of ϕ cannot be detected in the electron diffraction curves because of the small fraction of the molecules having small values of ϕ. It must be emphasized that in putting limits on V_0, the height of the barrier, we have assumed a certain shape for the potential curve. We have really only determined the shape of the potential curve near the *trans*-position of the molecule. At small values of ϕ the shape of the barrier may be quite different from that of a cosine function. If the actual barrier is steeper than the cosine function at small values of ϕ, our V_0 is small. If the actual barrier is flatter than the cosine function at small values of ϕ, our V_0 is too high. In any event, the barrier is high at small angles.

We wish to thank Professor Henry Eyring, Professor Linus Pauling and Professor Charles P. Smyth for many valuable discussions on this subject.

Calculations of the Lower Excited Levels of Benzene

M. GOEPPERT-MAYER, *Department of Physics, The Johns Hopkins University, Baltimore, Maryland*

AND

A. L. SKLAR,* *Department of Physics, The Catholic University of America, Washington, D. C.*

(Received August 3, 1938)

The energy of the first excited levels of benzene is calculated by the method of antisymmetrized molecular orbitals. The results predict two weak bands, due to forbidden electronic transitions, at $\lambda=2500$ and $\lambda=2100$ and a strong band at $\lambda=1500$. No empirical data except the carbon-carbon distance in benzene were used.

IN a previous paper,[1] one of the authors calculated the excited electronic levels of some organic molecules, among them benzene, on the basis of the Heitler-London method of approximation. The same calculation is undertaken here for benzene with the method of antisymmetrized products of molecular orbitals.[2]

I. THE ORBITALS

Of the four valence electrons of each carbon atom those in the $2s$-eigenfunctions and in the $2p$-eigenfunctions whose node is normal to the plane of the benzene molecule give rise to sp^2 hybridized single bonds to neighboring carbon atoms and to the hydrogens. The angles between the three sp^2 hybridized wave functions determine the geometry of the benzene molecule. The remaining 6 electrons, one for each carbon, are in the $2p\pi$ atomic eigenfunctions whose node coincides with the plane of the benzene ring. These electrons are responsible for the aromatic properties of benzene and for the lower absorption bands.[1] We are here concerned with the different molecular states of these 6 electrons only.

The electrons shall be denoted by Greek letters $\nu, \mu, 1, \cdots, 6$. The different carbon atoms will be denoted by k. The $2p\pi$ eigenfunction of the kth carbon atom will be written $K(\nu)$; specifically $I(\nu), \cdots, VI(\nu)$. They are all taken to be positive on the same side of the benzene plane.

The interaction between the 6 electrons is at first neglected. The potential H_0 acting on the electrons has then the symmetry of the benzene molecule and may be written as a sum of the contributions from each atom.

$$\mathrm{H}_0=\sum_K H_K. \tag{1}$$

Of the 6 K-functions the following 6 mutually orthogonal orbitals have to be formed[3]

$$\phi_l(\nu)=(6\sigma_l)^{-\frac{1}{2}}\sum_{k=1}^{6}\exp^{2\pi ilk/6}K(\nu), \quad \phi_l{}^*=\phi_{-l} \tag{2}$$

with $l=0, \pm1, \pm2, 3$. The coefficients $\sigma_l{}^{-\frac{1}{2}}$ take care of the normalization. If the overlapping integral $\int I(\nu)II(\nu)d\tau_\nu$ is neglected, all σ's become unity.

With this approximation, and neglecting of integrals over products of K's which are not neighbors, the energies of the orbitals are:

$$\epsilon_l=\int I(T+H_0)Id\tau + 2\cos(2\pi l/6)\int I(T+H^0)IId\tau, \tag{3}$$

where T is the kinetic energy. In section IV the energies will be evaluated more exactly.

It is seen that the energies of the orbitals increase with $|l|$ since $\int I(T+H^0)IId\tau$ is negative. The energy depends only on the absolute value $|l|$, showing that the levels with $|l|=1$ and $|l|=2$ are doubly degenerate.

* This work was supported by a grant from the Penrose Fund of the American Philosophical Society.

[1] A. L. Sklar, J. Chem. Phys. **5**, 669 (1937).

[2] R. S. Mulliken, J. Chem. Phys. **1**, 492 (1933); Phys. Rev. **32**, 186, 761 (1928); **33**, 730 (1929); **40**, 55, **41**, 49, 751; **43**, 279 (1932–3). J. E. Lennard-Jones, Trans. Faraday Soc. **25**, 668 (1929). G. Herzberg, Zeits. f. Physik **57**, 601 (1929).

[3] E. Hückel, Zeits. f. Physik **70**, 204 (1931).

The energy of the molecule is lowest if the orbitals ϕ_0, ϕ_1, ϕ_{-1} contain two electrons each. The eigenfunction of the ground state in this order of approximation is the product

$$\psi_0=\phi_0(1)\phi_0(2)\phi_1(3)\phi_1(4)\phi_{-1}(5)\phi_{-1}(6). \quad (4)$$

The first excited level arises if one electron from the state $l=+1$ or $l=-1$ is lifted to $l=2$ or $l=-2$. Its energy above the ground state is $\epsilon_2-\epsilon_1$. To this level belong four different eigenfunctions:

$$\begin{aligned}
\psi_1&=\phi_0(1)\phi_0(2)\phi_{+1}(3)\phi_{+1}(4)\phi_{-1}(5)\phi_{+2}(6),\\
\psi_2&=\phi_0(1)\phi_0(2)\phi_{-1}(3)\phi_{-1}(4)\phi_{+1}(5)\phi_{-2}(6),\\
\psi_3&=\phi_0(1)\phi_0(2)\phi_{+1}(3)\phi_{+1}(4)\phi_{-1}(5)\phi_{-2}(6), \quad (5)\\
\psi_4&=\phi_0(1)\phi_0(2)\phi_{-1}(3)\phi_{-1}(4)\phi_{+1}(5)\phi_{+2}(6),\\
\psi_1&=\psi_2^*; \quad \psi_3=\psi_4^*.
\end{aligned}$$

II. Group Theoretical Considerations

The way in which this 4-fold level of the molecule as a whole splits up, due to electronic interaction, and the behavior of the resultant molecular states can be determined without calculation by the application of group theory. The potential H_0 has the symmetry of the benzene ring, which is transformed into itself by rotations and reflections forming the group D_{6h}. The group operations transform any orbital ϕ_l into a linear combination of orbitals of the same energy, with coefficients which are the matrix elements of an irreducible representation of the group. The same holds true for a state of the molecule as a whole. The interaction between the electrons cannot alter this; it is only capable of splitting up "accidental" degeneracies, namely to separate the energies of states belonging to different irreducible representations which happened to be energetically equal in the zero*th* approximation.

We wish therefore to investigate which irreducible representations of the benzene group are contained in the reducible fourth order representation determined by the transformation properties of the functions (5).

From the group table[4] of D_{6h}, by the usual method of comparison of the characters, the irreducible representations of the one electron orbitals can be found immediately. They are

$$\phi_0 \subset \Gamma_8(A_{2u}); \quad \phi_1, \phi_{-1} \subset \Gamma_6(E_{1g});$$
$$\phi_2, \phi_{-2} \subset \Gamma_{11}(E_{2u}); \quad \phi_3 \subset \Gamma_4(B_{2g}),$$

where the symbols in brackets are the notation of Mulliken and Placzek.[5] Every closed shell transforms like the identical representation $\Gamma_1(A_{1g})$, that is, remains unchanged under the operations of the group. We find therefore for the eigenfunction of the ground state

$$\psi_0 \subset \Gamma_1(A_{1g}).$$

The four eigenfunctions of the excited level transform like the products $\phi_{\pm1}$, $\phi_{\pm2}$, namely:

$$\psi_1 \cdots \psi_4 \subset \begin{matrix} \Gamma_6 \times \Gamma_{11} = (\Gamma_9 + \Gamma_{10} + \Gamma_{12}) \\ E_{1g} \times E_{2u} = (B_{1u} + B_{2u} + E_{1u}) \end{matrix}.$$

The excited level will therefore split up into two single states belonging to Γ_9 and Γ_{10}, and one doubly degenerate one belonging to the two-rowed representation Γ_{12}.

Transitions between an excited state and the ground state with emission or absorption of light occur only if the integral of at least one component of the electric moment P multiplied by the eigenfunctions of ground- and excited state does not vanish. This is the case if the integrand is completely symmetrical, or at least contains an additive part which has this property. In other words, an excited level will be active in combination with the ground state only if the direct product of its representation and the representation of P contains the identical representation Γ_1. The transformation properties of P are the following:

$$P_z \text{ (normal to benzene plane)} \subset \Gamma_8(A_{2u});$$
$$P_x, P_y \text{ (in the plane)} \subset \Gamma_{12}(E_{1u}).$$

None of the products of Γ_8 with Γ_9, Γ_{10} or Γ_{12} contains Γ_1 nor do the products of Γ_{12} with Γ_9 and Γ_{10}. Only $\Gamma_{12} \times \Gamma_{12}$ contains a totally symmetrical part, so that Γ_{12} is the only active level, and is capable of emitting light polarized in the benzene plane, that is, perpendicular bands.

[4] Bright Wilson, Phys. Rev. **45**, 706 (1934).

[5] Mulliken, Phys. Rev. **43**, 279 (1933).

Transitions from the states Γ_9 and Γ_{10} to the ground state are, however, possible with simultaneous emission or absorption of vibrational energy, for instance of one quantum of vibration frequency of symmetry $\Gamma_5(E_{2g})$ that is of a degenerate, Raman active vibration (frequencies ν_6, ν_7, ν_8, ν_9 in the notation of E. Bright Wilson); or in combination with emission or absorption of two quanta of any degenerate vibration. It is to be expected that these transitions are weak, since they would vanish completely if the eigenfunction of the total molecule could be expressed as a product of vibrational and electronic functions.

The linear combinations of the four product eigenfunctions ψ (5) which have the symmetries Γ_9, Γ_{10}, Γ_{12} respectively are:

$$\begin{aligned} \Gamma_9(B_{1u})\Psi &= 2^{-\frac{1}{2}}(\psi_1+\psi_2), \\ \Gamma_{10}(B_{2u})\Psi &= 2^{-\frac{1}{2}}(\psi_1-\psi_2), \\ \Gamma_{12}(E_{1u})&\begin{cases} \Psi_3=\psi_3, \\ \Psi_4=\psi_4. \end{cases} \end{aligned} \tag{6}$$

III. Electronic Interaction

The change of energy of the states due to the electronic interaction

$$H^1=\sum_{\substack{\nu=1 \\ \mu<\nu}}^{6}\frac{e^2}{r_{\nu\mu}} \tag{7}$$

will now be calculated.

The molecular eigenfunctions of the ground state (4) and the excited states (6) must be multiplied by an appropriate spin function and made completely antisymmetrical with respect to the exchange of electrons. The two possible spin functions for the νth electron will be denoted by $\alpha(\nu)$, $\beta(\nu)$. If two electrons are in the same orbital, they must necessarily have opposite spins. For the ground state, therefore, the spin function

$$\chi_0=\alpha(1)\beta(2)\alpha(3)\beta(4)\alpha(5)\beta(6) \tag{8}$$

gives the most general result.

For the excited states two cases must be distinguished. The spins of electrons 5 and 6, the only ones which are unpaired, may be either opposite or parallel. In the first case, the spin function must be made antisymmetric in 5 and 6, namely

$$\chi_s=2^{-\frac{1}{2}}\alpha(1)\beta(2)\alpha(3)\beta(4) \times[\alpha(5)\beta(6)-\beta(5)\alpha(6)]. \tag{9}$$

In the second case it must be symmetric in 5 and 6, which can be done in three different ways, corresponding to the three orientations of the sum of the spins in space, one of which is

$$\chi_t=\alpha(1)\beta(2)\alpha(3)\beta(4)\alpha(5)\alpha(6), \tag{10}$$

while the others contain $\beta(5)\beta(6)$ and

$$2^{-\frac{1}{2}}[\alpha(5)\beta(6)+\beta(5)\alpha(6)].$$

Since the perturbing potential H^1 (7) is spin independent, spin states (9) and (10) do not interact. We shall refer to the states described by eigenfunctions obtained with (9) as singlet states, to those obtained with the three spin functions symmetric in 5 and 6, of which (10) is one, as triplet states. The energy of the latter three is the same in this approximation. The magnetic interaction between spin and orbit may however, bring about a fine structure splitting.

The totally antisymmetric eigenfunctions are then obtained by performing all 6! permutations P of electrons on the product of spin and coordinate function, multiplying the result by -1 to the order (odd or even) of the permutation and adding. For instance, for the ground state

$$\mathbf{\Psi}_0=(6!)^{-\frac{1}{2}}\sum_P(-1)^P P\Psi_0\chi_0.$$

Since the molecular orbitals ϕ_l are *strictly* orthogonal, the average value of H^1 for any such function can be expressed without any approximation, since all integrals over products of functions in which more than two electrons are in different molecular orbitals are zero. The energy will contain Coulomb terms, of the form

$$\gamma_{ll'}=\int\int\frac{e^2}{r_{\nu\mu}}|\phi_l(\nu)|^2|\phi_{l'}(\mu)|^2 d\tau_\nu d\tau_\mu \tag{11}$$

and exchange terms

$$\delta_{ll'}=\int\int\frac{e^2}{r_{\nu\mu}}\phi_l(\nu)\phi_{l'}(\mu)[\phi_l(\mu)\phi_{l'}(\nu)]^* d\tau_\nu d\tau_\mu. \tag{12}$$

Of the product eigenfunctions (4), ψ_3 and ψ_4 interact with none of the permutations of any

other one, bearing out the fact that the eigenfunctions (6) are the correct ones. The interaction between ψ_1 and ψ_2 brings in two more integrals,

$$\xi=\int\int\frac{e^2}{r_{\nu\mu}}\phi_1(\nu)\phi_{-1}{}^*(\nu)\phi_2(\mu)\phi_{-2}{}^*(\mu)d\tau_\nu d\tau_\mu$$

$$=\int\int\frac{e^2}{r_{\nu\mu}}\phi_1{}^2(\nu)\phi_2{}^2(\mu)d\tau_\nu d\tau_\mu, \quad (13)$$

$$\eta=\int\int\frac{e^2}{r_{\nu\mu}}\phi_1(\nu)\phi_2(\nu)\phi_1(\mu)\phi_2(\mu)d\tau_\nu d\tau_\mu. \quad (14)$$

All integrals γ, δ, ξ, η are real.

The energies, including electronic interaction, are then for the ground state

$$E_0=2\epsilon_0+4\epsilon_1+\gamma_{00}+8\gamma_{01}+6\gamma_{11}-4\delta_{01}-2\delta_{1-1}, \quad (15)$$

where ϵ_0 and ϵ_1 are the energies of the orbitals (3).

For the excited singlet states, the energies are

$$\begin{aligned} E_{1s}&=E^{(1)}+\delta_{-12}-\delta_{12}-\xi+2\eta, && {}^1\Gamma_9(B_{1u}),\\ E_{2s}&=E^{(1)}+\delta_{-12}-\delta_{12}+\xi-2\eta, && {}^1\Gamma_{10}(B_{2u}), \quad (16)\\ E_{3s}&=E^{(1)}-\delta_{-12}+\delta_{12}, && {}^1\Gamma_{12}(E_{1u}), \end{aligned}$$

and for the triplet states

$$\begin{aligned} E_{1t}&=E^{(1)}-\delta_{-12}-\delta_{12}-\xi, && {}^3\Gamma_9(B_{1u}),\\ E_{2t}&=E^{(1)}-\delta_{-12}-\delta_{12}+\xi, && {}^3\Gamma_{10}(B_{2u}), \quad (17)\\ E_{3t}&=E^{(1)}-\delta_{-12}-\delta_{12}, && {}^3\Gamma_{12}(E_{1u}), \end{aligned}$$

where the term E^1 which all excited levels have in common is

$$E^{(1)}=2\epsilon_0+3\epsilon_1+\epsilon_2+\gamma_{00}+6\gamma_{01}+2\gamma_{02}$$
$$+3\gamma_{11}+3\gamma_{12}-3\delta_{01}-\delta_{02}-\delta_{1-1}. \quad (18)$$

The subscripts 1, 2, 3 correspond to those on the eigenfunctions (6).

IV. The Energies in Terms of Atomic Integrals

The next task is to express all the integrals γ, δ, ξ, η over molecular orbitals in terms of integrals over the atomic eigenfunctions $K(\nu)$ through the use of (2).

The normalization coefficients σ_l of the orbitals are first determined by the relation:

$$\sigma_l=\tfrac{1}{6}\int\sum_K\{K^2(\nu)+2\cos(2\pi l/6)K(\nu)(K+I)(\nu)$$
$$+2\cos(4\pi l/6)K(\nu)(K+II)(\nu)$$
$$+(-1)^lK(\nu)(K+III)(\nu)\}d\tau_\nu$$
$$=1+2\cos(2\pi l/6)\int I(\nu)II(\nu)d\tau_\nu$$
$$+2\cos(4\pi l/6)\int I(\nu)III(\nu)d\tau_\nu$$
$$+(-1)^l\int I(\nu)IV(\nu)d\tau_\nu.$$

The functions $K(\nu)$ are assumed to be normalized. If the "overlap integrals" between neighbors are denoted by s_1, between next to neighbors s_2 and between opposite places in the ring s_3, the above expression can be written

$$\sigma_l=1+2s_1\cos\frac{2\pi l}{6}+2s_1\cos\frac{4\pi l}{6}+(-1)^ls_3. \quad (19)$$

The integrals $\gamma_{ll'}$ and $\delta_{ll'}$ contain the terms $\sigma_l\cdot\sigma_{l'}$ in the denominator, the integrals ξ and η the term $\sigma_1\cdot\sigma_2$. The expansions of the orbital integrals contain molecular integrals of Coulomb type between electrons on the same and on different atoms,

$$A_K=\int\int\frac{e^2}{r_{\nu\mu}}I^2(\nu)\cdot(K+I)^2(\mu)d\tau_\nu d\tau_\mu, \quad (20)$$

secondly a mixed exchange and Coulomb integral the interaction between an electron on one atom with one that is shared between the same and the neighboring atom,

$$B=\int\int\frac{e^2}{r_{\nu\mu}}I^2(\nu)I(\mu)II(\mu)d\tau_\nu d\tau_\mu, \quad (21)$$

and finally the exchange integral between electrons on neighboring atoms

$$C=\int\int\frac{e^2}{r_{\nu\mu}}I(\nu)II(\nu)I(\mu)II(\mu)d\tau_\nu d\tau_\mu. \quad (22)$$

Interactions between electrons which are partially on atoms which are not nearest neighbors shall be neglected, except for the purely Coulomb terms (20). All integrals A, B, C, s_ν are positive.

In this nomenclature, formulae(16) and (17) for the energies of the excited states take the form

$$\begin{aligned}
E_{1s} &= E^{(1)}+(1/6\sigma_1\sigma_2)\{\quad A_0-6A_1+8A_2-3A_3+\ C\}, && {}^1\Gamma_9(B_{1u}),\\
E_{2s} &= E^{(1)}+(1/6\sigma_1\sigma_2)\{\ -A_0-2A_2\qquad +3A_3+5C\}, && {}^1\Gamma_{10}(B_{2u}), \quad (23)\\
E_{3s} &= E^{(1)}+(1/6\sigma_1\sigma_2)\{\qquad 3A_1-3A_2\qquad -3C\}, && {}^1\Gamma_{12}(E_{1u}),\\
E_{1t} &= E^{(1)}+(1/6\sigma_1\sigma_2)\{-3A_0+2A_1\qquad +\ A_3+\ C\}, && {}^3\Gamma_9(B_{1u}),\\
E_{2t} &= E^{(1)}+(1/6\sigma_1\sigma_2)\{\ -A_0\qquad -2A_2+3A_3-7C\}, && {}^3\Gamma_{10}(B_{2u}), \quad (24)\\
E_{3t} &= E^{(1)}+(1/6\sigma_1\sigma_2)\{-2A_0+\ A_1-\ A_2+2A_3-3C\}, && {}^3\Gamma_{12}(E_{1u}).
\end{aligned}$$

The order of the singlet terms will be shown to be $E_{2s}<E_{1s}<E_{3s}$, that of the triplet states $E_{1t}<E_{3t}<E_{2t}$, with the triplet states lower than the singlets.

The common term $E^{(1)}$ (18) of the excited states, as well as the energy of the ground state E_0 (15) are too complicated, due to the different normalization factors, to be written down in the general form. We are, here, however, interested only in the height of the excited levels above the ground state, and therefore in $E^{(1)}-E_0$. Using the numerical values of s_1, s_2, s_3, and therefore of the normalization coefficients σ_0, σ_1, σ_2 (see Table I), we obtain

$$\begin{aligned}
E^{(1)}-E_0 &= \epsilon_2-\epsilon_1-2\gamma_{01}+2\gamma_{02}-3\gamma_{11}\\
&\quad +3\gamma_{12}+\delta_{01}-\delta_{02}+\delta_{1-1}\\
&= \epsilon_2-\epsilon_1+0.4_1A_0+0.8_1A_1+0.64A_2\\
&\quad +0.23A_3-1.15B-1.26C.
\end{aligned} \qquad (25)$$

Lastly, we are confronted with the calculation of the energies ϵ_l of the orbitals due to the potential of the benzene rings. An approximate form for these was given in (3). The complete expression is

$$\epsilon_l=\frac{1}{\sigma_l}\int I(\nu)(T+H_0)\{I(\nu)+2\cos(2\pi l/6)II(\nu)+2\cos(4\pi l/6)III(\nu)+(-1)^lIV(\nu)\}d\tau_\nu. \qquad (26)$$

The effect of the hydrogen atoms will be neglected completely. In the expression

$$H_0=\sum_K H_K$$

the potential H_K is then simply the attraction of the carbon nucleus and the repulsion of the other five carbon electrons. Since $I(\nu)$ is supposed to be an atomic eigenfunction, the relation

$$(T+H_I(\nu))I(\nu)=W_{2p}I(\nu) \qquad (27)$$

holds, where W_{2p} is the energy of a $2p$ electron in a carbon atom in the valence state. This term occurs once in every one of the 4 terms of ϵ_l (26), with coefficients that add up to σ_l, precisely canceling the σ_l in the denominator. W_{2p} therefore drops out of the difference $\epsilon_2-\epsilon_1$ since its coefficient in each ϵ_l is independent of l.

In the potential H_K the two electrons of the inner shell of the carbon atom shall be treated as if they were located in the nucleus. $H_K(\nu)$ is then the electrostatic potential at the place ν of a nucleus of charge 4 plus one electron in each of the three $2sp\sigma$ hybridized wave functions, or, which is the same, of the nucleus and one electron each in a $2s$ and the two $2p\sigma$ eigenfunctions. The calculation of the new integrals can be simplified by noticing that H_K is the potential of a neutral carbon atom with one electron in the $2s$ and each of the three $2p$ functions, minus the potential of a $2p\pi$ electron. The potential of the neutral carbon atom, $\mathbf{H}_K$ is a spherically symmetrical

TABLE I.

$s_1=\int I(\nu)II(\nu)d\tau_\nu$	= .26
$s_2=\int I(\nu)III(\nu)d\tau_\nu$	= .04
$s_3=\int I(\nu)IV(\nu)d\tau_\nu$	= .02
$A_0=\int\int e^2/r_{\nu\mu}I^2(\nu)I^2(\mu)d\tau_\nu d\tau_\mu$	= 16.82 volts
$A_1=\int\int e^2/r_{\nu\mu}I^2(\nu)II^2(\mu)d\tau_\nu d\tau_\mu$	= 8.78
$A_2=\int\int e^2/r_{\nu\mu}I^2(\nu)III^2(\mu)d\tau_\nu d\tau_\mu$	= 5.64
$A_3=\int\int e^2/r_{\nu\mu}I^2(\nu)IV^2(\mu)d\tau_\nu d\tau_\mu$	= 4.95
$B=\int\int e^2/r_{\nu\mu}I^2(\nu)I(\mu)II(\mu)d\tau_\nu d\tau_\mu$	= 4.47
$C=\int\int e^2/r_{\nu\mu}I(\nu)II(\nu)I(\mu)II(\mu)d\tau_\nu d\tau_\mu$	= .87
$Q=-\int\mathbf{H}_I(\nu)II^2(\nu)d\tau_\nu$	= .83
$R=-\int\mathbf{H}_I(\nu)I(\nu)II(\nu)d\tau_\nu$	= 1.89

$I(\nu)$, $II(\nu)$ designate $2p\pi$ carbon functions (32) around nuclei I, II, respectively, $\mathbf{H}$ is the potential of a neutral carbon atom (33).

attraction and we may write

$$H_K(\nu)=\mathbf{H}_K(\nu)-\int\frac{e^2}{r_{\nu\mu}}K^2(\mu). \tag{28}$$

If (27) and (28) are inserted into (26) the second part gives rise to integrals of the types A and B (20), (21), the first part to new integrals, namely the effect of one neutral carbon atom on an electron at another nucleus,

$$Q=-\int\mathbf{H}_I(\nu)II^2(\nu)d\tau_\nu \tag{29}$$

and the effect of the potential on an electron partially on the same and on the neighboring atom

$$R=-\int\mathbf{H}_I(\nu)I(\nu)II(\nu)d\tau_\nu. \tag{30}$$

The minus sign is introduced in order to make both Q and R positive. All terms involving $\mathbf{H}_K$ which arise from interactions of non-neighbors are small enough to be neglected. The difference of ϵ_2 and ϵ_1 is then

$$\begin{aligned}\epsilon_2-\epsilon_1&=\frac{\sigma_1-\sigma_2}{\sigma_1\sigma_2}\{-2Q-2A_1-2A_2-A_3\}\\&\qquad+\frac{\sigma_1+\sigma_2}{\sigma_1\sigma_2}\{R+B\} \qquad (31)\\&=-1.12Q+2.22R-1.12A_1\\&\qquad-1.12A_2-0.56A_3+2.22B.\end{aligned}$$

If (31) is put into (25) we obtain the final result for the part of the energy common to all excited states above the ground state

$$\begin{aligned}E^{(1)}-E_0=&-1.12Q+2.22R+0.41A_0\\&-0.31A_1-0.48A_2-0.33A_3\\&+1.07B-1.26C. \qquad (32)\end{aligned}$$

V. Numerical Values

The eigenfunctions used for the calculation of the numerical integrals are $2p\pi$ hydrogen like functions at the different nuclei,

$$K(r,\theta,\phi)=\left(\frac{z^5}{32\pi}\right)^{\frac{1}{2}}r\exp(-zr/2)\sin\theta\cos\phi. \tag{33}$$

The screening constant z was chosen to be $z=3.18$, a value which was obtained by Zener[6] on the basis of a variational calculation minimizing the energy of the ground state of one carbon atom. This screening constant is not necessarily the most advantageous one for our molecular calculation. Minimizing the energy of one carbon atom in its valence state would presumably give a more correct value for z.

The distance between carbon atoms is $r_0=1.39A$,[7] which leads to $zr_0=8.37$ in atomic units.

The numerical values of the integrals used are collected in Table I.

The overlap integrals s can be calculated in closed form.[8] A_0, the repulsion between two electrons on the same atom, was calculated for this paper. The Coulomb repulsions between electrons on different atoms, A_1, A_2, A_3, as well as the exchange integral C were taken from the tables of Bartlett.[9]

The integral B, the repulsion between one electron on one atom and one shared between the same and a neighboring atom was not to be found in the literature. The evaluation was complicated and details of the calculation will be published shortly by one of the authors and R. H. Lyddane.

The attraction of a neutral carbon atom, in the valence state for an electron is:

$$\mathbf{H}_I=-\frac{4e^2}{r_\nu}+\frac{1}{r_\nu}\int_0^{r_\nu}e^2\sigma(r)r^2dr+\int_{r_\nu}^{\infty}e^2\sigma(r)rdr, \tag{34}$$

where

$$\begin{aligned}\sigma(r)=4\pi\{&|\psi_{2s}|^2+|\psi_{2p_x}|^2\\&+|\psi_{2p_y}|^2+|\psi_{2p_z}|^2\}. \qquad (35)\end{aligned}$$

r_ν signifies the distance of the electron from the nucleus of the carbon atom I.

Since

$$\int_0^{\infty}\sigma(r)r^2dr=4$$

(34) may be simplified to

$$\mathbf{H}_I=-\int_{r_\nu}^{\infty}\left(\frac{r}{r_\nu}-1\right)\sigma(r)rdr. \tag{36}$$

[6] Zener, Phys. Rev. **36**, 51 (1930).
[7] *Handbuch der Physik*, Vol. 24, No. 2, p. 143.
[8] *Handbuch der Physik*, Vol. 24, No. 1, p. 643.
[9] J. H. Bartlett, Phys. Rev. **37**, 507 (1931). In Bartlett's notation, $A=i_1+\frac{1}{2}i_7$ and $C=i_2+\frac{1}{2}i_8$.

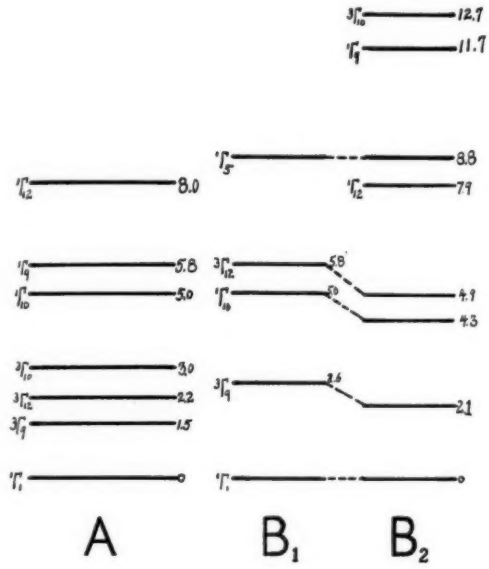

FIG. 1.

The effects of this potential of carbon atom I on an electron on the neighboring nucleus II, Q, as well as on an electron shared between atoms I and II, R, were calculated. Since the potential $\mathbf{H}_I$ decreases rapidly with distance, its effect on other than neighboring electrons was found to be completely negligible.

VI. RESULTS

The levels calculated in this manner are shown in Fig. A. The numbers at the right of the lines give the energy in volts of the levels above the ground state. Since only the excitation of one electron from $l=1$ to $l=2$ has been considered, only the lowest levels are obtained. The next higher ones, however, arising from the excitation of one electron from $l=1$ to $l=3$, one electron from $l=0$ to $l=2$ or two electrons from $l=\pm1$ to $l=\pm2$ have different symmetry properties from any of those obtained here (for instance Γ_5) and therefore do not interact with the states considered.

Figures B_1 and B_2 show for comparison the level scheme obtained from the Heitler-London method of calculation.[1] Figure B_1 contains the levels as calculated from nonpolar terms, B_2 those obtained by the inclusion of some polar configurations. The contribution of the polar terms is somewhat uncertain since not all possible polar terms, but only the lowest ones, were considered, and since the energy depends on two parameters which can only be roughly determined empirically.[10]

The energy of the lowest singlet state, of symmetry ${}^1\Gamma_{10}$ agrees very well in the two methods. Experimentally, a band of oscillator strength $f=10^{-4}$ is observed at $\lambda=2600$A or energy about 4.7 volts. The small transition probability indicates that this band is due to a forbidden electronic transition. Analysis of the band structure shows that the observed vibrational progressions are in agreement with a symmetry character ${}^1\Gamma_{10}(B_{2u})$ for the excited electronic state.

Of the other singlet states, the energies of ${}^1\Gamma_{12}(E_{1u})$ agree well in both calculations. A glaring discrepancy occurs however in the position of the level ${}^1\Gamma_9$. In the Heitler-London calculation both ${}^1\Gamma_9$ and ${}^1\Gamma_{12}$ are purely polar terms. They are obtained in that method really as a second approximation, and it would not be surprising if the calculated energy would turn out to be too high. On the other hand, in the method of this paper, polar configurations enter with too large coefficients into all states, causing the polar states to be relatively too low, as will be discussed later. But the agreement for the level ${}^1\Gamma_{12}(E_{1u})$ must then be regarded as purely accidental.

The experimental evidence in the region of the far ultraviolet is not completely conclusive. The measurements of Henri[11] in solution, evaluated by Chako[12] show a band of oscillator strength one-tenth at about 2070A, or 6.0 ev. One must be inclined to attribute this to the electronic level ${}^1\Gamma_{12}$, since this is an allowed transition. On the other hand, the measurements of Carr and

---

[10] The two parameters are the difference between the Coulomb energy of a polar and a nonpolar state and the resonance integral $\int\psi_a(1)\psi_b(2)H\psi_a^*(1)\psi_a^*(2)$. Their values were estimated from the absorption frequency of pentene 2 (since cyclohexene has not been measured), and from the resonance of cyclohexene. States like and were omitted since they introduced new variables and complicated the determinant.

[11] V. Henri, J. de. Phys. **3**, 181 (1922).

[12] N. Chako, J. Chem. Phys. **2**, 644 (1934).

Stücklen[13] in the gas seem to indicate the presence of two bands at 2040A and 1850A, of 6.0 ev and 6.7 ev respectively, the band at longer wave-length being the weaker one. This would be in reasonable agreement with the calculations of this paper, which predict a state forbidden in combination with the ground state, therefore a weak band, at 5.8 ev, and an allowed band at 8.0 ev. Since in solution the 2600A band of benzene is considerably shifted to longer wave-length, it is conceivable that a strong band at 1850A might be shifted sufficiently in the liquid to mask a weak band at 2040A, which would correlate the experiments of Henri with the appearance of the bands in vapor.

The energy of the triplet states turns out to be uniformly lower in the molecular orbital than in the Heitler-London calculation. The best agreement is obtained for $^3\Gamma_9$, the worst for $^3\Gamma_{10}$. That the energy, calculated on the basis of molecular orbitals, is lower for the triplet states than the singlet states can be seen qualitatively. Since the eigenfunctions used are antisymmetrized they allow no more than two electrons of opposite spin to be simultaneously at one nucleus, but they allow this to happen very frequently. Terms corresponding to two electrons on one carbon atom give rise to a large repulsion and therefore an increase in the energy. Now in the triplet states, where four electrons have spin α, two spin β, this piling up of two electrons of opposite spin will not occur as often as in the singlet states, causing the calculated energy of the triplet states to be lower than that of the singlets. For the true electronic eigenfunctions two electrons will not accumulate as freely on one carbon atom, so that one must expect the true difference between the energies of the excited singlet and triplet states to be smaller than that calculated on the basis of molecular orbitals. In other words, the absolute value of the energies of all states computed on the basis of molecular orbitals are too high, but those of the singlet states more too high than those of the triplet states. Since we calculate the energies of all excited states above the ground state, which is a singlet state, it may be expected that the energies of the singlet states are more reliable than those of the triplet states.

[13] E. P. Carr and H. Stücklen, J. Chem. Phys. **6**, 55 (1938).

VII. Summary

The eigenfunctions used for the description of the states of the benzene molecule are built from products of molecular orbitals. They are made completely antisymmetric. The orbitals in turn are assumed to be linear combinations of the $2p\pi$ atomic eigenfunctions of the six carbon atoms. No assumptions other than these were made. The energy is obtained as a sum of integrals over atomic eigenfunctions. Except for the Coulomb term, interactions between electrons farther apart than on neighboring atoms were neglected. This approximation is not necessary, since the other occurring integrals can be estimated very easily. There exist, however, a great number of them, and the calculation of the coefficients with which they enter into the energy of the various levels becomes extremely tedious. We took into account the effect of quite a few of them and found that they tend to cancel. No other approximations were made and no empirical data were used, except the C-C distance in benzene.

The energies depend then on the form of the atomic eigenfunctions. The integrals which are most sensitive to a change in the screening constant are the overlapping integrals s, and they also enter rather critically into the energy. The screening constant used here was 3.18.

The authors wish to express their thanks to Professors K. F. Herzfeld and J. E. Mayer for their interest and for many valuable discussions.

LETTERS TO THE EDITOR

This section will accept reports of new work, provided these are terse and contain few figures, and especially few halftone cuts. The Editorial Board will not hold itself responsible for opinions expressed by the correspondents. Contributions to this section must reach the office of the Managing Editor not later than the 15th of the month preceding that of the issue in which the letter is to appear. No proof will be sent to the authors. The usual publication charge ($3.00 per page) will not be made and no reprints will be furnished free.

The Absorption Coefficients of the Acetyl Halides

The absorption coefficients of acetyl chloride, bromide and iodide for some of the lines of the mercury arc spectrum have been measured with a thermopile and monochromator. The values obtained are listed in Table I. The long wave-length limits for the absorption, as estimated by an extrapolation of these data, are 2900, 3100, and 4000A for the chloride, bromide, and iodide, respectively. The absolute values of the absorption coefficients and these limits may be in error a few percent because of the reactivity of the compounds and, in the case of the chloride and iodide, the separation of condensed phases as the result of the reaction occurring.

Preliminary analyses of the products formed in the decomposition of these compounds caused by the absorption of ultraviolet light indicate that the reactions involved are quite complex. No hydrogen, ethane, or ethylene was detected by suitable tests for each.[1] The non-condensable (in liquid air) gases consisted of carbon monoxide and methane. The non-condensable portion obtained from acetyl chloride on illumination with $\lambda = 2537$A was 60 percent carbon monoxide and that obtained from the bromide or iodide was approximately 90 percent carbon monoxide. The condensable products contained the corresponding methyl halide but otherwise showed marked variations.

In the case of acetyl chloride a liquid product separated out during the course of the illumination. This substance appeared first as a white mist which became yellow as it settled on the walls and finally it changed to a dark brown. The presence of some hydrogen chloride and unchanged acetyl chloride interfered with the analysis of the liquid but the carbon and hydrogen percentages were found to be in fair agreement with the hypothesis that this substance is a polymer of either diacetyl or ketene. Tests of water solutions of the condensable gases for carbonate and oxalate (from $(COCl_2)$ ions) were negative.

Acetyl bromide did not yield a liquid such as was obtained from the chloride. In addition to methyl bromide the condensable products contained some bromine and compounds containing more than one atom of bromine per molecule, probably ethylene bromide. The products from acetyl iodide contained considerable quantities of free iodine and some liquid which was not analyzed on account of the small amount obtained.

Detailed studies of the decomposition of these three compounds are in progress.

TABLE I. *Absorption coefficients.*

Wave-length A	Acetyl chloride	Acetyl bromide	Acetyl iodide
2537	21.6	64.8	468
2652	10.3	46.8	324
2699	9.2	30.6	—
2753	4.5	12.6	216
2804	2.9	5.0	—
2894	—	—	126
3130	—	—	46.8
3650	—	—	6.5

$\epsilon = 1/cl \log_{10} I_0/I$ (c in moles/liter, l in cm)

D. H. ETZLER
G. K. ROLLEFSON

Department of Chemistry,
University of California,
Berkeley, California,
August 25, 1938.

[1] Blacet and Leighton, Ind. Eng. Chem. Anal. Ed. **3**, 266 (1931); Blacet, MacDonald and Leighton, ibid. **5**, 272 (1933); Blacet and MacDonald, ibid. **6**, 334 (1934); Blacet and Volman, ibid. **9**, 44 (1937).

Raman Frequencies of Hexamethylene Glycol

In the course of preparation of a series of glycols, Mr. George W. Anderson of the Department of Chemistry of this University supplied the writer with a specimen of hexamethylene glycol ($HO \cdot (CH_2)_6 \cdot OH$), with a melting point of 40.9 deg. C, and a boiling point range of 135 5 to 136.5 deg. C at a pressure of 8 mm Hg.

In determining the Raman frequencies for this compound, mercury arcs in pyrex were used for excitation. In some runs a filter consisting of a saturated solution of sodium nitrite was used to eliminate the Raman lines resulting from the mercury 4047A group of lines. An iron spark spectrum adjacent to the Raman spectrum was used for the purpose of interpolating the wave numbers of the Raman lines.

The values are as follows, with estimated relative intensities and mercury line sources according to the Kohlrausch designations:

814 (2-*e*), 852 (2-*e*), 874 (2-*e*), 915 (1-*e*), 1000 (2-*e*), 1052 (3-*e*), 1084 (3-*e*), 1298 (4-*ek*), 1435 (4-*ekc*), 1472 (4-*ekc*), 2855 (8-*ek*), 2905 diffuse (8-*ek*).

R. C. WILLIAMSON

Department of Physics,
University of Florida,
Gainesville, Florida,
September 15, 1938.

Structure of Liquid Aliphatic Amines

The Table I below gives the results of x-ray diffraction study in five liquid di-acyl amines and in *n*-amyl and tri-*n*-amyl amines. The usual technique of production of x-rays and of obtaining diffraction haloes in liquids was employed. The second column gives the Bragg spacing d, calculated from the diameter of the diffraction halo. The third column gives the constant k, in Raman[1] and Ramnathan's theory, i.e., the ratio of d to $(m/p)^{\frac{1}{3}}$, which for spherical molecules should have a value between 0.8 and unity.

It is seen that the value of Bragg spacing has the constant value 4.46A for all the normal di-acyl amines examined. This value is close to 4.60A, which is the diameter of a carbon-atom-chain in aliphatic liquid molecules found by previous workers.[2] This constant value for the spacing cannot represent the distance between two carbon-chains in the same molecule of an acyl amine, since the diffraction haloes are far from sharp. The possible explanation of this value of the spacing is, therefore, that it represents the distance between two carbon-chains belonging to two adjacent molecules of the amine.

We may assume that the flat pyramidal shape of the NH_3 molecule is maintained in the acyl amine molecule, in which one, two or three carbon-chains replace the hydrogen atoms. Taking into account the tendency of long chains to arrange themselves parallel to one another and adopting Stewart's[3] idea of "Cybotactic state" in liquid, the required condition for diffraction is obtained if we suppose that in the liquid, the molecules are piled up one above the other, the vertices of the adjacent pyramids fitting into each other and the corresponding edges lying close and parallel. Here, the Bragg spacing will be the mean distance between two carbon-chains lying along corresponding edges of adjacent pyramids and this will be nearly equal to the thickness of the chain, since the packing can be as close as possible. The whole arrangement of the molecules will, therefore, somewhat resemble a row of rather flat tripods, placed one above the other, the three legs of one lying close and alongside those of its neighbor. It is found that in the haloes of the tri-acyl amines, there is considerable intensity within the diffraction halo but the outer edge is sharply defined. This is readily explained on the above picture, as the outer limit corresponds to the closest approach of one edge of a pyramid towards the corresponding one of its neighbor. Any disarrangement of the row of pyramids will increase the mean distance between corresponding carbon-chains and give the inner scattering of the halo.

It will be also seen from the table that the spacing for an iso-amine is larger than that for the normal one—an effect of the side linkage in the chain. Also, the value of the constant k in the last column is, in all cases but one, below 0.7, showing that the molecules are not spherical in shape. Only in the case of di-iso-propyl amine, it is more than .8. This must be due to the fact that this molecule is more nearly spherical in shape, since there is a side linkage attached to a short carbon-chain.

TABLE I.

Liquid	$d = \frac{\lambda}{2 \sin \theta/2}$	k
Di-*n*-propyl amine	4.46A	0.730
Di-iso-propyl amine	5.48A	.890
Di-*n*-butyl amine	4.46A	.685
Di-*n*-amyl amine	4.46A	—
Di-iso-amyl amine	4.84A	.693
n-amyl amine	4.34A	.624
Di-*n*-amyl amine	4.46A	—
Tri-*n*-amyl amine	4.70A	.603

B. V. THOSAR

Physics Department,
College of Science,
Nagpur (C.P.), India,
August 16, 1938.

[1] Raman and Ramnathan, Proc. Ind. Ass. Cult. Sci. p. 127 (1923).
[2] Stewart and Morrow, Phys. Rev. **30**, 232 (1927).
[3] Stewart, Rev. Mod. Phys. **2**, 116 (1930).

Mayer's Theory of Condensing Systems

Mayer's general results[1] can be derived almost immediately from the theory of dissociating assemblies, thus avoiding much of his preliminary argument. Fowler's general method[2] for gaseous assemblies with any number of components and reactions is at once applicable to a gas of one component and any number of reactions—clustering processes or collisions. The dissociating molecule of type S is now a collision or cluster of S atoms. Fowler's equations (479) and (484), giving the law of mass action and the external pressure on the gas, are then, with classical partition functions, almost obviously identical with Mayer's equations (43) and (37) when recast into the notation there used. The present more general argument is applicable to any type of partition function, proving very directly the generality of Mayer's results.

WILLIAM BAND

Department of Physics,
Yenching University,
Peking, China,
August 1, 1938.

[1] Joseph E. Mayer, J. Chem. Phys. **5**, 67 (1937).
[2] R. H. Fowler, *Statistical Mechanics*, 2nd Edition, §5·3.

On the Symmetries of the Fields About Ions in Solution. Equilibrium between Forms of Different Symmetry

The absorption spectra of solutions of trivalent europium are so sharp that it is possible to resolve the multiplets induced by the electrical fields about the europium ions. It was found[1] that the multiplets consisted of different numbers of components depending upon the nature of the solutions. Such differences were sought as a parallel to the different structures which arise in the spectra of crystals when a rare earth is subject to crystal fields of various symmetries.

In this note we shall describe new features in the spectra of aqueous solutions of europium nitrate and of europium chloride, especially in the blue region which contains lines rather easy to follow. This group consists of four lines in the chloride and three lines in the nitrate of different spacing, sharpness and relative intensities.[2] These

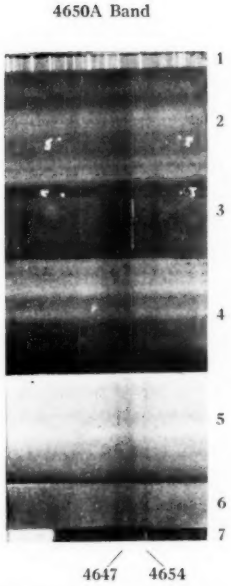

FIG. 1. 1-Fe arc. 2-$EuCl_3$ .0025 M. 3-$EuCl_3$ .95 M. 4-$Eu(NO_3)_3$ .0025 M. 5-$Eu(NO_3)_3$ .009 M. 6-$Eu(NO_3)_3$ .95 M. 7-Fe arc.

separate patterns remain unchanged from about 1.5 M to about 0.01 M as observed with a 21-ft. grating. On diluting to 0.0007 M, we could discover no change in the pattern of the chloride but when the nitrate was diluted to 0.0007 M, its group which had consisted of three lines now had changed over to four, indistinguishable in character from those of the chloride. At concentrations between 0.01 M and 0.0007 M, the nitrate showed both spectra and with increased dilution the chloride pattern gained intensity at the expense of the nitrate pattern. (See Fig. 1.)

Europium nitrate in aqueous solution has then distributed itself between two discrete configurations in equilibrium corresponding to different symmetries of the fields about the europium ions. There is some resemblance here to the situation in which two allotropic modifications of a crystal are present together, with this difference, that the equilibrium in the solution of the nitrate takes place within one phase.

In a forthcoming note it will be shown that europium nitrate and europium chloride are strong electrolytes similar to and of the same order of strength as lanthanum nitrate and lanthanum chloride which have served as standard salts in thermodynamic studies of trivalent ions. Because of the close resemblance of europium to other rare earths, we regard the existence of discrete forms of different symmetry as no rare phenomenon—among trivalent ions, at any rate.

SIMON FREED AND H. F. JACOBSON

G. H. Jones Laboratory,
University of Chicago,
Chicago, Illinois,
September 2, 1938.

[1] S. Freed and S. I. Weissman, J. Chem. Phys. **6**, 297 (1938).
[2] Since the publication of the previous note, we have discovered that G. Urbain (J. Chem. Phys. **4**, 243 (1906)) had observed differences between the spectrum of europium nitrate and of europium chloride in aqueous solution.

Symmetries of the Fields About Ions in Solution and Electrolytic Dissociation

Recent experiments[1] have shown that the fields about the ions of trivalent europium in aqueous solution are sharply defined in their intensities and orientations and that these differ with the nature of the solution. However, with a solution of a given salt, the structures in the spectra which respond to changes in the fields are not affected when the solution is diluted. The wave-lengths of the lines, their sharpness, relative intensities, the spacings within the multiplet, all remain unchanged, from concentrated to dilute solutions. Europium chloride has four lines in a particular group in the blue region. No change could be observed in the character of the lines when the concentration was varied from about 1.5 M to 0.0007 M. Corresponding to this group of lines, europium nitrate has three lines, altogether different in quality from the four of the chloride. These lines experience no change when the solution is diluted, even though a new additional form makes its appearance[2] at about 0.01 M. The spectrum of the new form is indistinguishable from that of the chloride. As dilution proceeds the "chloride-structure" of the nitrate becomes more intense relative to the original "nitrate-structure." Nevertheless, even though the total intensity of each structure varies, the relative intensities within the structure, the sharpness, and the intervals remain invariable throughout dilution.

The theory of Bethe[3] prescribes into how many components a particular energy level will be decomposed by an electrical field of given symmetry. The magnitude of the intervals between the components is a measure of the strength of the fields. We have found that the spectrum of a crystal of hydrated europium nitrate contains three lines in its blue group, having roughly the same intervals as originate from a solution of the nitrate. We are then to conclude that the fields about the europium ions in the crystal are roughly of the same intensity as the fields about the ions in solution. Furthermore this intensity does not change with dilution.

A natural assumption to make at this point is that the salts of europium are revealing bonds which are permanently oriented. If that description is to be correct, it must not exclude the electrolytic dissociation of the salts since, as we shall show, salts of europium are strong electrolytes in about the same measure as the salts of lanthanum. The latter have repeatedly served to illustrate and test the inter-ionic attraction theory.

There is such a mass of different data on the close resemblance among the ions of the rare earths[4] that there can be little doubt concerning the resemblance with respect to ionization also. As a final check on these inferences, which, to be sure, involve little interpolation, Mr. I. M. Klotz of this laboratory measured the electrical conductivities of solutions of europium nitrate and of europium chloride and found them to be nearly of the same magnitude as those of the corresponding lanthanum salts. Mr. Klotz will publish his data shortly. As to thermodynamic behavior—the freezing point lowering of lanthanum nitrate at 0.01 M is 3.35 times[5] that of the same concentration of mannose and at 0.001 M it is 3.75 times.

Judging from the spectra we have been led to assign rather permanent, discrete geometrical configurations to the fields about the ions of europium notwithstanding the fact that such configurations have long been imagined characteristic of non-electrolytes. This behavior is not limited to salts of europium. It is not due to some singular electronic distribution which europium possesses,[6] since europium ion acts in its salts and solutions like the *spherically* symmetrical gadolinium *ion* (^8S). Salts of these two ions are almost inseparable by fractional crystallization; they are next to each other in the periodic table.

The model for the structure of these electrolytes which the spectra seem to place before us has little resemblance to the model evolved by the interionic attraction theory. There is, for example, no sign of a diffuse ionic atmosphere changing continuously in extent and field intensity with dilution. The spectra give no suggestion that at greater dilution discrete structures will disappear. The fact is that when one discrete structure disappears another as discrete and fixed takes its place.

There may, of course, be somewhat similar phenomena with bivalent ions but there seems little likelihood that they are prominent in univalent ions where the Debye-Hückel theory has been so conspicuously successful. However, with simple trivalent ions in the range of concentrations we have investigated, there are, it seems, sufficient reasons for expecting the Debye-Hückel theory to be in disagreement with the experimental results.

SIMON FREED

G. H. Jones Laboratory,
University of Chicago,
Chicago, Illinois,
September 9, 1938.

[1] S. Freed and S. I. Weissman, J. Chem. Phys. (1938).
[2] S. Freed and H. F. Jacobson, J. Chem. Phys., in this issue.
[3] H. Bethe, Ann. der Physik **3**, 133 (1929).
[4] The osmotic coefficients of the salts of those rare earths which have been measured (C. M. Mason, J. Am. Chem. Soc. **60**, 1638 (1938)) differ extremely little. The isomorphism of the crystals, their miscibility with each other, the slight differences in the ionic sizes and in the molal volumes and especially the great difficulty of separating them by fractional crystallization.
[5] *International Critical Tables.*
[6] The exceptionally sharp lines, that is, the exceptionally weak coupling which Eu^{+++} has with the oscillations, rotations, etc., of the environment, may, perhaps, be related to the zero value of the angular momentum of the electronically activated state, i.e., $J=0$. The basic state of Eu^{+++} is actually $J=0$ and the thermally activated states are $J=1$ etc. Transitions between these and an activated state $J=0$ are very probable.

The Separation of the Carbon Isotopes by Diffusion

The results to be described were obtained with a battery of 51 Hertz-type pumps as modified by Professor W. Bleakney of Princeton.[1] Preliminary experiments on mixtures of argon-helium, carbon dioxide-nitrogen and carbon dioxide-argon permitted the determination, for these mixtures, of the best operating conditions in respect to applied heat and working pressure. With respect to the latter, our results confirm those of Barwich.[2] As for the question of the presence or absence of a capillary between the pump units we have found that the yield is better without a capillary. For the two mixtures carbon dioxide-argon and carbon dioxide-nitrogen we have obtained separation factors of 2.4 and 5.4 respectively. From these values it is possible to calculate, for methane, a theoretical separation factor of 1.18. Experimentally we found that, for methane, better separation of the carbon isotopes could be obtained with higher heats than in the cases of the above mixtures. In spite of this, however, the experimental separation factor is less than the theoretical value, in agreement with the data of Sherr.[1] At the present time, with an adequate system of purification and circulating a large volume of methane, we have obtained in thirty hours of pumping a yield of 300 cc of methane at 1.8 mm Hg pressure and containing from 30 to 32 percent of carbon 13. This is indicated by the relative intensities of the Swan bands $C^{12}-C^{12}$, $C^{12}-C^{13}$ and $C^{13}-C^{13}$ reproduced in Fig. 1.

We wish particularly to thank Messrs. Breyre and Coppens of the Institut National des Mines at Paturages, who placed at our disposal specially purified methane.

P. CAPRON
J. M. DELFOSSE
M. DE HEMPTINNE
H. S. TAYLOR

Institut de Physique,
Université de Louvain,
Louvain, Belgium,
September 15, 1938.

[1] R. Sherr, J. Chem. Phys. **6**, 251 (1938).
[2] Barwich, Zeits. f. Physik **100**, 166 (1936).

The Diamagnetism of Gaseous Nitrosyl Chloride*

In a recent paper Jahn[1] suggested that nitrosyl chloride (NOCl) exists in a triplet normal state, perhaps with a low-lying singlet state, in order to explain the apparent excess entropy of $R \ln 3$ or $R \ln 4$ calculated from equilibrium measurements over that calculated from structural and spectroscopic information. This triplet ground state would lead to paramagnetism of the substance. Wilson[2] made magnetic measurements on liquid nitrosyl chloride and found it to be diamagnetic. There remains, however, the possibility that polymerization of the molecules in the liquid state might reduce the paramagnetism of the substance, as is the case with oxygen at sufficiently

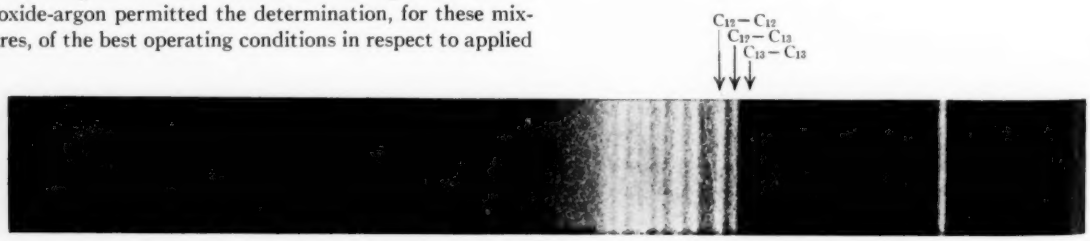

FIG. 1.

low temperatures. We have therefore carried out measurements on the gaseous compound.

The susceptibility was measured at 25° by the Gouy method, making comparison with oxygen as the substance of known paramagnetism ($\kappa = +0.142 \times 10^{-6}$ c.g.s.m. at 20°).[3] A glass tube of 19 mm diameter was separated into two compartments by a glass septum and equipped at either end for sealing off. This was suspended from the arm of an analytical balance, and the apparent change in weight (Δw in mg) of the tube was determined when the magnet was excited with two different currents. The absolute values of the magnetic fields obtained were 8080 and 9350 oersteds at 9.00 and 14.00 ampere readings. With both ends evacuated there were found for the corresponding readings $\Delta w = +0.10$ and 0.16 (average of at least two determinations); with the upper end evacuated and dried tank oxygen at 701 mm pressure at 25° in the lower end, $\Delta w = -8.29$ and -11.08; with the upper end evacuated and pure nitrosyl chloride at 790 mm pressure at 25° in the lower end, $\Delta w = +0.11$ and 0.14. The probable error in the determination of Δw is of the order of ± 0.05 mg. The nitrosyl chloride was prepared from nitric oxide and chlorine which had been carefully purified for use in equilibrium measurements. A large excess of nitric oxide was allowed to react with the chlorine, and the nitrosyl chloride was then frozen out in the tube and pumped free from volatile impurities.

The predicted values of Δw for nitrosyl chloride in a $^3\Sigma$ state at the pressure and temperature of measurement are -9.3 and -12.5; the predicted values for equipartition between three $^3\Sigma$ and one $^1\Sigma$ states (quantum weight four) are -7.0 and -9.3; the predicted values for a singlet state (diamagnetic), taking into account the estimated molecular diamagnetism of -30×10^{-6}, are $+0.19$ and 0.28 respectively. Correction for an estimated dissociation of 0.5 percent[4] into chlorine and paramagnetic nitric oxide would lower the diamagnetic values to $+0.15$ and $+0.24$ respectively. The observed Δw values are in satisfactory agreement with this last prediction. We conclude therefore that nitrosyl chloride is diamagnetic and in a singlet state.

CARROL M. BEESON
CHARLES D. CORYELL

Gates and Crellin Laboratories of Chemistry,
California Institute of Technology,
Pasadena, California,
August 23, 1938.

* Contribution from the Gates and Crellin Laboratories of Chemistry, California Institute of Technology, No. 663.

[1] F. P. Jahn, J. Chem. Phys. **6**, 335 (1938).
[2] E. B. Wilson, Jr., J. Am. Chem. Soc. **56**, 747 (1934).
[3] *International Critical Tables*, VI, 354 (1929).
[4] Extrapolation of unpublished equilibrium data of C. M. Beeson and D. M. Yost.